



State-of-art review on the process-structure-properties-performance linkage in wire arc additive manufacturing

Han Zhang, Runsheng Li, Junjiang Liu, Kaiyun Wang, Qian Weijian, Lei Shi, Liming Lei, Weifeng He & Shengchuan Wu

To cite this article: Han Zhang, Runsheng Li, Junjiang Liu, Kaiyun Wang, Qian Weijian, Lei Shi, Liming Lei, Weifeng He & Shengchuan Wu (2024) State-of-art review on the process-structure-properties-performance linkage in wire arc additive manufacturing, Virtual and Physical Prototyping, 19:1, e2390495, DOI: [10.1080/17452759.2024.2390495](https://doi.org/10.1080/17452759.2024.2390495)

To link to this article: <https://doi.org/10.1080/17452759.2024.2390495>



© 2024 The Author(s). Published by Informa UK Limited, trading as Taylor & Francis Group



Published online: 05 Sep 2024.



Submit your article to this journal [↗](#)



Article views: 2527



View related articles [↗](#)



View Crossmark data [↗](#)



Citing articles: 5 View citing articles [↗](#)

State-of-art review on the process-structure-properties-performance linkage in wire arc additive manufacturing

Han Zhang^a, Runsheng Li^b, Junjiang Liu^a, Kaiyun Wang^a, Qian Weijian^a, Lei Shi^c, Liming Lei^c, Weifeng He^d and Shengchuan Wu^a

^aState Key Laboratory of Rail Transit Vehicle System, Southwest Jiaotong University, Chengdu, People's Republic of China; ^bAviation Services Research Centre, The Hong Kong Polytechnic University, Hong Kong, People's Republic of China; ^cTaihang Laboratory, Chengdu, People's Republic of China; ^dSchool of Mechanical Engineering, Xi'an Jiaotong University, Xi'an, People's Republic of China

ABSTRACT

Wire Arc Additive Manufacturing (WAAM) can well offer improved design flexibility and manufacturing versatility for the integrated molding of large components. However, it is challenging to achieve high productivity in arc additive metal part applications, as it requires consistent manufacturing, reliable quality, and predictable performance. The service performance of arc additively manufactured components is often influenced by microstructure, widely distributed defects, deep residual stresses, and complex surface roughness. To this regard, investigating the Process-Structure-Property-Performance (PSPP) relationships via both experimentation and simulation is a proven strategy for furthering the capabilities of additive manufacturing. Nowadays, Machine Learning (ML) can also be a powerful tool for modelling these complex, nonlinear relationships. This paper begins with a brief overview of WAAM process classification, and a generic description of process control. It then proceeds to a comprehensive review and discussion of how component microstructure, internal defects, surface roughness, and residual stress, all impact mechanical and fatigue properties of WAAM components. Additionally, it includes a detailed exploration of the latest advancements in using ML to predict these effects, focusing on PSPP modelling. Finally, the paper discusses the current limitations of ML approaches in PSPP modelling, and outlines future trends and technological prospects.

ARTICLE HISTORY

Received 31 May 2024
Accepted 31 July 2024

KEYWORDS




Wire arc additive manufacturing; microstructure and mechanical properties; internal defect; residual stress; fatigue performance assessment; machine learning

1. Introduction

Additive manufacturing(AM), renowned for its ability to build three-dimensional objects layer by layer through advanced digital designs, is a revolutionary technology, very different to traditional manufacturing processes, such as casting, forging, and machining [1]. Besides, it is a representative in the new technological evolution, mainly due to its unique advantages in enhancing design freedom, reducing production cycles, and approaching near-net shaping without requiring the expensive mold any more [2].

Over the past four decades, the community has not only developed various AM processes, but has also applied them extensively across major industries, including automotive, aerospace, and biomedical areas, making it one of the fastest-growing disciplines. Researchers around the world are paying more attention to such cutting-edge technology, to achieve short-cycle, high-precision, high-performance manufacturing [3–6].

With the advancement of AM, a variety of AM processes have emerged. At present, the two main categories of AM processes for metallic components are Powder Bed Fusion (PBF) and Directed Energy Deposition (DED), as outlined in ISO/ASTM 52900:2015. In the PBF process, metal powder particles are selectively fused, either sintered, or melted layer-by-layer by a heat source. PBF is particularly suited for manufacturing small parts, ranging from 200 mm to 350 mm in the maximum dimension [1]. Despite the higher precision and better surface quality of PBF products compared to other AM technologies, it remains only economically feasible for optimised parts in high-value components [7]. Compared with the PBF process, DED offers a higher material deposition rate and is primarily used for producing medium to large parts, with dimensions ranging from 350 mm to 5000 mm [1]. DED enables the direct formation of high-performance metal

CONTACT Shengchuan Wu  wusc@swjtu.edu.cn; Junjiang Liu  jun_j_lu@foxmail.com  State Key Laboratory of Rail Transit Vehicle System, Southwest Jiaotong University, Chengdu 610031, People's Republic of China; Liming Lei  biamfirst@126.com  Taihang Laboratory, Chengdu 610213, People's Republic of China

© 2024 The Author(s). Published by Informa UK Limited, trading as Taylor & Francis Group

This is an Open Access article distributed under the terms of the Creative Commons Attribution-NonCommercial License (<http://creativecommons.org/licenses/by-nc/4.0/>), which permits unrestricted non-commercial use, distribution, and reproduction in any medium, provided the original work is properly cited. The terms on which this article has been published allow the posting of the Accepted Manuscript in a repository by the author(s) or with their consent.

components, which typically require minimal machining. In addition, DED is also employed for the rapid repair and remaking of locally damaged components and structures [8].

To meet the manufacturing requirements of large-scale, complex and integrated components, Wire Arc Additive Manufacturing (WAAM) has undergone considerable developments. WAAM stands out from DED technologies due to its efficient deposition rates, relatively low equipment costs, excellent material utilisation, and eco-friendly characteristics [9–12], hence its description as ‘Green Technology’ [13]. Moreover, WAAM technology can shorten the manufacturing and subsequent processing times by 40–60% and 15–20%, respectively, depending on the component sizes [10]. This is particularly evident in the production of complex components, such as aircraft landing gear, where it can reduce raw material use by up to 78%, compared to traditional subtractive manufacturing processes [9]. To date, WAAM technology has been applied to manufacturing processes using various engineering materials, including titanium [14], aluminium [15], nickel alloys [16], and steel [17], demonstrating tremendous potential. Yi et al. [18], presented an overview of recent advancements in wire innovations that have expanded the range of materials available for WAAM. Figure 1 provides a detailed analysis of WAAM, as indexed by the Science Citation Index, categorising the data by publication year, research institution, research direction, field, and literature type [18]. Over the past decades, metal WAAM technology has been extensively studied by numerous research institutions worldwide, with a significant surge in literature post-2016. This period accounts for about 97.16% of all WAAM publications, highlighting its rapid emergence as a major field of study.

Although the mechanical performance of WAAM fabricated components compares well with those conventional techniques, the manufacturing process of WAAM components involves huge challenges. Rapid cooling and thermal cycling in WAAM processes can affect the size and shape of material grains, and the process is prone to defects such as porosity, cracking, and high residual tensile stresses [19–21]. These issues can severely detriment the mechanical performance and fatigue resistance of WAAM treated components, introducing significant variability in fatigue life and posing major challenges for material design, manufacturing processes, properties, and performance. Given that fatigue failure is one of the most common event and critical failure modes during the service life of engineering components, ensuring the long-term service reliability and safety of WAAM components is of prime concern. Thus, an integrated assessment method of

Process-Structure-Properties-Performance (PSPP), which focuses on microstructure, defects, residual stress, and roughness on service life becomes particularly important.

In the field of WAAM, the development of traditional physical models and their intricate relationship with processes, structure, properties and performance, is a comprehensive multi-level systematic approach [22]. This ranges from micro to macro levels, including real-time monitoring, performance prediction, failure analysis, and process optimisation. Real-time monitoring techniques are integrated to optimise process parameters, ensuring stability in the manufacturing process and high product quality [23]. By thoroughly analysing the microstructure, defects, residual stresses, and surface roughness of WAAM parts, the macroscopic mechanical properties can be meticulously evaluated, and fatigue life and failure modes can be predicted in terms of the service environment [21]. Metallurgical theory and simulation equations based PSPP models, not only captures the intricate behaviour of materials during the manufacturing, but also lays a robust theoretical foundation for optimising processes, and enhancing performance. This advancement significantly furthers triggers a broader application of WAAM technology.

However, traditional investigations tend to rely on methods such as experimental analysis, theoretical modelling, and numerical solutions, to construct PSPP models. These approaches still have significant limitations and boundaries in exploring the intricate, multi-factor coupling relationships between process parameters, influencing factors, and mechanical properties in metal additive manufacturing. This results in difficulties in meeting the requirements for accuracy and efficiency, in predicting macroscopic mechanical properties. Furthermore, the WAAM process is highly sensitive to variations in process parameters, including welding current, voltage, and wire feed speed, among others [24]. Metals exhibit pronounced nonlinear behaviour during rapid melting, solidification, and cooling processes, leading to changes in parameters like thermal conductivity and yield strength [25]. Traditional physical models may encounter difficulties in handling the nonlinear behaviour, thereby struggling to accurately describe real material responses.

It still remains challenging to determine a non-linear relationship among PSPP in a high-dimensional space. As a data-driven science, Machine Learning (ML) provides effective ways to handle the intricate relationships within high dimensions. By using ‘Additive Manufacturing’ and ‘Machine Learning’ as keywords in the Web of Science database, a total of 1,419 academic papers were retrieved (as of March 2024). The quantity of

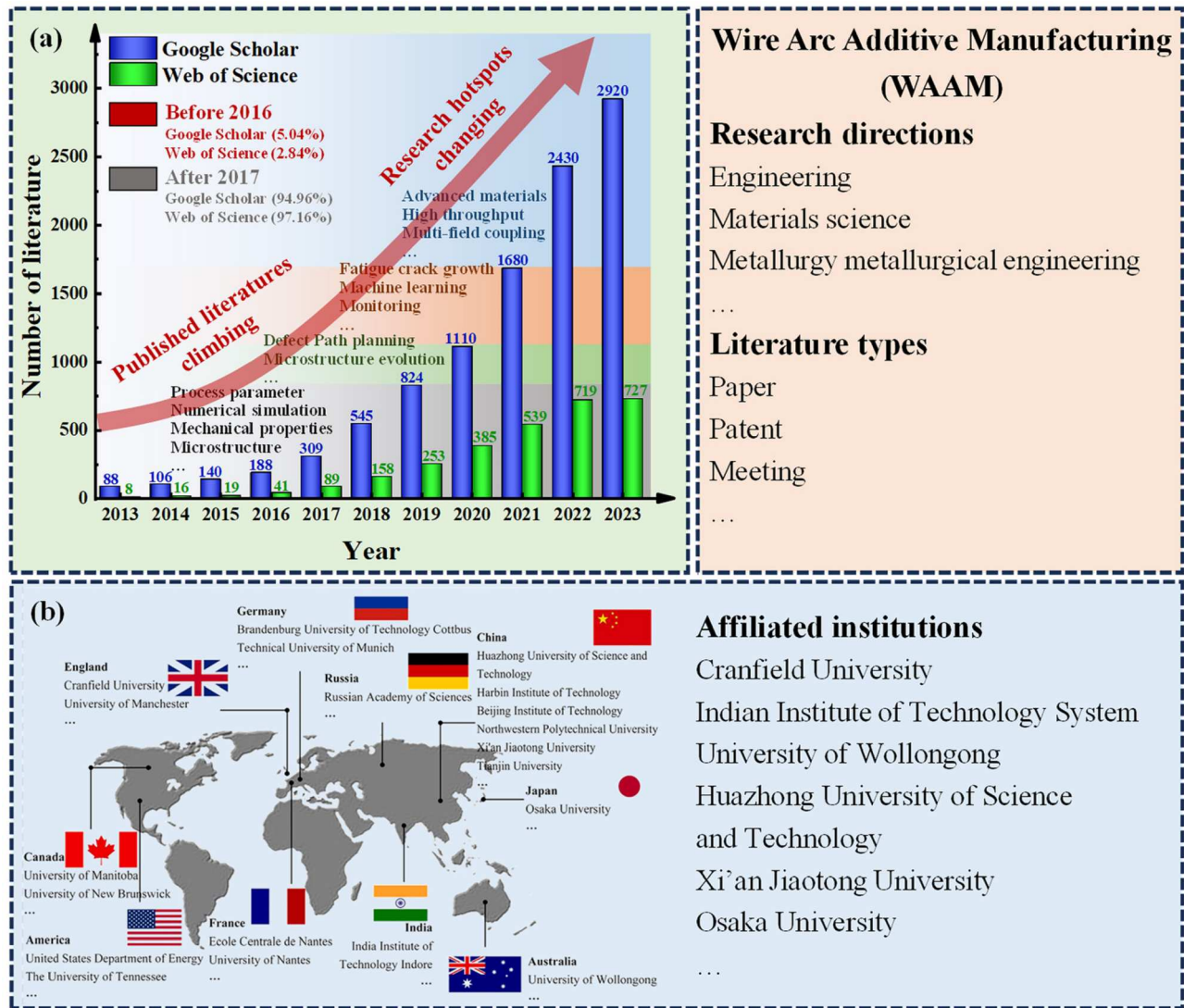


Figure 1. Analysis of research trends in WAAM, (a) based on the Science Citation Index, utilising Data from Web of Science, Google Scholar, (b) affiliated institutions [18].

published papers has seen an almost exponential surge in the past four years, underscoring the increasing interest in ML-based AM technology, across diverse sectors.

ML models surpass traditional physical models in identifying the complex nonlinear relationships between process parameters, microstructures, and mechanical properties [26]. By training on extensive datasets that include process parameters, microstructural features, and mechanical property data, these models can autonomously identify and learn hidden patterns and correlations, thereby constructing highly accurate predictive models [27]. Moreover, through methods like cross-validation and evaluation using independent test sets, ML models ensure the accuracy and reliability of their predictions [28]. Integrating multi-source data from experiments, simulations, and field tests, these models comprehensively predict and analyse factors

ranging from process parameters and microstructures to mechanical properties and service performance [29]. This integrated approach not only deepens our understanding of the WAAM process, but also provides a scientific basis and technical reference for the precise adjustment of process parameters and the intelligent improvement of metal WAAM processes.

Figure 2 depicts the principal research process for establishing PSPP relationships, in the field of ML within WAAM research. It aims to further the PSPP methodology, assisting in customising ultimate high-performance metal components, in more universal material selection, in more comprehensive virtual manufacturing, and aiding actual production. This is in order to inform more advanced printing. In short, clarifying the PSPP relationships is becoming a promising development strategy for WAAM technology.

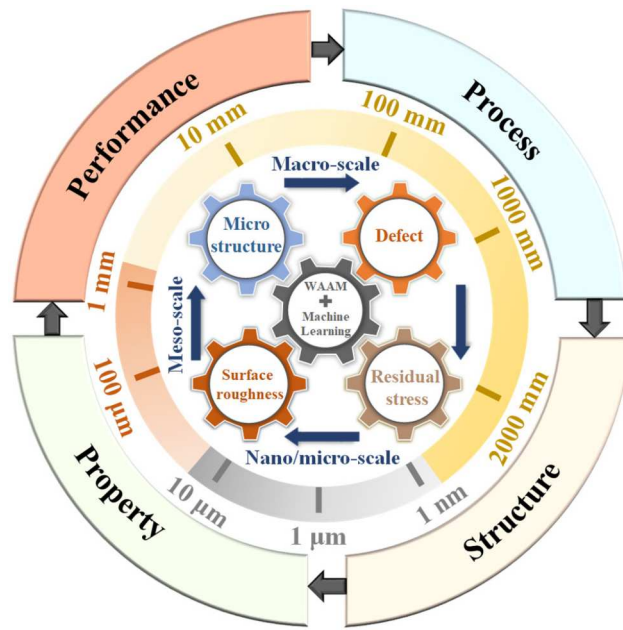


Figure 2. Schematic of establishing PSPP relationships in the field of ML within WAAM research.

2. Wire arc additive manufacturing process

2.1. Classification of WAAM

Wire arc additive manufacturing solution is a wire-based DED method, which usually uses an electric arc as a fusion source, to melt wire feedstock and deposit part preforms layer-by-layer [30]. Depending on the form of

thermal energy applied, the WAAM process can be broadly categorised into three types: Gas Metal Arc Welding (GMAW) based, Gas Tungsten Arc Welding (GTAW) based, and Plasma Arc Welding (PAW) based [10]. As shown in Figure 3, each category of WAAM technology has distinct characteristics. The deposition rate for GMAW-based WAAM is 2-3 times higher than that of GTAW or PAW-based methods. Nevertheless, the GMAW-based WAAM method shows less stability and generates more welding fumes and spatter, due to the direct application of current to the raw material. Based on this classification, the choice of WAAM technology directly affects the processing conditions and productivity of the target component.

2.2. Hybrid WAAM

Despite the numerous advantages of WAAM over traditional manufacturing methods, there are still some problems. It is hard, when using the WAAM process, to produce the desired characteristics and required accuracy of the finished part, which hinders its large-scale application in industry. Hybrid-AM has received significant attention recently [33]. Hybrid-AM involves two or more sequential processes being employed to create the finished part. The limitations of WAAM can be overcome by imposing auxiliary fields, including magnetic fields [34,35], acoustic fields [36], thermal fields [37] and deformation fields [38]. Besides, there are some

Processes	Technical parameters	Features	Merits & Demerits	Applications
<p>GMAW</p>	<ul style="list-style-type: none"> Energy source: GMAW Feedstock: Metal welding wire Build rate: 3-7 kg/hour Build size: up to 3 m³ Part accuracy: ±0.5-1.0 mm Roughness: 6.3-12.5 μm 	<ul style="list-style-type: none"> Electrode type: Consumable Separate feed wire: not required Typical deposition rate: 3-4 kg/hour Energy density: High, 0.4-0.87 kJ/mm 	<ul style="list-style-type: none"> High efficient and low cost Low initial set-up cost Co-axial feeding of wire Low arc stability High spattering Poor surface roughness 	<ul style="list-style-type: none"> Automotive Shipbuilding Construction General Manufacturing Repair Robotics Structural Steel
<p>GTAW</p>	<ul style="list-style-type: none"> Energy source: GTAW Feedstock: W electrode or filler Build rate: 0.5-2 kg/hour Build size: up to 1 m³ Part accuracy: ±0.1-0.5 mm Roughness: 1.6-6.3 μm 	<ul style="list-style-type: none"> Electrode type: Non-consumable Separate feed wire: required Typical deposition rate: 1-2 kg/hour Energy density: Low, 0.2-1.49 kJ/mm 	<ul style="list-style-type: none"> Smooth surface finish High part accuracy Reduced porosity Off-axial feeding of wire Necessity of rotation of wire and torch 	<ul style="list-style-type: none"> Aerospace Precision Welding Pipelines Nuclear Pressure Vessels Pharmaceutical Artistic Sculpture
<p>PAW</p>	<ul style="list-style-type: none"> Energy source: Plasma Feedstock: W electrode or filler Build rate: 1-4 kg/hour Build size: up to 1 m³ Part accuracy: ±0.3-0.8 mm Roughness: 6.3-12.5 μm 	<ul style="list-style-type: none"> Electrode type: Non-consumable Separate feed wire: required Typical deposition rate: 2-4 kg/hour Energy density: Highest, 0.7-1.30 kJ/mm 	<ul style="list-style-type: none"> Narrow high temperature zone High welding speed Off-axial feeding of wire Necessity of rotation of wire and torch 	<ul style="list-style-type: none"> Thin Materials Medical Devices Electronics Jewelry Metalworking Research and Development

Figure 3. Overview of typical metal additive manufacturing processes utilised by WAAM [10,24,31,32].

novel external field-assisted techniques that utilise plasma fields, electric fields and coupled multiple fields as auxiliary energy fields [39].

Figure 4(f)–(g) depict acoustic field assisted WAAM. Adding an auxiliary external set of acoustic fields can affect the deposition and curing process of the material. Acoustic waves can help to adjust the alignment and distribution of the material particles, resulting in a more homogeneous and compact material, which can help to minimise holes and defects, thus improving the properties and quality of the manufactured product [40]. As shown in Figure 4(e), the use of a magnetic field in WAAM exerts a significant influence on melt pool convection, due to TEMC and damping effects, resulting in a reduction in the melt pool velocity, the inhibition of reflux, and changing of the melt pool temperature gradient [41]. An auxiliary thermal field does not affect the melt pool dynamics.

However, it can control the thermal history of the WAAM part. One of the main motivations for applying

a thermal field is crack elimination. The underlying mechanism is that the auxiliary thermal field reduces the thermal gradient and cooling rate, which results in a more uniform temperature field and reduces the thermal stresses on the deposited sample [47].

In contrast to magnetic and thermal fields, both interacting with the material without direct contact, deformation fields, as shown in Figure 4(a)–(d), primarily affect the manufacturing layer through contact, resulting in plastic deformation of the part. This process, known as dynamic recrystallisation, leads to high energy storage in the deposited material, which in turn leads to the formation of more dislocations and preferential nucleation sites [48].

Hybrid *in situ* rolled wire-arc additive manufacturing (HRAM) is a hybrid-AM process, capable of printing large-scale parts, by combining *in situ* micro-rolling with standard WAAM [49]. As illustrated in Figure 5, Huazhong University of Science and Technology (HUST) has successfully used HRAM technology to

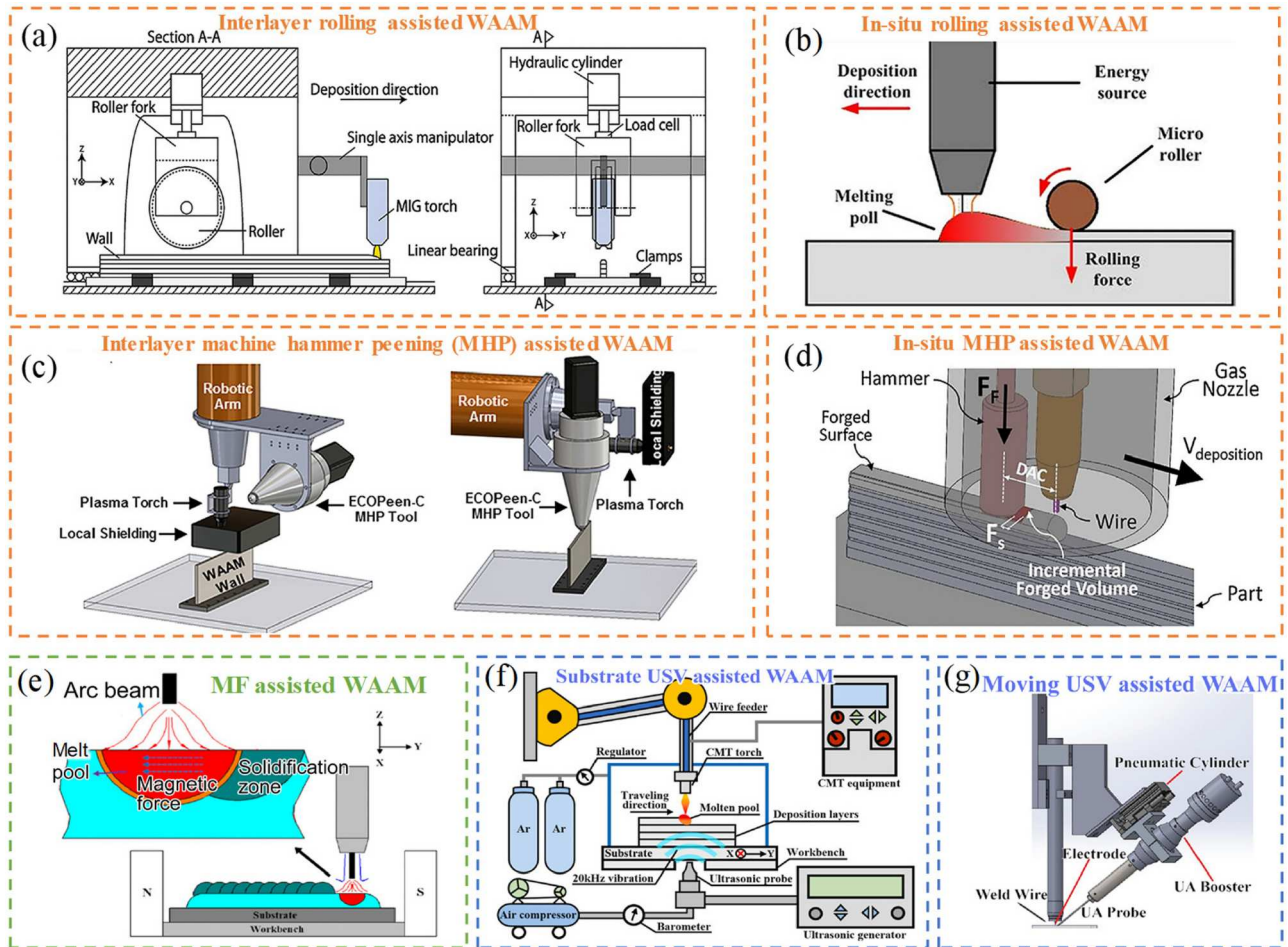


Figure 4. Schematics of WAAM with assisted field: (a) Interlayer rolling assisted WAAM [42]; (b) *In situ* rolling assisted WAAM [43]; (c) Interlayer Machine Hammer Peening (MHP) assisted WAAM [44]; (d) *In situ* MHP assisted WAAM [33]. (e) Auxiliary Magnetic Field (MF) assisted WAAM [45]. (f) Substrate Ultrasonic Vibration (USV)-assisted WAAM [36]; (g) Moving USV-assisted WAAM [46].

print air spring mounting beams, achieving both high efficiency and quality [50]. The study demonstrates that HRAM can be employed to generate near-final blanks expeditiously and economically, in conjunction with conventional casting techniques. With regard to the mechanical properties, as Figure 5(c) demonstrates, the strength and ductility of alloys produced by HRAM exceeded the acceptance index values for conventional materials. This work provides a solution for the integrated molding of large, critical load-bearing components.

Multi-robot collaborative WAAM manufacturing represents a prominent hybrid additive manufacturing process, distinguished not only by added assistance fields, but also by its integration of robotic systems with WAAM technology [51]. This approach employs multiple robotic deposition heads operating simultaneously on a single platform [52]. This approach expands manufacturing capabilities, to include producing fine details at the sub-meter scale to constructing large-scale structures of several metres, significantly improving manufacturing flexibility and freedom [53]. However, achieving successful multi-robot collaboration demands extensive expertise, including both hardware and software developments to overcome

challenges and to ensure the production of defect-free parts [18]. Importantly, WAAM suits a diverse range of applications. By carefully assessing different factors and understanding the capabilities and limitations of each WAAM process, manufacturers can make informed decisions, and choose the most appropriate method for their specific application and product requirements.

2.3. WAAM process and control

In WAAM, integrating manufacturing is key for enhancing process control and efficiency. This integration typically includes the real-time monitoring systems, which are fitted with various sensors. They continuously track and evaluate the manufacturing process and material properties, as shown in Figure 6, detecting any deviations or potential defects early in the process, facilitating immediate corrective actions.

Advanced control algorithms that utilise sensor data to adjust process parameters such as arc power, travel speed, and wire feed rate in real-time, are crucial for intelligent WAAM. Dynamic adjustments of parameters are crucial for maintaining optimal conditions throughout the material deposition process, which ensures the

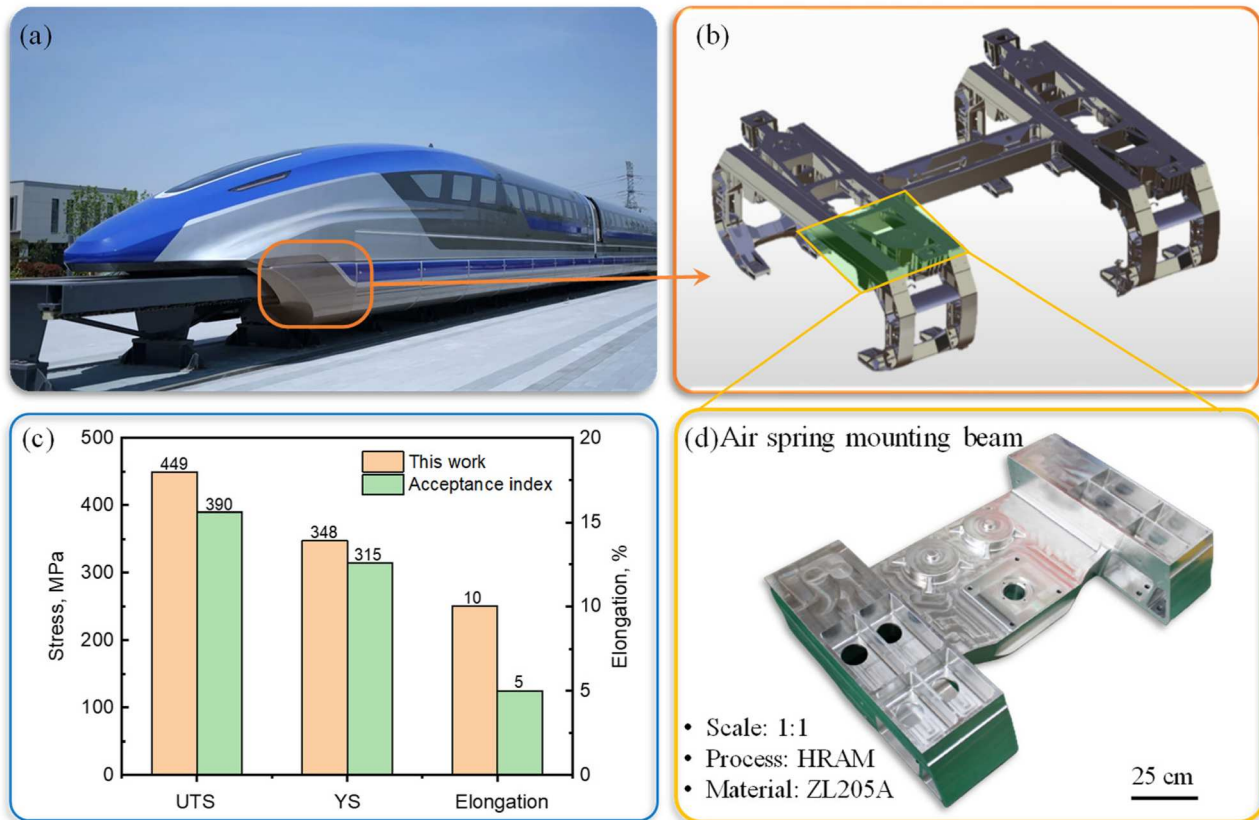


Figure 5. (a) Transit system with the maximum design speed of 600 km/h; (b) Bogie of the high-speed maglev; (c) Mechanical properties of the HRAM produced ZL205A alloy, together with the acceptance index. (d) Air spring mounting beam produced by HRAM.

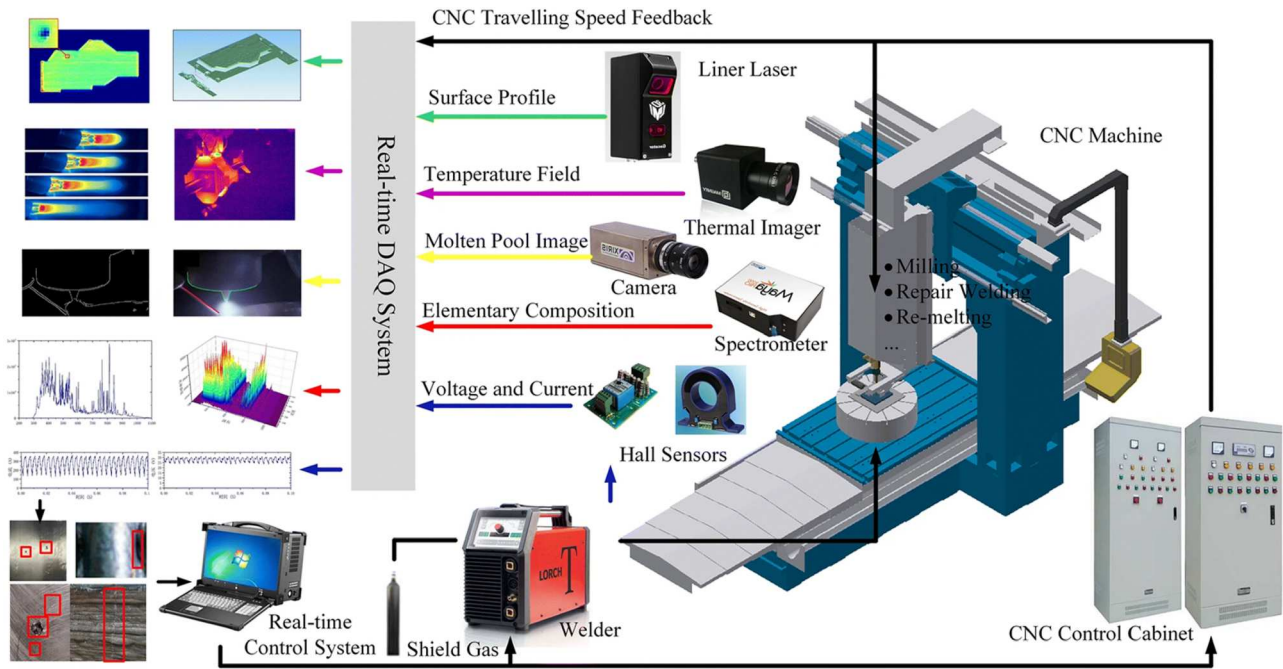


Figure 6. Schematic diagram of a closed-loop quality control WAAM system based on multi-sensor data fusion technology [54].

structural integrity and dimensional accuracy of the final product. Moreover, ML models can improve the accuracy of control by using historical data from real-time monitoring, to make reasonable predictions. WAAM process control allows the development of a fully automated, self-optimising system, which can minimise manual intervention, reduces material waste, and improves the overall quality and efficiency of the metal WAAM process.

2.3.1. WAAM fabrication process

In WAAM, arc welding is usually combined with a wire feeding mechanism. As illustrated in Figure 7, the raw metal wire is melted using the heat of the arc, after which the molten metal is deposited layer by layer on a given substrate, using bead deposition guided by 3D CAD model data. Robots or gantry systems are employed to continuously deposit these beads, ultimately forming a complete 3D metal component.

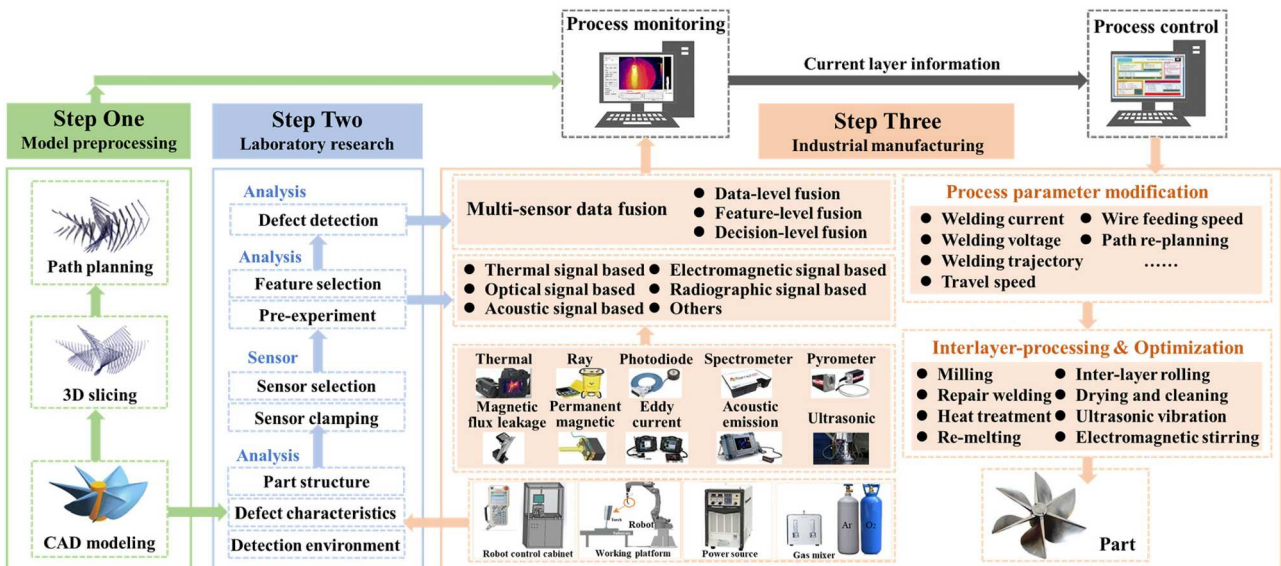


Figure 7. Schematic diagram of WAAM system.

The manufacturing of engineering parts using WAAM generally involves three main steps: process planning, deposition, and post-processing [55]. With a given CAD model, 3D slicing and programming software can generate the necessary robot motions and welding parameters to achieve manufacturing with high geometrical accuracy. Based on welding deposition models specific to the materials used for component fabrication, the 3D slicing and programming software provide automated path planning and process optimisation to avoid potential process defects. During the manufacturing process, robots conduct precise movements of the welding gun, to construct the component layer-by-layer. In addition, advanced WAAM systems can also be equipped with various sensors, to capture the welding signals, deposited weld geometry, metal transfer behaviour, and temperature, thus enabling process monitoring and control for achieving higher product quality. This work describes a burgeoning area of current and future research interest, which has the potential to significantly enhance the performance of WAAM processes.

2.3.2. Real-time monitoring of WAAM process

The formation of WAAM components is achieved through a layer-by-layer deposition process. During this process, single weld passes are closely spaced and stacked, and a number of physical processes are involved, including heat transfer from the arc to the wire, changes in droplet morphology during wire melting, solidification, and changes in the geometry of the weld passes. These events influence the performance and quality of the finished product to significant extent [56]. In order to achieve effective control in WAAM, it is necessary to have real-time access to the process parameters during the manufacturing process. Figure 8 gives the parameters that may affect the final product, for different processes carried out during WAAM. Existing research methods generally monitor the melt pool geometry, brightness and thermal distribution, through physical sensors [57]. The images

obtained from the monitoring process are then quantified and analysed, and the collected data is used to design control strategies and provide effective data support for model creation and modification. The key to effective monitoring is the accurate and efficient analysis of the collected data, generally divided into three categories: one-dimensional (1D), two-dimensional (2D) and three-dimensional (3D) data [58].

In the WAAM process, 1D data is relatively straightforward to obtain and fast to process. This data typically covers arc welding current and voltage, wire feed rate, and welding speed, which can be collected at low cost. Given the complexity of the WAAM process, 1D data does not usually provide sufficient information for analysis. Consequently, in order to acquire more detailed information about the shape of the part, 2D data is required. As shown in Figure 9, considerable numbers of researchers have worked on offline parameter management in order to obtain 2D data [59]. 2D data is primarily acquired by sensors, including industrial cameras, photodiodes, laser scanners and X-ray cameras, in order to find surface topography and to detect defects.

To improve the reliability of the WAAM process, it is crucial to gather 3D data with comprehensive information, using a non-destructive monitoring system to detect process anomalies. In WAAM, alterations in the melt pool can be monitored in real time by X-ray computed tomography (X-CT) and temperature field control [60]. Aucott et al. [61] demonstrated the ability of synchrotron X-ray imaging to capture, visualise and quantify the *in situ* melt pool evolution of metal alloys. This technique allows for the observation and understanding of the formation and evolution of the melt pool for the WAAM manufacturing process. X-CT is a non-destructive, non-contact inspection method that allows for real-time monitoring of internal microstructures formed during the welding process. This enables the detection of otherwise undetected defects, using 1D and 2D data.

However, the real-time effects of process parameters on stress evolution cannot be accurately estimated

WAAM Process			
Process Parameters	Product Quality	Process Signatures	Post Processing
<ul style="list-style-type: none"> ◆ Welding current ◆ Wire feed speed ◆ Shielding gas ◆ Travel speed ◆ 	<ul style="list-style-type: none"> ◆ Surface quality ◆ Physical properties ◆ Mechanical properties ◆ Fatigue performance ◆ 	<ul style="list-style-type: none"> ◆ Melt pool ◆ Flow field ◆ Grain growth ◆ Residual stress ◆ 	<ul style="list-style-type: none"> ◆ Peening ◆ Heat treatment ◆ Post machining ◆ Stress release ◆

Figure 8. The decisive factors during WAAM process.

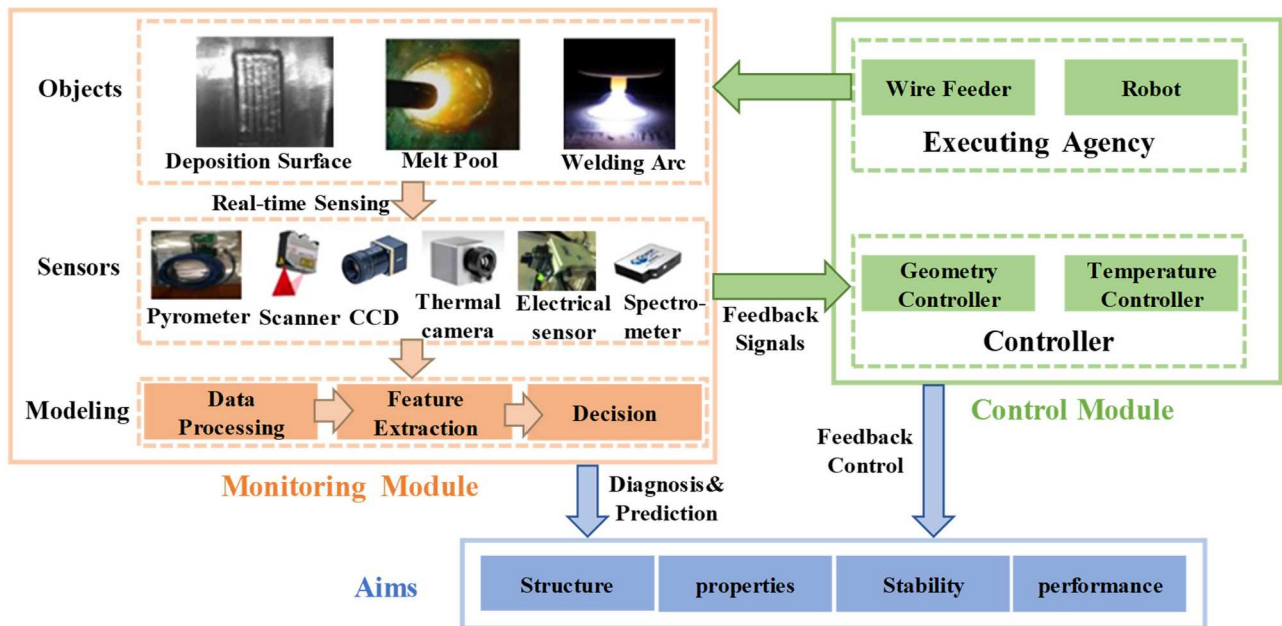


Figure 9. Monitoring and control framework of WAAM [59].

using conventional techniques [62]. In recent years, the rapid development of neutron diffraction technology has provided new means for non-destructive measurement of 3D residual stresses in critical load-bearing components. Nycz et al. [63] quantified the residual stresses in large-scale AM components before and after stress relaxation, using neutron diffraction, which provides a crucial foundation for optimising process parameters for printing AM components. As shown in Figure 10, Plotkowski et al. [64] used neutron diffraction to investigate the transient phase transitions and lattice strain evolution of crystal transformed steel during AM. The findings provide a novel approach to the design of residual stress states and property distributions in AM components. These insights could potentially aid in regulating residual stress distributions, thereby enhancing fatigue life and resistance to stress corrosion cracking.

The primary goal of the monitoring and control system is to improve process stability, precision in shape, and production quality, while also enabling real-time detection of defects in WAAM. Advances in process control have significantly enhanced WAAM technology, leading to notable improvements in surface finish and material properties. Moreover, these advancements have minimised variability between components and reduced the occurrence of material discontinuities, ensuring reliable performance in service.

2.3.3. Offline inspection of WAAM parts

One of the main challenges in WAAM is ensuring that components not only have enhanced mechanical

properties but also maintain robust structural integrity. To achieve this, it is crucial to meticulously control and optimise the local microstructure, during the entire manufacturing process. Also, employing multidimensional and multiscale characterisation techniques is essential. These techniques enable a detailed analysis of the microstructure and localised properties, within specific material zones across different spatiotemporal scales, thereby allowing a thorough understanding of the material mechanical behaviour. The ultimate goal is to establish a quantitative mapping relationship within the PSPP framework, which is instrumental in refining the material processes and microstructure. This mapping significantly contributes to the rapid, cost-effective development and deployment of high-performance metal materials and components.

Therefore, to establish a comprehensive PSPP system, it is necessary to utilise materials characterisation techniques with different spatial resolutions to obtain information on various scales, such as dislocations, precipitates, grain size, grain boundary characteristics, texture, elemental segregation, and manufacturing defects. This multiscale correlation of data can provide good information on materials and structures, which is indispensable for accurately predicting their service performance, and for establishing theoretical models. Material structure characterisation techniques mainly fit into two categories: traditional 2D destructive and advanced 3D non-destructive methods. Burnett and Withers [65] emphasised that sample preparation and foundational for materials characterisation, especially for high-resolution characterisation.

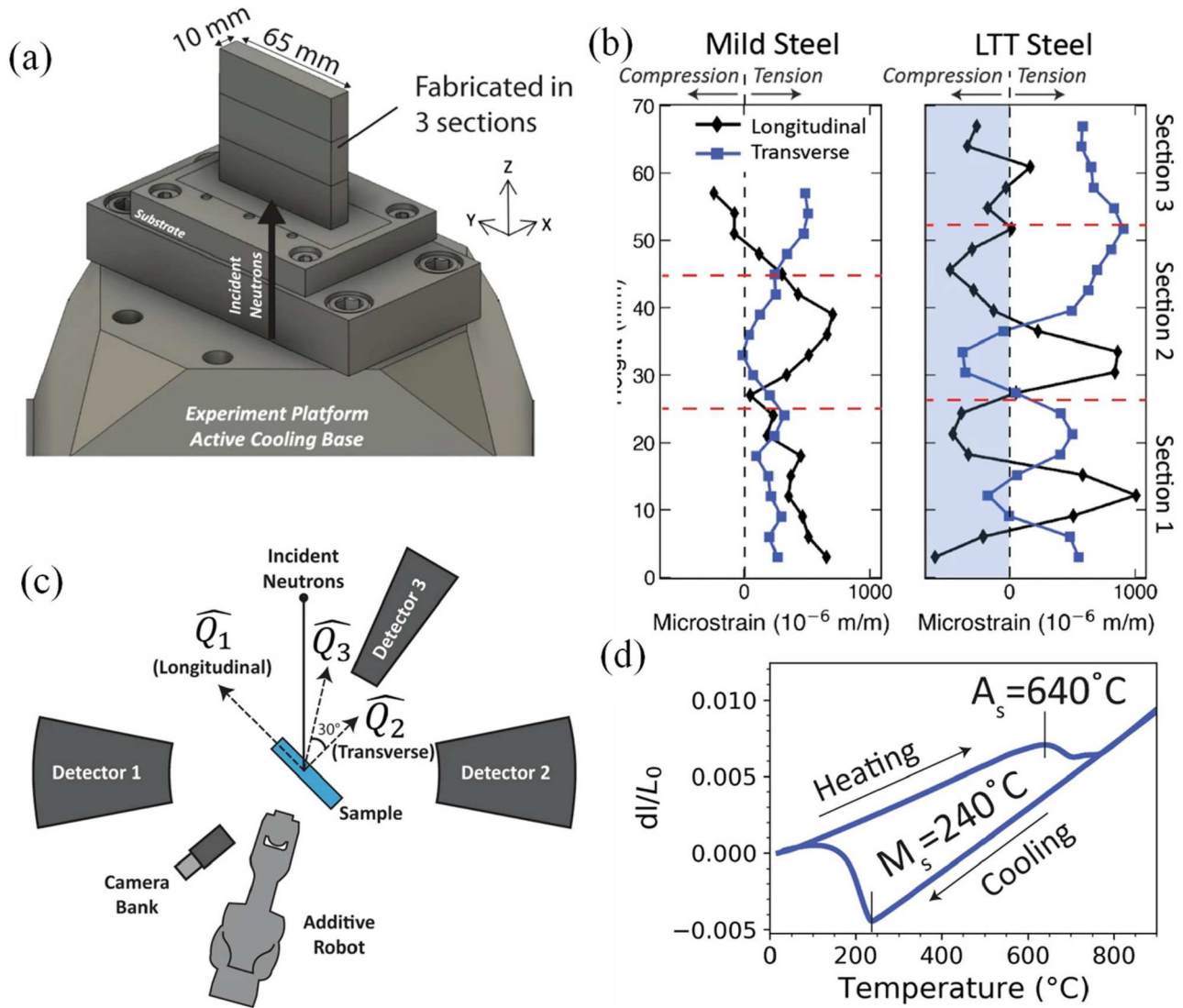


Figure 10. Schematic of the monitoring modes for obtaining 3D data. (a) *In situ* WAAM experimental setup diagram of Ex-situ neutron diffraction measurements (b) Ex-situ neutron diffraction measurements conducted at HFIR showing elastic lattice strain variations along the centreline at different heights. (c) Ex-situ neutron diffraction measurements (d) *In situ* WAAM experimental setup diagram to monitor temperature and phase transformations at different heights [64].

Offline imaging involves unloading the specimen after reaching a predetermined damage stage, followed by microstructural characterisation, and subsequent cyclic loading and unloading, for further analysis. Conversely, *in situ* imaging allows an application of load that is concurrent with structural characterisation, allowing a real-time and dynamic assessment of material damage evolution. Figure 11 illustrates the nucleation and growth of voids in the WAAM Ti6Al4 V alloy using multidimensional and multiscale correlated imaging [49]. This kind of visualisation shows the damage evolution mechanisms, and offers semiquantitative scientific support when investigating material degradation mechanisms, and constructing life prediction models.

Specifically, Figure 11 utilises multiscale structural characterisation methodology focused on a particular stage of material damage, analysing the voids' nucleation and growth, looking at the local microstructure, chemical composition, and dislocation dynamics. To monitor the progression of internal damage, prevalent methods integrate advanced light sources with offline or *in situ* high-resolution imaging techniques. For example, Xie et al. [66] employed high-resolution synchrotron radiation X-ray micro-computed tomography, to image defects in the WAAM process. This approach enabled the researchers to gather information about internal defects, and identify critical defects. The complex thermal conditions present in WAAM lead to the formation of equally complex residual stress patterns.

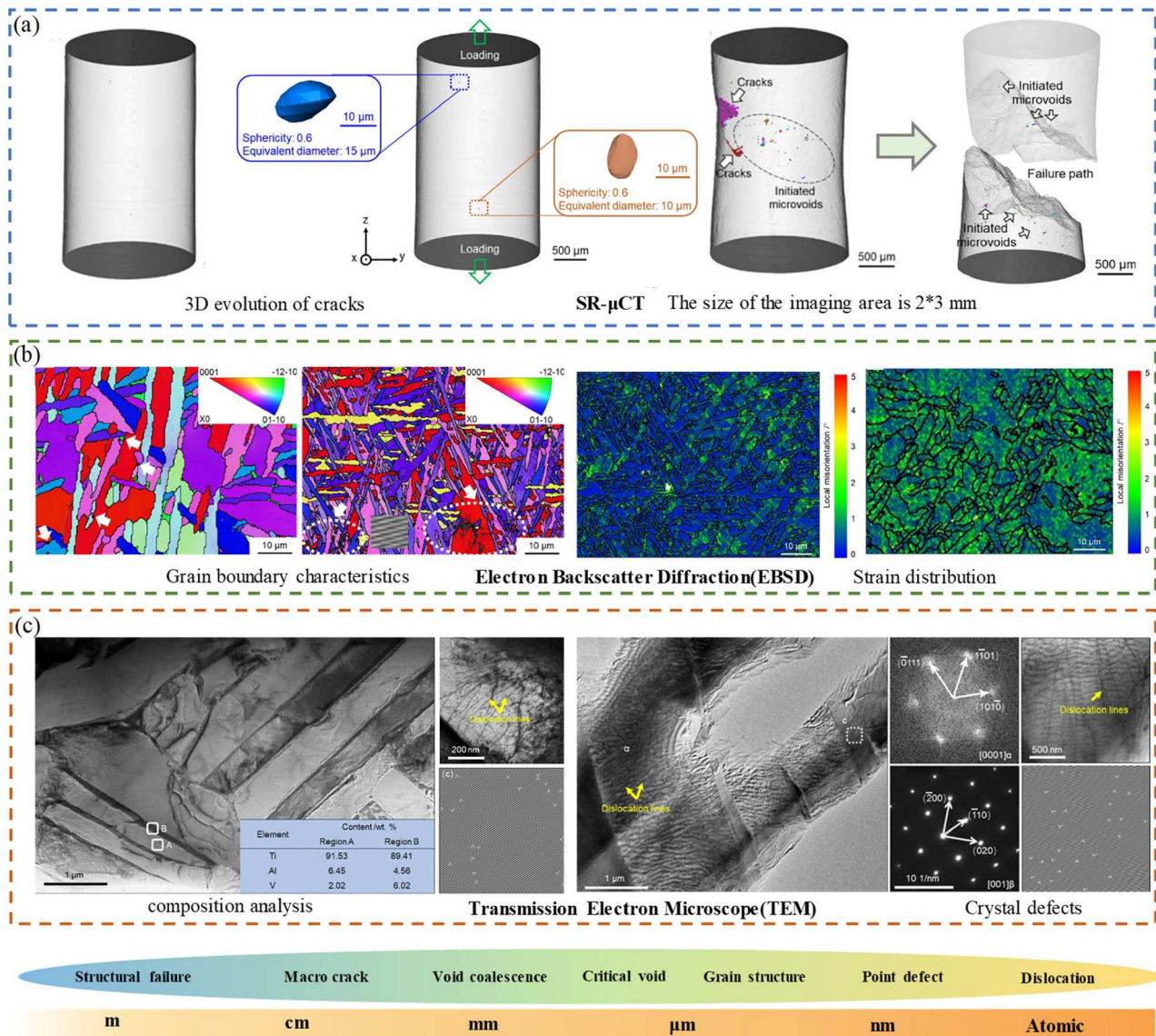


Figure 11. Multidimensional and multiscale correlated imaging characterisation of fatigue damage behaviour in WAAM Ti6Al4 V alloy [49].

In the context of damage evolution of behaviour by utilising *in situ* high-resolution tomography, it is noteworthy that the development of *in situ* mini loading devices is progressing towards incorporating a number of things and events. These include a broader spectrum of near real service conditions, (such as monotonic tension, cyclic bending, low-cycle fatigue, high-cycle fatigue, and ultra-high-cycle fatigue), more complex environments, (including ultra-high temperatures, ultra-low temperatures, corrosive atmospheres, and irradiation), and integrating functions for mechanical loading and sample environment control. This progress is driving research on material service damage in interdisciplinary and multiscale directions. At the same time, in order to understand material service damage

mechanisms, there is a continual fusion of various techniques, such as X-ray imaging and diffraction techniques, as well as neutron diffraction and imaging techniques.

Following the acquisition of the damage evolution landscape during material service, it is imperative to correlate it with mechanical and fatigue performance studies, to finally identify the multidimensional and multiscale mechanisms of near service damage failure, thereby refining fatigue damage prediction models.

3. PSPP based on physical modelling

WAAM offers extensive opportunities to meet flexible design requirements and enhance product performance.

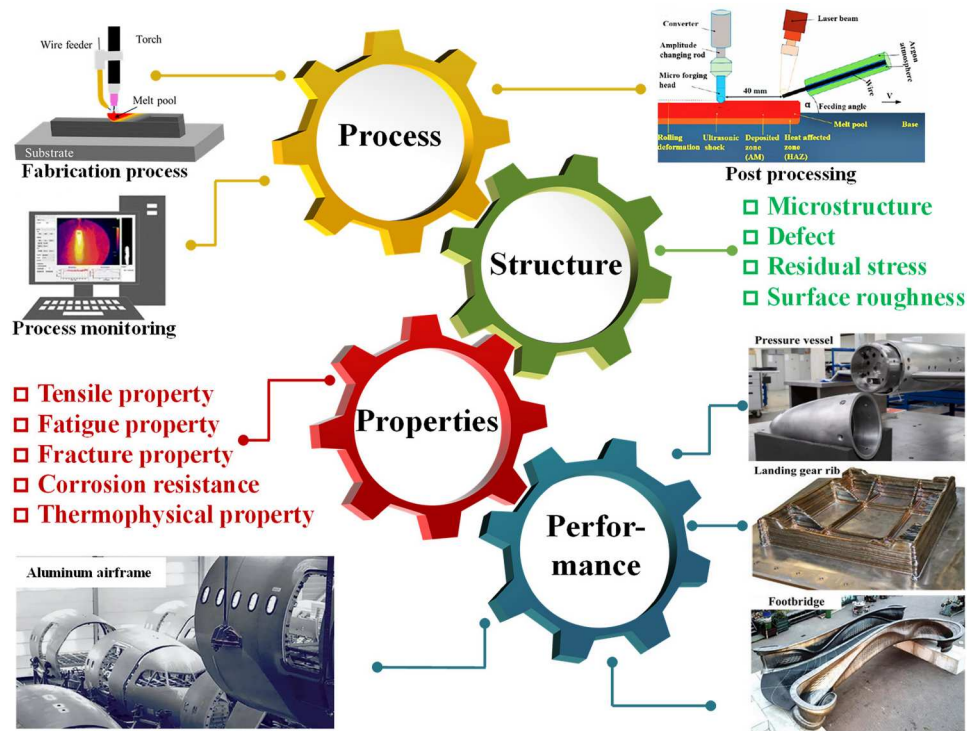


Figure 12. Schematic of the principal PSPP relationships for metallic materials produced by WAAM [18,72,73].

Despite this potential, there remains a significant lack of understanding of the dynamic and complex processes involved in WAAM, (such as microstructure formation, porosity, residual stress, and surface roughness (SR) etc.) and their impact on the service performance of the final products. This significantly hinders the widespread adoption of WAAM technology. To advance the understanding of WAAM, it is crucial to identify the PSPP relationships.

Recently, researchers have been developing multi-scale models to define PSPP relationships [41–43,47, 48,67–71], aiming to quantitatively understand AM processes. These models specifically analyse the effects of AM's distinct layer-by-layer fabrication techniques on material evolution, on both local and global scales. This analysis guides the optimisation of structural characteristics, which in turn enhances the mechanical properties and service performance of the final products. As depicted in Figure 12, both microstructure evolution and performance can be affected by the process parameters, and by the defects. Although many types of defects can be mitigated through post-process heat treatments, designing the manufacturing stages can substantially improve microstructure, and boost mechanical properties. Therefore, conventional metallurgical models continue to be valuable tool to understand some of these intricate process-structure relationships.

The fatigue performance of AM treated is influenced by four main factors: microstructure, internal defects, residual stresses, and surface roughness [74]. These factors are closely related to differences during manufacturing, so it is necessary to fully understand WAAM technology and its influence on the mechanical properties and fatigue performance of parts. In order to clarify the relationship between these factors and process parameters, some investigations usually involve exploring the interaction mechanisms between them, aiming at establishing a systematic relationship among process, structure and performance. This characterisation serves as the primary basis for selecting a numerical scheme for predicting the microstructure of final additive manufacturing materials and establishing connections between their configuration, composition, and performance, i.e. the PSPP relationship. This approach is intended to gain valuable insights and enhance the optimisation of the WAAM process, and of component design, and enables a deeper understanding of the potential relationships between material changes and manufacturing processes, thus facilitating the modelling of dynamic processes across multiple scales.

3.1. Microstructure-properties links and control

In the WAAM process, materials are built layer-by-layer, melting and depositing onto a solid substrate. This

process occurs without interfacial thermal resistance, leading to rapid thermal conduction. Consequently, non-equilibrium solidification takes place, due to high temperature gradients and rapid cooling rates. The solidification thermodynamics and kinetics become complex under such conditions. Each deposit experiences a brief but intense cycle of heating and cooling, undergoing rapid, variable-temperature transformations, that differ from what occurs in traditional manufacturing processes. This leads to a unique, multilayered, and heterogeneous microstructure, characterised by large columnar grains. Although these grains are beneficial to creep resistance at high temperature, they usually have lower strength, toughness, and corrosion resistance at normal working temperatures, compared with fine equiaxed grains [75,76].

Acquiring fine equiaxed crystals in WAAM is very challenging. The growth of these grains usually extends beyond the epitaxial growth area of the substrate, leading to a competitive environment. In the competitive environment, due to the decrease of the total number of grains, fewer but larger grains are formed. Generally, grain growth is consistent with the strongest thermal gradients. However, the lower energy density arc of WAAM produces weaker thermal gradients and slower solidification rates, which, combined with the heat dissipation capacity of the substrate, promotes the growth of large columnar grains perpendicular to the welding direction [77]. The limited mechanisms of nucleation of new grain in WAAM allow this growth to continue without restriction [78], leading to the development of poor and anisotropic mechanical properties. Consequently, achieving columnar to equiaxed transition (CET) presents a significant challenge in WAAM due to the high local heat input, and the large temperature gradients.

WAAM is similar to welding process, in that nucleation initiates at the base-metal grains located along the fusion line, that serve as a substrate. These grains then expand to the weld's centre through epitaxial growth (Figure 13(a)). The molten melt pool, which is in close contact with these base-metal grains, fully saturates them due to its complete wetting property [79]. Figure 13(b) illustrates that solidification occurs directionally, moving from the previously deposited substrate towards the molten liquid, driven by the loss of heat in the direction of the solid substrate. The barrier to heterogeneous nucleation is minimal, leading to the dominance of grain growth in shaping the final microstructures. As grains expand, solute atoms are expelled into the surrounding liquid, forming a solute-rich layer ahead of the advancing solid-liquid interface. This accumulation broadens the freezing range as

depicted in Figure 13. Consequently, constitutional supercooling, prompted by micro segregation. This supercooling occurs, coupled with the morphological stability of the solid-liquid interface, significantly affects the outcome of the rapid solidification process.

According to classical solidification theory [82], the microstructure of metal alloys during directional solidification is governed by local conditions in the melt pool, primarily the temperature gradient (G) and the solidification rate (R) (Figure 13(c)). These parameters collectively dictate the solidification microstructure. The ratio of the temperature gradient to the solidification rate (G/R) influences the grain morphology, while their product ($G \times R$) determines the cooling rate, which in turn affects the microstructure's size. With increasing subcooling, the microstructure transitions from a planar front to an equiaxed dendritic morphology. According to the classical nucleation and growth theory, the critical conditions for CET can be given by the following equations:

$$G = |\nabla T| \quad (1)$$

$$R = (1/G)(\partial T / \partial t) \quad (2)$$

$$\begin{aligned} \frac{G^n}{R} &> C_{\text{CET}} \text{Columnargrain} \\ \frac{G^n}{R} &= C_{\text{CET}} \text{Transitionline} \\ \frac{G^n}{R} &< C_{\text{CET}} \text{Equiaxedgrain} \end{aligned} \quad (3)$$

where C_{CET} is a critical value related to the undercooling at heterogeneous nucleation sites, and n is a material-dependent constant. As shown in Figure 13(d), in the lower right part of the CET diagram (when the temperature gradient is high, and $G^n/R > C_{\text{CET}}$), formation of columnar grains is favoured during solidification, which is prevalent in additive manufacturing. In WAAM, a steep thermal gradient and high cooling rate favour the formation of dendritic columnar structures. As subcooling increases, the microstructural evolution marks a morphological shift from planar fronts to isotropic dendrites [81].

Based on the above theoretical analysis, it is obvious that the change of temperature history, peak values, gradients and cooling, and curing rate, will affect the formation of microstructure. WAAM can be described at three different scales: macro, meso, and micro (see Figure 14). The phase transformations and grain growth in WAAM can be effectively predicted by combining the temperature curve generated by the macro-scale model with the transient metallurgical equation obtained by the hardenability algorithm [59–61,83–85]. However, the macro model faces challenges in

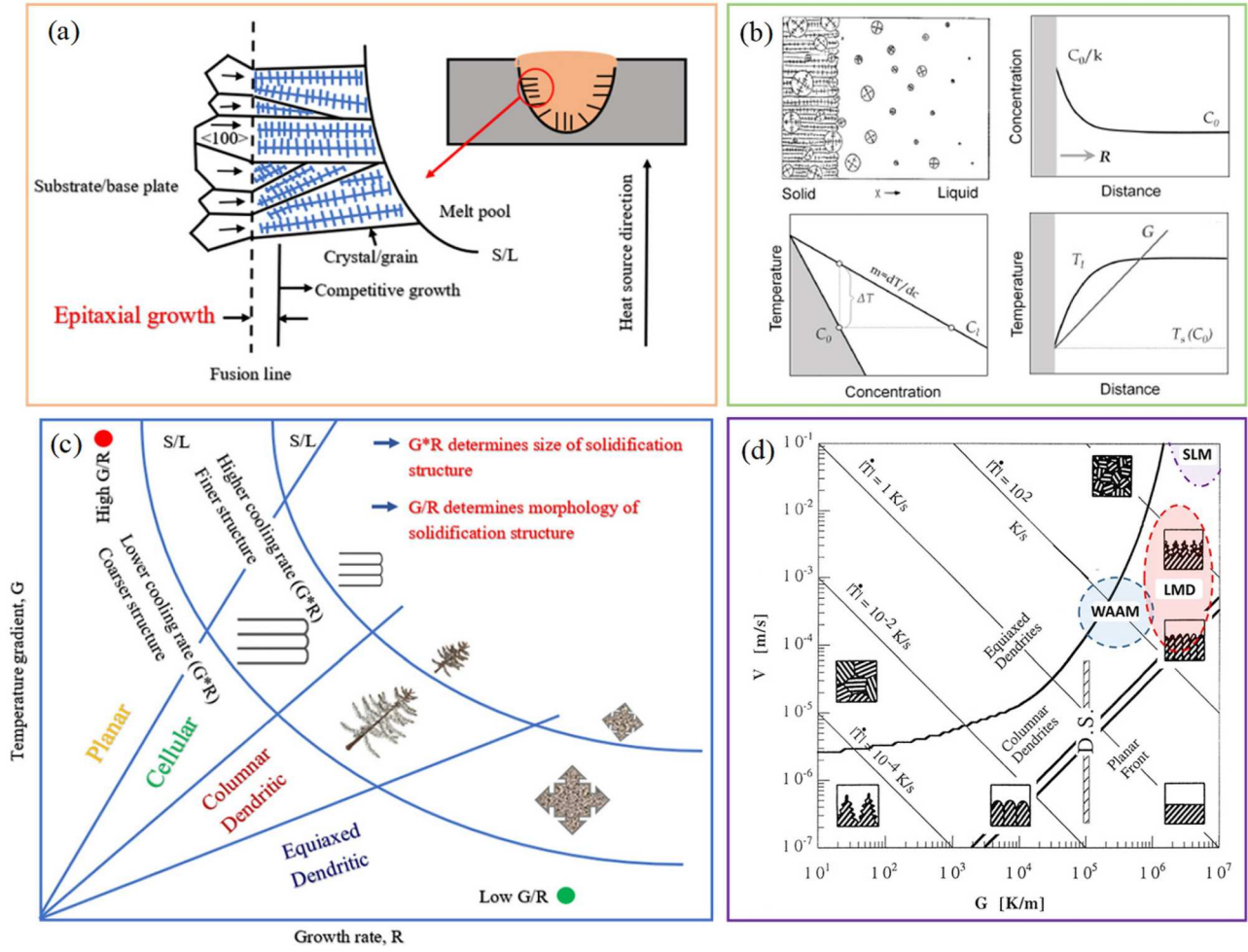


Figure 13. Schematic illustrations demonstrate the impact of growth conditions on microstructure during rapid solidification in AM processes. (a) epitaxial growth in AM process, similar to conventional welding [79]; (b) the dynamics of grain growth, solute segregation, and constitutional supercooling at the solid-liquid interface during rapid solidification processes [80]; (c) temperature gradient G and growth rate R on the morphology and size of solidification microstructure [79]; (d) the combined effect of thermal gradient and solidification rate on the microstructure of solidification [81].

accurately describing the dynamic processes of arc heat transfer and the behaviour of droplets. These phenomena require analysis at the mesoscale through a sophisticated multi-physics model that accounts for interactions among different states of matter, these being plasma, gas, liquid, and solid [62–64,86–88]. Hu and Tsai [89] developed a unified model that incorporates various phenomena, suggesting that droplet transfer and alterations in the weld pool surface both affect the transient distributions of current density, arc temperature, and arc pressure.

These parameters are often assumed to maintain constant Gaussian profiles in conventional macro-scale heat source models. To broaden the practical applicability of these complex meso-scale multi-physics models, it is essential to integrate fundamental equations that govern mass conservation (4), momentum (5), energy (6), and current continuity (7) with the actual dimensions

of the metal parts.

$$\frac{\partial \rho}{\partial t} + \nabla \cdot (\rho \mathbf{v}) = 0 \quad (4)$$

$$\rho \left(\frac{\partial \mathbf{v}}{\partial t} + \mathbf{v} \cdot \nabla \mathbf{v} \right) = -\nabla p + \mu \nabla^2 \mathbf{v} + \frac{1}{3} \mu \nabla (\nabla \cdot \mathbf{v}) + \rho \mathbf{f} \quad (5)$$

$$\rho \dot{w} = \sigma : D + \dot{q} - \nabla q \quad (6)$$

$$\nabla^2 \Phi + \Sigma = 0 \quad (7)$$

where ρ is the density, μ is the viscosity, t is the time, \mathbf{v} is the velocity vector, p is the pressure, \mathbf{f} is the internal forces (forces per unit of mass), w is the internal energy rate per unit of mass, σ is the cauchy stress tensor, D is the rate of deformation tensor, \dot{q} is the heat generation rate per unit of volume, q is the heat flux vector, Φ is the electric potential, and Σ is the electric potential source [90].

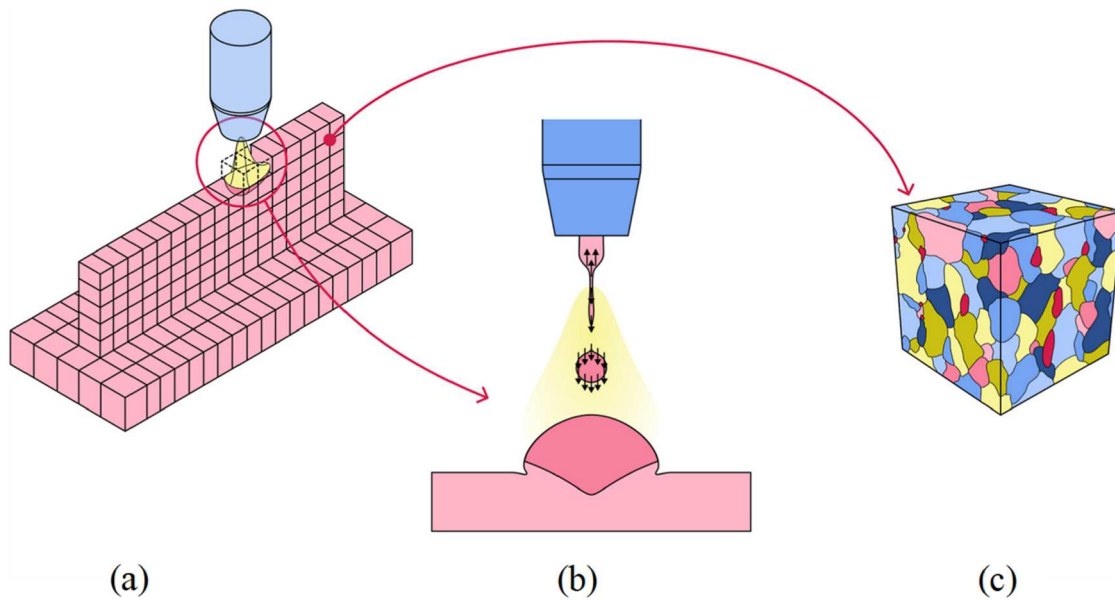


Figure 14. WAAM modelling at the three different scales: (a) macro, (b) meso and (c) micro [90].

While the mesoscale model effectively illustrates how droplet transfer and weld pool deformation influence arc characteristics, its practical application is constrained by high computational demands, and the transient nature of these phenomena. Conversely, while models provide direct simulations of metal solidification, grain growth, and phase transformations, implementing them within realistic manufacturing timescales presents significant challenges, as shown in Figure 14. In addition, randomisation methods such as the Monte Carlo method and cellular automata provide alternative approaches to checking the changes in material microstructure [91]. Wang et al. [92] proposed multi-scale experiments and modelling to reveal the physical basis of structure evolution and control, in the WAAM process. The multi-scale models are important for revealing the thermal dynamics and structural dynamics of the manufacturing processes of metal structures.

Recent advancements in WAAM have focused on enhancing the microstructure and properties of metallic materials [93,94]. Strategies that have been employed include optimising process parameters, applying high-pressure rolling, using ultrasonic shot peening, and incorporating alloying elements. The focus of some research has been on optimising process parameters to modify and enhance the microstructure, in order to achieve specific properties of the material. Peng et al. [95] enhanced homogeneity by integrating TiC particles into WAAM, eliminating columnar crystals. Wu et al. [96] refined ferrite grains in duplex stainless steels, through *in situ* alloying, controlling subcooling rates to influence grain formation. Zhuo et al. [97] explored

grain morphology in titanium alloys, comparing monolayer and multilayer deposition methods. Wang et al. [98] investigated arc mode effects on the stability and integrity of WAAM structures. In addition to traditional experimental approaches, many researchers have employed thermo-mechanical coupling models, to macroscopically describe WAAM [99,100]. These models are particularly effective in identifying and optimising process parameters.

Beyond optimising process parameters, several researchers have refined WAAM by enhancing deposition techniques to achieve targeted properties. Cai et al. [101] introduced OL-WAAM, a laser-assisted technique that refines microstructures by maintaining high laser energy densities to remelt each layer. This method, as shown in Figure 15, alters grain growth dynamics compared to conventional WAAM, introducing more nucleation sites and shifting temperature gradients dynamically due to laser oscillation effects. Zhang et al. [102] applied high-energy ultrasonication to reduce grain size and enhance mechanical properties. Gong et al. [103] tailored microstructures to achieve higher strength and reduced anisotropy. By applying specific post-processing techniques, such as heat treatment and surface finishing, the microstructure of materials is refined, and corresponding mechanical properties are enhanced. Guo et al. [104] improved the mechanical strength of commercial Al alloys, through microstructural control via WAAM machining and T6 treatment, surpassing 500 MPa in yield strength and 550 MPa in ultimate strength. It can be seen that the modulation of the microstructure can change, and

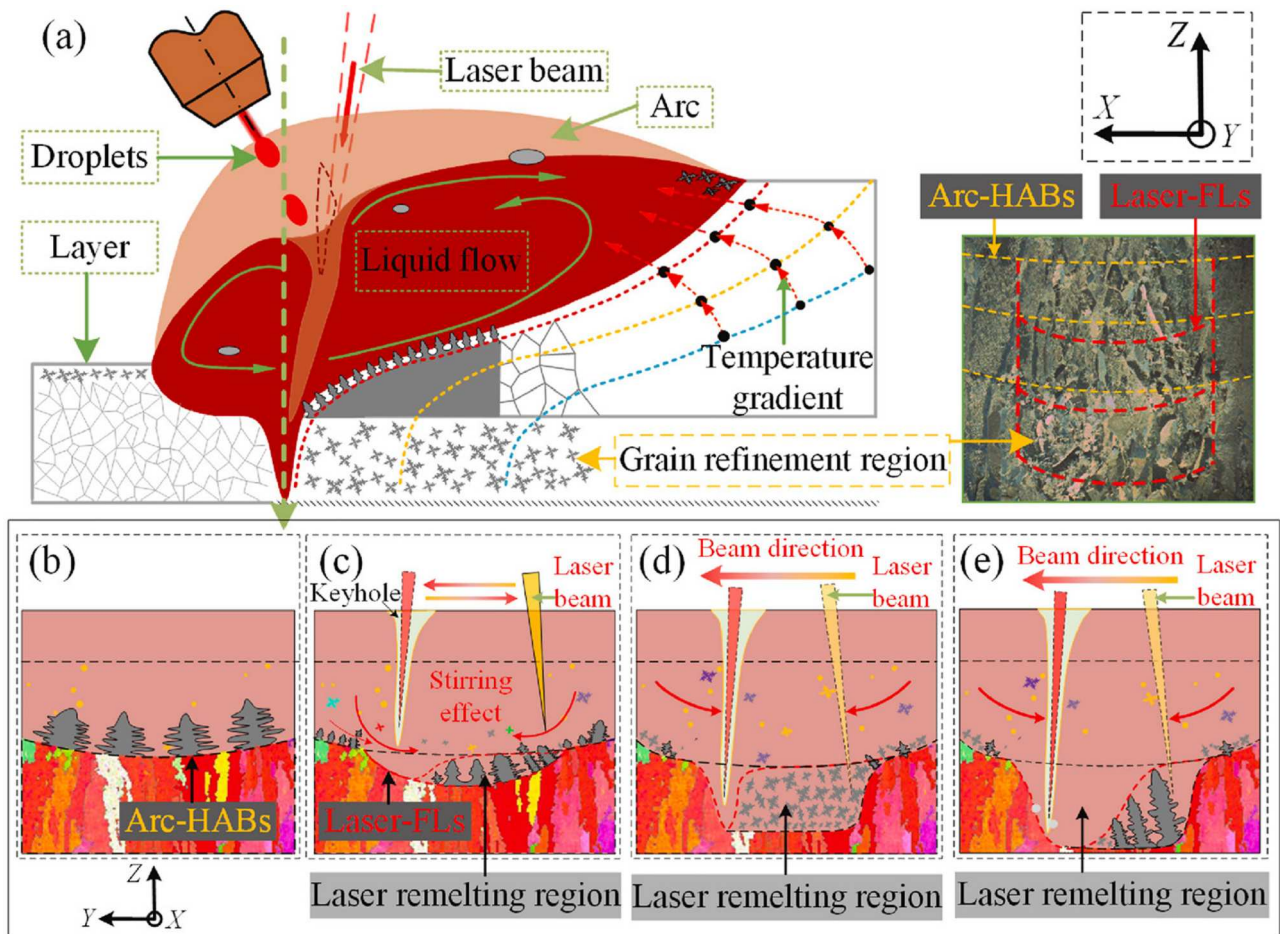


Figure 15. Schematic illustration of the flow and grain evolution in the melt pool of OL-WAAM, (a) the characteristics of grain growth. (b) 0 W (c) 1200 W (d) 1600 W (e) 2000 W [101].

potentially enhance, the mechanical properties of the material. It is not easy to analyse how microstructure continually influences mechanical properties, due to the complex and variable nature of material behaviour.

Table 1 summarises the relationships between process parameters, microstructure, and mechanical properties, for various metallic materials. Refining the microstructure of materials such as SS316L stainless steel, Al-Mg alloy, and HSLA steel, significantly enhances their strength and toughness, while reducing defects and stress concentrations. This improvement in microstructural integrity demonstrates the link between microstructure and macroscopic properties, and opens up new areas of research for material optimisation. Different microstructural morphologies, such as columnar and equiaxial crystals, impact mechanical properties by influencing the distribution of grain boundaries, phase boundaries, and dislocations. Specifically, equiaxial crystals improve ductility due to their isometric nature, whereas columnar crystals introduce anisotropy, affecting directional strength properties. Furthermore,

advanced processing techniques like optimised parameter settings, advanced rolling, and stirring friction processing can enhance WAAM, strategically guiding microstructural evolution, to significantly improve mechanical properties. The influence of thermal cycling on microstructure evolution also plays a critical role, as demonstrated by the formation of equiaxial dendrites in the top layer of AZ31 magnesium alloy during welding. This example highlights the intricate relationship between thermal cycling, microstructure, and material properties.

The corrosion resistance of additively manufactured steels is strongly influenced by their microstructure. Specifically, a uniform microstructure distribution notably enhances corrosion resistance. Austenitic phases, in particular, are more effective at reducing corrosion rates than martensitic and ferritic phases, with a dense surface further improving resistance [116]. Optimising process parameters and heat treatments can significantly enhance these properties [117]. Additionally, the performance of WAAM components under

Table 1. Microstructure and mechanical properties of metals fabricated by WAAM.

Material	Process factor	Microstructural features	Mechanical properties
SS316L [98]	Arc modes Deposition rate	Smaller secondary dendritic arm spacing	UTS 540 MPa YS 418 MPa
Ti-6Al-4 V [101]	Deposition models laser power	The prior- β grains decreases first and then increase as the laser power increases,	Vertical UTS 1322 MPa Horizontal UTS 1309 MPa
Al-Mg4.5Mn alloy [105]	<i>In situ</i> rolled	Columnar and isometric crystal composition	UTS 285.9 MPa Elongation 23.3%
SS316 [106]	Heat source	Numerous columnar dendrites extend in the direction of construction	UTS 541.50 MPa YS 506 MPa
Al-Mg alloys [107]	Heat inputs	Achieved modification columnar grain to equiaxed	UTS 249-262 MPa YS 119-141 MPa
HSLA steel [108]	Heat inputs	Mainly of pearlite and ferrite	UTS 860 - 950 MPa YS 530 - 620 MPa Fatigue 263 MPa (10^6)
AZ31Mg [109]	Heat source (CMT)	Hybrid vertical columnar dendrites and direction-changed columnar dendrites. The top layer appears as equiaxed dendrites due to columnar to equiaxed transition (CET)	Building direction UTS 210.5 ± 3.5 MPa YS 131.6 ± 4.2 MPa Travel direction UTS 151.9 ± 12.9 MPa YS 71.2 ± 4.5 MPa
Al-Si alloy [110]	travel speed of welding torch	Alpha-Al dendrites, eutectic Si particles and Fe-rich intermetallic compounds	UTS 205.6 MPa YS 98.0 MPa
Nickel-aluminium bronze [111]	Deposition tracks	Consisted of an α -Cu phase (light area), a β' phase (dark area), and intermetallic κ phases mainly composed of Fe	WAAM-NAB has better corrosion resistance than cast alloys in artificial seawater.
High strength steel [112]	Deposition strategy cooling rates	Displayed a mixture of acicular ferrite, bainite and martensite phases	/
5183Al [113]	Deposition dimensions	Equiaxed grains are dominant	74.98 ± 2.70 HV0.2 UTS 265.05 - 278.43 MPa YS 156 - 169 MPa
2219Al [114]	WAAM + interlayer Friction stirs (FSP)	Coarse eutectic phases were broken and dissolved into the α -Al matrix	UTS 277 MPa YS 143 MPa Ultimate fatigue strength 139 MPa
AWS ER100S-G steel [115]	Heat source (GMAW)	High amounts of acicular ferrite (AF), some pro-eutectoid ferrite (PF)	VHCF 390 MPa at 109 cycles

high temperatures warrants attention. The strength and stability of materials at elevated temperatures are critical factors in assessing their high-temperature mechanical properties. Appropriate heat treatment processes, such as solid solution treatment and aging, not only reduce residual stresses and refine grain structure, but also improve creep resistance [118]. These improvements are essential for enhancing the mechanical properties of WAAM components in high-temperature environments.

In summary, the intricate correlation between processing, structure, and properties forms the cornerstone of strategies aimed at material modification and performance enhancement. In order to optimise the grain structure with AM, it is necessary to control the shape by refining the grain size, so as to improve the mechanical properties of the produced components. AM parts generally exhibit inhomogeneity, leading to minimal directional dependence in their macro-mechanical properties. This effect provides a microstructure basis for developing multi-scale theoretical models. Typically, controlling and optimising grain structure involves creating equiaxed fine grains to improve both strength and ductility. However, the work hardening process leads to recrystallisation, and it is not suitable for AM.

Therefore, it is still challenging to establish a practical method to refine grain structure, in order to quantitatively enhance mechanical properties.

3.2. Defects-fatigue performance relationship

In the WAAM process, numerous factors, such as heat source parameters, scanning parameters, material composition, and part structure, significantly influence the quality of the final components. These factors lead to defects that are characterised by their broad distribution, diverse forms, wide size range, and complex origins. These defects critically reduce the fatigue strength of the components, and lead to greater variability in their fatigue life. Thus, understanding the mechanisms of defect formation in WAAM is essential. Minimising these defects and precisely predicting their impact on fatigue performance can guide the optimisation of process parameters, which in turn, enhances the reliability and applicability of additive components in engineering applications.

WAAM technology involves a multi-physical field interface process, where the complex, transient, and unbalanced physical, chemical, and metallurgical characteristics are susceptible to unsuitable process

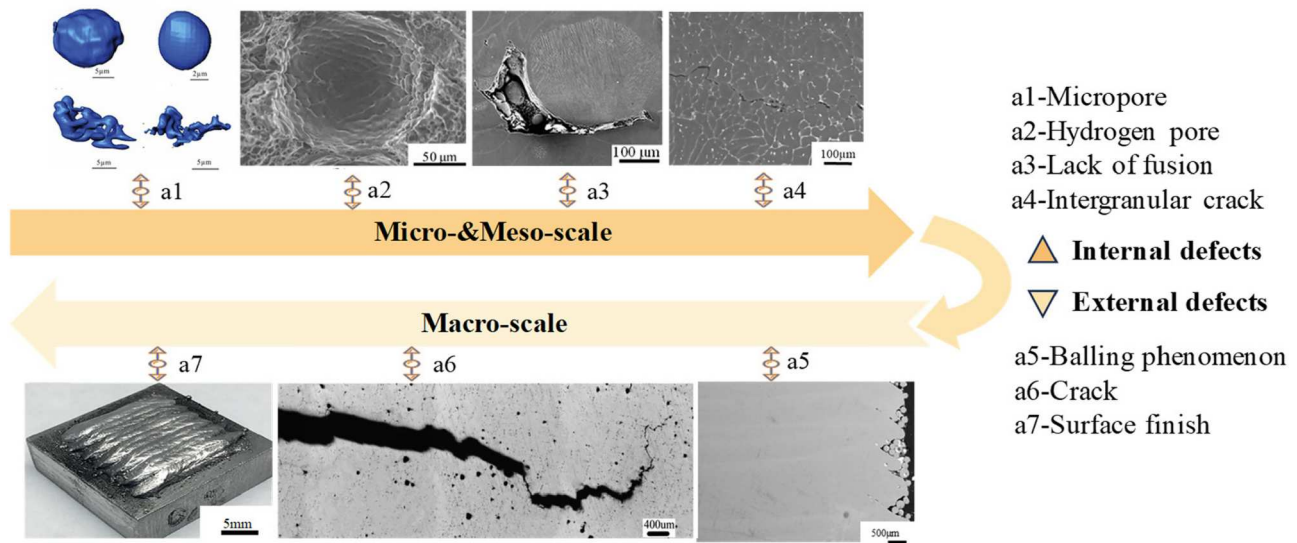


Figure 16. Various defects in WAAM metal, including internal pores and cracks, and external issues like balling, surface finish, and crack [119–123].

parameters. Changes in processing conditions during the manufacturing of components can lead to the development of internal defects. Moreover, the entrapment of impurities in the AM process can result in defect formation, thereby weakening the mechanical properties of components. Figure 16 shows that WAAM metal often exhibits various defects, such as internal issues including pores and intergranular cracks, alongside external problems like balling, surface finish, and cracks [119–123]. To achieve high-quality AM products, an in-depth understanding of the mechanisms of defect formation is required, along with strict control over process parameters to minimise the occurrence and development of defects.

One of the most critical defects influencing the quality of WAAM process parts is porosity, particularly in relation to internal porosity and fluid properties [124]. Figure 17, adapted from Yi et al. [125], provides a detailed analysis of the key factors influencing porosity in WAAM technology. These factors encompass various arc operation modes and adjustments in process parameters, including the settings of welding current and voltage, wire feed rate, and the speed of the welding head's movement. Furthermore, the selection of an appropriate shielding gas and its resultant atmosphere also play a crucial role in determining porosity levels. These internal porosities are commonly influenced by stirring, shrinkage, and partial dissipation within the melt pool [126]. As a result of alterations in pressure and solubility, minute pores will emerge and coalesce to form larger pores. These pores can be categorised according to their morphology, into two main types: Spherical ones, and irregularly shaped fusionless ones

[127]. Alternatively, they can be classified according to the formation mechanism, with raw material-induced pores, and process-introduced pores [128]. It is not uncommon for gaps or voids to be observed during complex deposition processes or sharp changes in the temperature field, particularly when insufficient sputtering or melting has occurred. The resulting pores are often irregularly shaped [10]. Furthermore, contaminants on the surfaces of wires and substrates, such as moisture, dirt, grease, and hydrocarbons, are difficult to eliminate completely. These contaminants can be

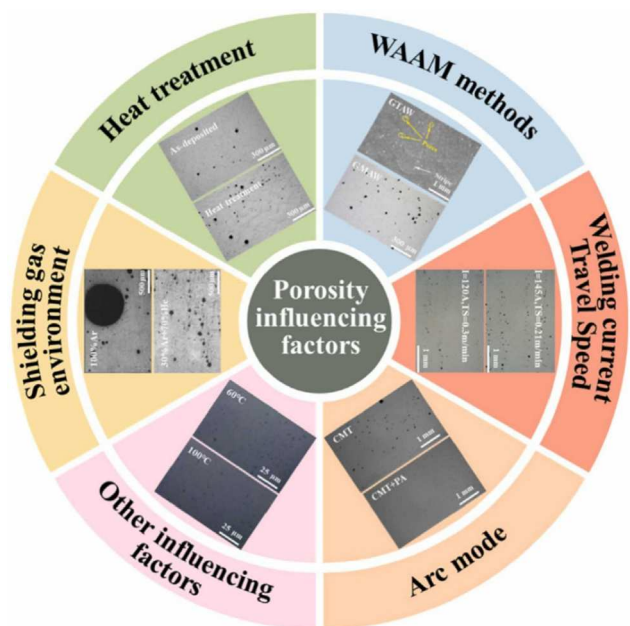


Figure 17. Porosity influencing factors of WAAM [125].

easily ingested by the melt pool, where they absorb energy during the deposition process and contribute to pore formation upon solidification [129]. Therefore, it can be concluded that ensuring the cleanliness of the raw materials is of utmost importance.

Researchers have strategically implemented a variety of techniques to minimise or eradicate porosity in aluminium alloy components during WAAM processes [125]. Innovative methods such as hybrid laser-arc additive manufacturing [125], ultrasonic vibration-assisted processes [130], and the application of external magnetic fields have proven effective in reducing porosity [41]. Cong et al. found that the critical factors that enable the WAAM process to control the porosity efficiently are the low heat input, a fine equiaxed grain structure and effective oxide cleaning of the wire [131]. Additionally, Romali Biswal et al. clarified that the porosity level has a significant impact on the fatigue behaviour of WAAM Ti-6Al-4 V structural components [132].

Defects resulting from processes such as lack of fusion (LOF), can diminish the fatigue strength and lifespan of AM materials. Lack of fusion defects typically have a flat, elongated shape and may evolve into sharp notches or even crack-like defects. The appearance of crack-like defects may also be attributed to the distribution of low melting point second phases along grain boundaries during subsequent deposition, and the thermal effects of tensile stresses. This can result in a significant deterioration of mechanical properties, with the potential for direct component failure [133]. Seow et al. [134] note that the orientation of crack-like defects influences the alloy's apparent fracture toughness. Consequently, orientation dependence should be a primary concern at each stage of characterising WAAM materials. Furthermore, the implications of orientation-dependent fracture properties on the assessment of structural integrity merit careful consideration.

Figure 18 illustrates the stress distribution nephogram around real pores and unfused defects in Al-Mg4.5Mn alloy, that was, manufactured using micro-area *in situ* forging and composite arc fuse additive [66]. In Figure 18(a), the stress concentration of lack of fusion defects is primarily located at sharp geometric transitions on the defect contour, with a stress concentration factor (K_t) of 1.92, which is greater than that of the porosity defects ($K_t=0.77$) in Figure 18(b). Stress concentration generated by porosity is relatively evenly distributed at the defect's edge perpendicular to the loading direction and passing through the central plane of the defect. In summary, it can be seen that defect with larger size and complex morphology near the material surface, have higher degrees of stress concentration, with the most critical areas being potential fatigue crack nucleation points [135]. Consequently, defects with higher stress concentration factors cause greater levels of risk.

The presence of sinkholes can diminish the fatigue strength of additive components and increase the variability in fatigue life. Establishing a direct mapping relationship between defect parameters and fatigue performance remains a central challenge in the field of additive manufacturing. Therefore, the priority is to minimise internal defects as much as possible and accurately predict the fatigue performance that results from these defects.

Macroscopically, the fatigue limit represents the maximum stress amplitude at which the material will endure infinite cycles without failure. On a microscopic scale, it corresponds to the critical stress for short crack propagation. In this context, fatigue crack initiation and short crack propagation are permissible when the external load remains below the fatigue limit. However, the short crack halts its propagation before extending into a long crack, forming a non-propagating crack. Considering non-propagating cracks, Murakami

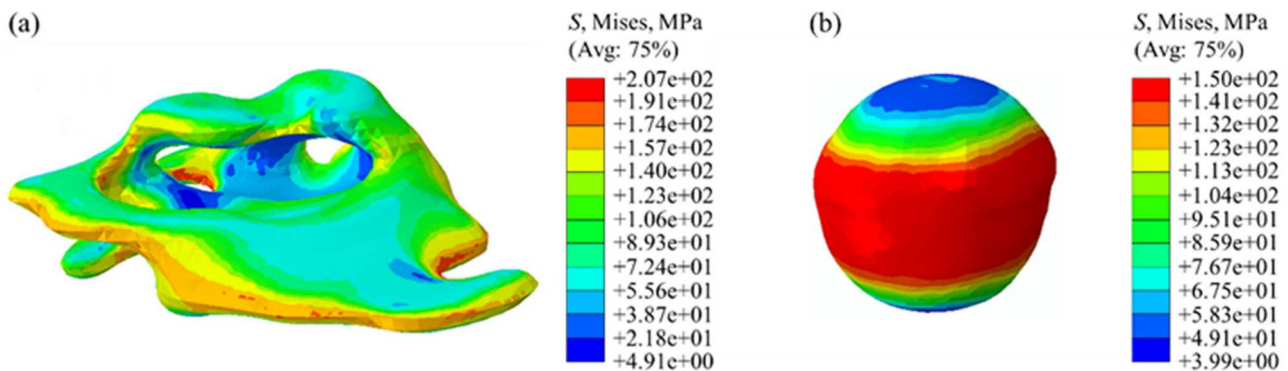


Figure 18. Mises stress distribution nephogram around defects in Al-Mg 4.5 Mn alloy produced through WAAM is described as follows: (a) lack of fusion; (b) porosity defects [66].

proposed the popular Murakami model, to quantify the impact of small-sized defects ($< 1000 \mu\text{m}$) on fatigue strength, based on the concept of defect tolerance [136]. The process of establishing the Murakami model can be described as follows:

In the Danninger-Weiss model, the long crack extension threshold $\Delta K_{\text{th,L}}$ combines the effects of defect location, size and material hardness. When the stress ratio $R = -1$, the expression for $\Delta K_{\text{th,L}}$ can be given by

$$K_{\text{th}} = g \cdot (HV + 120) \cdot [(\text{area})^{1/2}]^{1/3} \quad (8)$$

where g is the geometric correction factor characterising the location of the defect, $g = 3.3 \times 10^{-3}$ for surface defects and $g = 2.77 \times 10^{-3}$ for near-surface or internal defects; HV is the Vickers hardness of the material.

The stress intensity factor amplitude ΔK corresponding to small-sized defects ($< 1000 \mu\text{m}$) in the trap tolerance design is

$$K = Y \cdot \sigma \cdot \sqrt{\pi \cdot (\text{area})^{1/2}} \quad (9)$$

where $\Delta\sigma$ is the stress range, and Y is defined as with g . For surface defects, $Y = 0.65$, and for near-surface or internal defects, $Y = 0.5$.

The fatigue limit σ_w of the material is obtained by considering Eqs. (8) and (9) such that $\Delta K = \Delta K_{\text{th,L}}$. It is important to note that Eq. (8) is obtained for a stress ratio $R = -1$, and therefore, σ_w is the fatigue limit only at $R = -1$. In order to consider the effect of the stress ratio and solve for the material fatigue limit $\sigma_w(R)$ at any stress ratio R , the Walker factor $[(1-R)/2]^\gamma$ is introduced [137]:

$$\sigma_w(R) = \frac{C \cdot (HV + 120)}{[(\text{area})^{1/2}]^{1/6}} \left(\frac{1-R}{2} \right)^{-\gamma} \quad (10)$$

where C is the geometric correction factor, indicating the effect of defect location (surface defects, $C = 1.41$; near-surface defects, $C = 1.43$; and internal defects, $C = 1.56$), the exponent γ in the Walker factor depends on the type of material, and the Vickers hardness is satisfied when $\gamma = 0.226 + HV \times 10^{-4}$.

Eq. (10) is a form of the Murakami model, which delineates the relationship between a material's fatigue limit, and the size, location, and hardness of defects. This model defines the fatigue limit from a microscopic perspective as a non-propagating crack and has been extensively applied in evaluating the fatigue strength of materials containing different types of defects.

In order to accurately evaluate the influence of defects on the fatigue strength of materials, Japanese scholars Kitagawa and Takahashi put forward the famous Kitagawa-Takahashi (KT) diagram by combining nominal stress and fracture mechanics [138]. The

engineering significance of the KT diagram is that it combines the traditional nominal stress with the advanced damage tolerance, to evaluate the fatigue strength of the defect, including material fatigue strength, so as to achieve reliable evaluation. With the application and development of the classic KT diagram in relation to materials with defects, scholars have proposed a series of improved KT diagrams, the best known of which is the El-Haddad Model [139]. The El-Haddad model considers the influence of short cracks on the standard KT diagram, and introduces the intrinsic defect size $(\text{area}_0)^{1/2}$, to the original defect size $(\text{area})^{1/2}$ to be corrected. The mathematical expression of $(\text{area}_0)^{1/2}$ is as follows:

$$\sqrt{\text{area}_0} = \frac{1}{\pi} \left(\frac{K_{\text{th,L}}}{Y\sigma_0} \right)^2 \quad (11)$$

where $\Delta\sigma_0$ is the range of fatigue limits for defect-free materials.

The El-Haddad model replaces the $(\text{area})^{1/2}$ term in the traditional KT model with $(\text{area})^{1/2} + (\text{area}_0)^{1/2}$:

$$\sigma_e = \frac{K_{\text{th,L}}}{Y \sqrt{\pi (\sqrt{\text{area}} + \sqrt{\text{area}_0})}} \quad (12)$$

Introducing the intrinsic defect size $(\text{area}_0)^{1/2}$ transforms the horizontal line of the standard KT diagram into a smooth transition from the stress control zone to the threshold control zone. Consequently, the safety zone area decreases, reflecting a more conservative assessment of members capable of prolonged and safe service. In the El-Haddad model, the impact of $(\text{area}_0)^{1/2}$ can be disregarded only when the detected defect size significantly surpasses the intrinsic defect size, indicated by $(\text{area})^{1/2} \gg (\text{area}_0)^{1/2}$. Under such conditions, the calculation results of both the standard KT model and the El-Haddad model align closely.

In both the standard KT diagram and the El-Haddad model, the predicted results show a gradual decrease in fatigue strength with increasing defect size, in the larger defect size interval, which is consistent with the related research and engineering applications.

Figure 19 shows that components with pores exhibit lower fatigue strength and ductility, with porous specimens showing a 33% lower fatigue life, compared to defect-free specimens. The modified KT diagram, critical for calculating the threshold for crack initiation due to pores, assists in predicting fatigue limits for components with varying pore sizes. At the upper limit of this diagram, the fatigue limit for nearly defect-free materials with minimal defect size impact is established. As defect size increases, a corresponding decrease in fatigue strength is seen, where stress intensity factor amplitudes

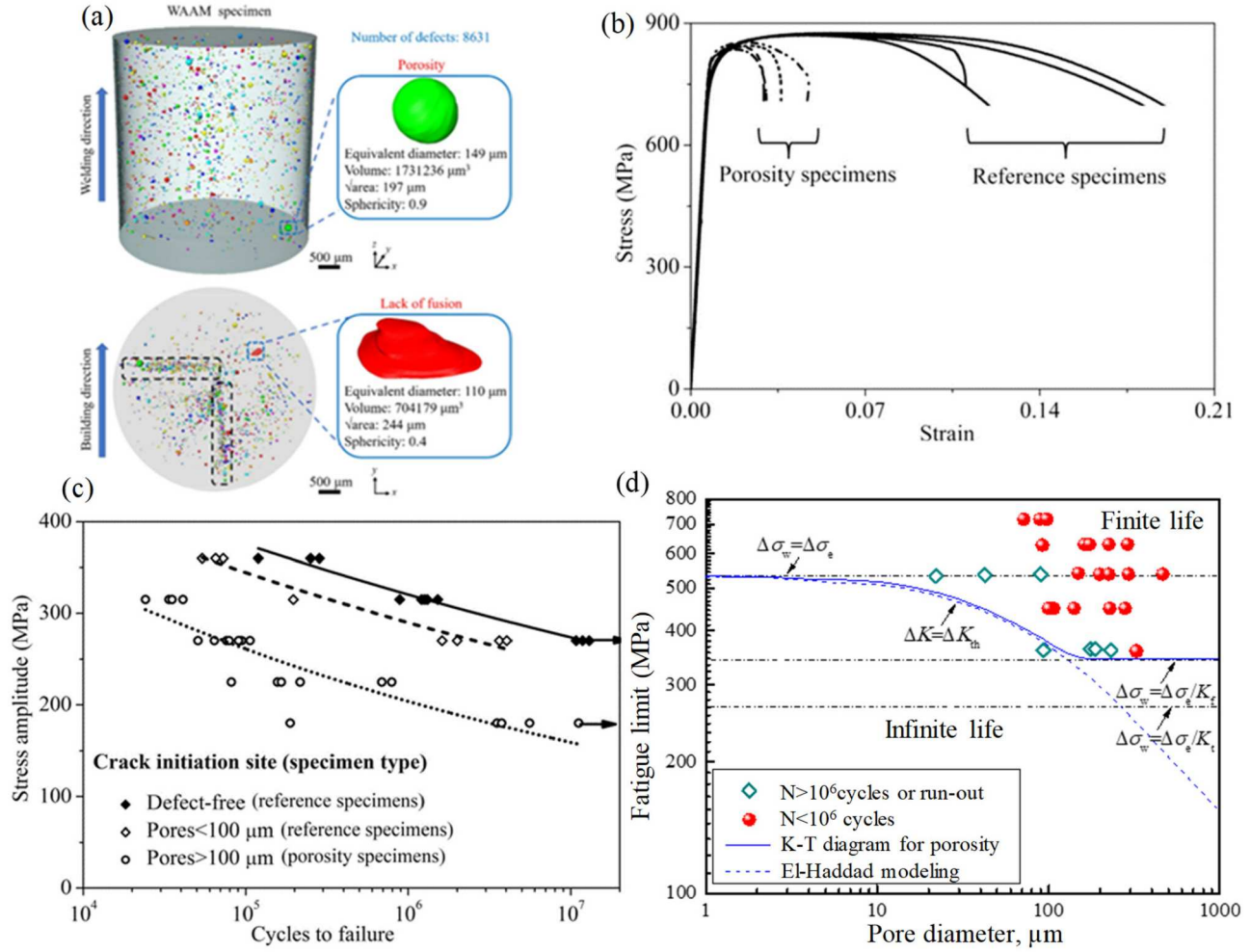


Figure 19. Typical impacts of porosity defects on mechanical properties of WAAM parts. (a) Defect characterisation (b) stress-strain relationships for tensile tests of reference specimens (solid lines) and porosity specimens (dashed lines); (c) three distinct S-N curves were identified depending on the crack initiation site and pore size; (d) calculated fatigue strength limit (solid line) for WAAM Ti-6Al-4V as a function of porosity diameter [66,132].

meet the threshold for long crack extension, as per linear elastic fracture mechanics. The lower limit of the fatigue strength reduction range in the KT diagram considers the notch effect, defined by the fatigue limit range $\Delta\sigma_e$ of smooth specimens and the stress concentration coefficients KT or Kf, as detailed in Figure 19(d). Biswal et al. [132] described the relationship between porosity levels and fatigue performance in WAAM Ti-6Al-4V components, highlighting its implications for optimising fatigue behaviour.

The adoption of process parameter optimisation and post-heat treatment can only serve to reduce the level of defects to a certain extent. These manufacturing defects, which are not easily avoided, act as a source of stress concentration, and induce fatigue crack nucleation, leading to a significant degradation of fatigue performance, and reduction in fatigue life. Cong et al. [131] concluded that unevenly distributed microstructure and

internal defects determine the fatigue performance of WAAM processed metallic materials. Wu et al. [140] and Hu et al. [127] accurately obtained the geometric parameters of defects using SR-µCT, and further proposed a modified three-parameter Kitagawa-Takahashi diagram, to relate critical defects to the applied stresses and fatigue life.

Defects can be considered as one of the important factors controlling the mechanical properties and fatigue performance of WAAM metals. Therefore, the influence of metallurgical defects on the mechanical properties of defective materials cannot be ignored. To accurately and effectively assess the service performance of WAAM alloys and quantitatively describe the relationship between geometric defect parameters and material fatigue performance, it is essential to establish the PSPP relationship based on process parameters. This involves considering defect characteristics such as

size, location, and morphology to evaluate the material's defect tolerance.

Internal defects are the main technical problem that WAAM metal parts must overcome, to be put into service. Quantitatively relating internal defects, including size, morphology, location, and quantity, to basic mechanics and fatigue performance, is a critical and ongoing research topic. In addition, this analysis informs structural design and technological processes, facilitating the development of mapping models that connect process, structure, and performance with shape control.

3.3. Residual stress formation and effects

AM undergoes a process of rapid local melting and rapid solidification of the surface material, accompanied by some degree of re-melting of the subsurface matrix. The inhomogeneous plastic deformation caused by the melting-solidification-remelting thermal cycle is the main source of residual stress in AM [141]. Debroy et al. [86] described three key factors: (1) spatial temperature gradients due to local heating and cooling of a moving heat source; (2) thermal expansion and contraction due to multiple heating and cooling; and (3) plastic and flow stresses. Figure 20 shows a representative residual stress profile and the subsequent deformation observed during the WAAM process [142]. In the WAAM-based manufacturing process, it is evident that excessive energy input, high deposition rates, and large temperature gradients typically induce residual tensile stresses in the top, bottom, and surface regions of the additive components. These stresses significantly reduce the resistance to fatigue crack nucleation and growth, thereby degrading mechanical properties, and shortening the fatigue life of the components. Therefore, it is particularly important to control and minimise residual stresses.

The selection of process parameters and residual stresses are intimately intertwined. Wu et al. [143] conducted an investigation to reveal the influence of three deposition patterns on the residual stresses and distortion, in multi-layer WAAM components made of Ti-6Al-4 V and Inconel 718. Further, Huang et al. [144] investigated the mechanism of residual stress formation at the top of the deposited layer, by studying the distribution of thermal stresses and welding deformation. It was observed that residual stresses appeared at the top of the deposited layer during the WAAM process, and increased and then decreased with the increase in the number of layers. Recognising this effect is essential in understanding the residual stress associated with WAAM process. The effects of processing conditions, such as substrate thickness, interlayer temperature, and deposition height, on the magnitude and distribution of residual stresses, were investigated by Derekar et al. [145]. With optimal process parameters, these residual stresses can be effectively minimised, particularly in large-scale metal fabrication. Residual stress control can be achieved by optimising deposition paths, substrate preheating, dwell times, plate rolling, and post-process heat treatments [80–84,146–150], which typically involve extensive and costly experimentation.

Theoretically, the evolution of residual stresses in WAAM can also be simulated using computational software, in a manner similar to the modelling of welding processes. As an alternative to experiments, it is possible to determine most of the physical fields, while balancing computational costs, to quickly and cheaply study the development of, and prevention of residual stresses in WAAM. Mughal et al. [151], Kumar et al. [152], Sun et al. [153], and Abusalma et al. [154], developed a finite element model, to simulate the evolution and distribution of thermal stresses during the WAAM process. Through experimental and simulation methods, the

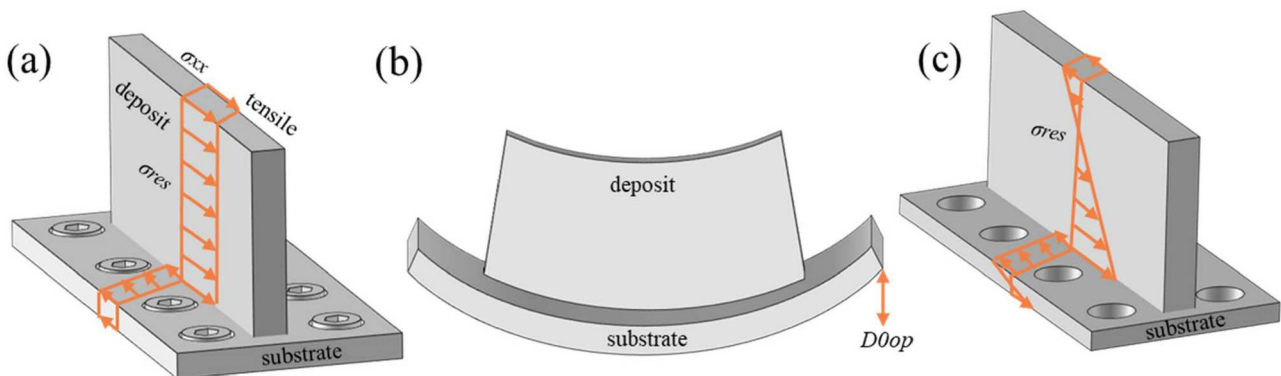


Figure 20. Typical residual stress profiles in WAAM and consequent distortion: (a) clamped residual stress profile; (b) out-of-plane distortion after unclamping; (c) redistributed and balanced residual stress profile after unclamping [142].

effects of different process parameters on residual stress have been studied, and many stress prevention methods have been proposed based on the principle of reducing the shrinkage difference between different parts, after solidification and cooling of the molten metal. This indicates that numerical simulations may offer a more comprehensive understanding of WAAM residual stress distributions.

Residual stresses in the deposition state of parts vary significantly in all directions due to the anisotropy of the fabricated parts. Feng et al. [155] numerically simulated the temperature field, stress field, and deformation during the WAAM process, revealing that both the inter-layer temperature and substrate thickness significantly influence residual stress distribution. Specifically, lower interlayer temperatures and thinner substrates can be effective in reducing tensile residual stresses. In another study, Fan et al. [156] developed a finite element model, to analyse the impact of cooling gas on the stress and deformation of WAAM parts. Their findings demonstrate that using a cooling source can significantly reduce longitudinal stress levels in the deposited layers. Moreover, Yang et al. [157] introduced a novel time-accelerated strategy for predicting residual stresses and deformations in WAAM, employing a semi-analytical method that separates the temperature into analytical and complementary fields. The numerical simulations have proven particularly effective in managing the complex thermodynamic and mechanical interactions during the fabrication of large metal parts, highlighting how the thermo-mechanical behaviour of parts is influenced by residual stresses [158].

To gain a deeper understanding of how process parameters affect residual stresses and deformation, some studies have focused on single-layer or single-pass scanning simulations, ignoring the stress accumulation effect of layer-by-layer stacking. Considering the multiscale nature of the AM process, Li et al. [159] developed an effective modelling approach. They derived an equivalent heat source from a microscale laser scanning model and integrated it into a mesoscale 'layer-by-layer deposition' model, to construct a comprehensive macroscale model. As shown in Figure 21, the method was shown to rapidly predict residual stresses and deformation of the component. In addition, new modelling techniques have emerged to reduce the computational time of multilayer forming simulations, such as selective cell activation [160] and dynamic mesh coarsening/refinement [161, 162].

It is widely acknowledged that residual stresses and deformations represent a significant challenge for the WAAM process. These factors not only affect part tolerances but can also lead to premature failure. Therefore,

the effective detection of residual stresses and the implementation of preventive optimisation during the WAAM process are crucial for achieving high precision and fast calculation for future large-scale WAAM components.

3.4. Surface roughness effects and evaluation

Although one of the advantages of AM is the ability to produce components with a near-net shape, the process of layer-by-layer melting and deposition, results in the surface of the material having a number of defect characteristics. These include spherical adhesion on the surface, localised depressions, uneven surfaces, asymmetric defects on the upper and lower surfaces, and a higher degree of roughness of the surface than that of traditional manufacturing methods. Surface roughness can affect the performance and functionality of the material or the component. A rough surface is a common source of stress concentration, which promotes fatigue crack initiation, significantly reducing the fatigue strength and life. Additionally, it compromises the material's resistance to abrasion and corrosion.

The surface roughness of as-deposited materials may be affected by a range of processing parameters, including the filler wire, shielding gas, travel speed (TS), wire feed speed (WFS), ratio of WFS to TS, heat accumulation, and solidification time [90–92, 163–165]. Qiu et al. [166] demonstrated the efficacy of Magnetic Arc Oscillation (MAO) in enhancing the surface finish of WAAM-fabricated materials. Li et al. [167] depicted that ultrasonic nanocrystalline surface modification treatment results in a reduction of surface roughness, accompanied by an increase in surface hardness of approximately 100%. To address issues related to poor material surface quality, a diverse range of surface post-treatments can be applied to AM metal parts [168], as shown in Figure 22.

It can be clearly found from Figure 22 that various post-treatment methods are available to improve surface roughness in arc additive manufacturing. The choice of method depends on several factors, including the material, shape, size, and desired surface quality of the part. In practice, it is essential to comprehensively evaluate the advantages and disadvantages of each method based on specific circumstances to select the most suitable technique for enhancing the surface quality of the parts.

In the field of WAAM, surface treatment technologies are pivotal in enhancing the surface finish of components. These technologies can significantly reduce surface roughness, thereby enhancing critical properties such as wear resistance, fatigue strength, and corrosion

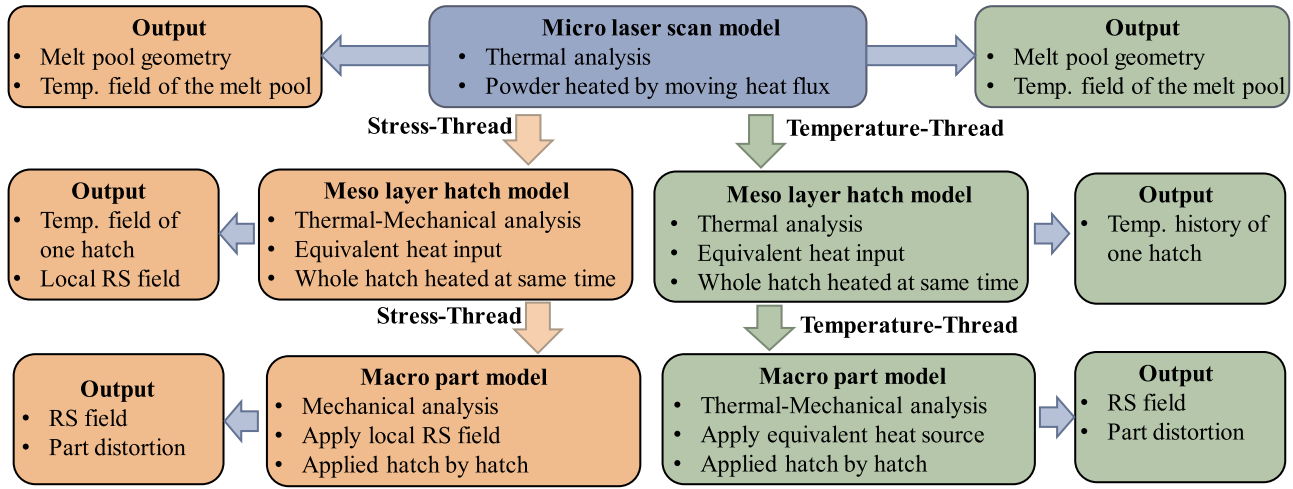


Figure 21. Finite element modelling and simplified computational approaches for residual stress prediction in AM components: a multiscale simulation modelling approach [159].

resistance [169]. Table 2 shows the impact of various surface treatment techniques on improving the surface roughness of parts fabricated using WAAM.

In general, any measures to reduce the surface roughness or internal defects of the part will have a positive impact on fatigue life [136]. SR is usually encountered in the form of a surface notch or defect, and it often becomes the source that initiates a fatigue crack. The geometric characteristics of a notch or defect have significant influence on the duration of the crack initiation stage of fatigue. For high-cycle fatigue, the crack initiation stage accounts for a high proportion of fatigue life, so it is considered that surface roughness

has a significant influence on high-cycle fatigue dominated by elastic strain. However, surface roughness has little effect on low cycle fatigue with high plastic deformation. The strain-life curve of low cycle fatigue is usually described by the Manson-Coffin formula [175]:

$$\varepsilon_a = \varepsilon_{ea} + \varepsilon_{pa} = \frac{\sigma'_f}{E} (2N_f)^b + \varepsilon'_f (2N_f)^c \quad (13)$$

where ε_a is the total strain amplitude; ε_{ea} is the elastic strain amplitude; ε_{pa} is the plastic strain amplitude; E is the elastic modulus; ε'_f is the fatigue ductility coefficient, which is dimensionless like strain; c is the fatigue ductility index.

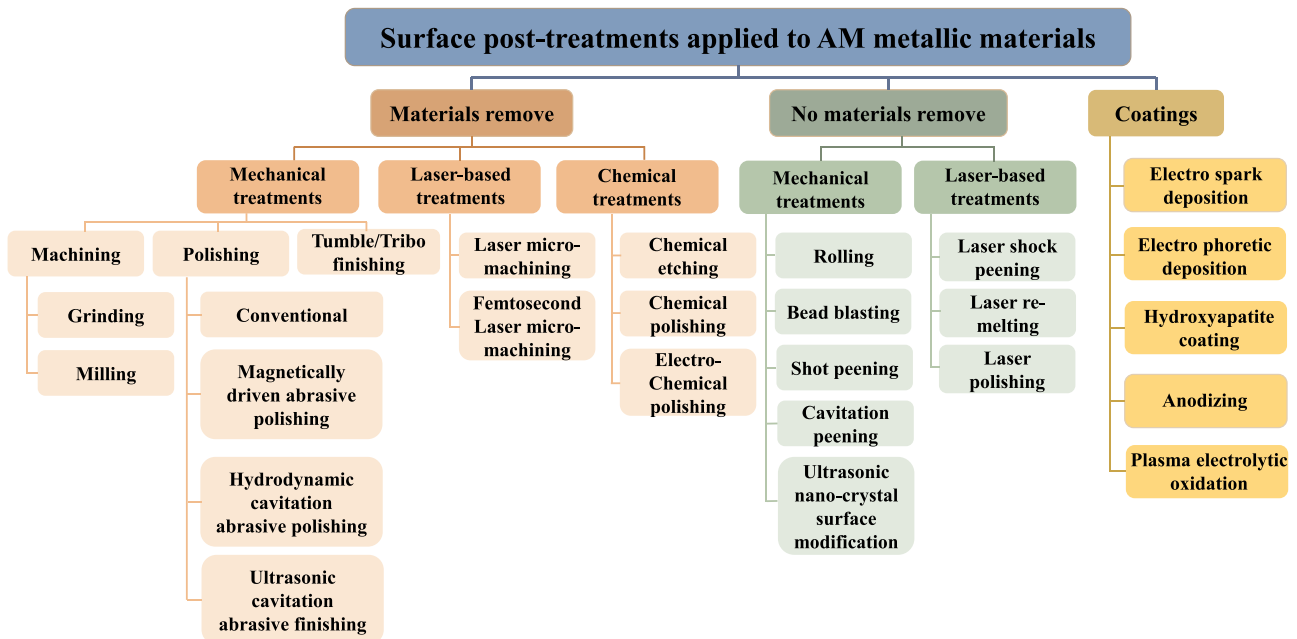


Figure 22. Categorisation of the surface post-treatments applied to AM metallic materials [168].

Table 2. Effects of different surface treatments in improving the surface roughness of WAAM parts.

Post-treatment	Materials	Initial Ra value (μm)	Post-treatment Ra value (μm)	Percentage improvement
Magnetic Arc Oscillation [166]	Ni-base alloy	198.64	144.69	27%
Ultrasonic Nanocrystal Surface Modification [167]	2356 aluminium alloy	10.40	2.34	77%
Laser Polishing [170]	SS316L	14.80	9.45	36%
Plasma Spray Coating [171]	Duplex stainless steel 2205	0.33	0.22	33%
Waterjet Machining [172]	Al alloy	35.00	6.50	81%
Shot Peening [173]	304 Steel	5.19	3.26	37%
Friction Stir Processing [174]	Ti6AL4V	35.00	6.20	82%

Since only the elastic portion of the strain-life curve is affected by surface roughness, Equation (13) is modified accordingly, as shown in Eq. (14) [176]:

$$\varepsilon_a = \varepsilon_{ea} + \varepsilon_{pa} = \frac{\sigma'_f}{E} (2N_f)^{b-0.143 \log(K_f)} + \varepsilon'_f (2N_f)^c \quad (14)$$

Figure 23 compares the difference between the predicted fatigue life value and the experimental value considering surface roughness [176]. The predicted values of high-cycle fatigue life controlled by stress are given in Figure 23(a), and values of low-cycle fatigue life controlled by strain are given in Figure 23(b). These results show that Eq. (13) and Eq. (14) can be effective in predicting high-cycle and low-cycle fatigue life, considering surface roughness, and have significant potential for fatigue life evaluation and prediction relating to metal WAAM components.

Near-net-shape AM presents challenges, such as poor surface quality, low dimensional accuracy, and difficulty in achieving high durability. A rough surface is considered to have multiple defects or notches. As a common source of stress concentration, it accelerates

the early initiation of fatigue cracks, significantly compromising fatigue properties. Therefore, controlling surface roughness is essential for the successful application of WAAM, especially for complex parts that must meet stringent performance criteria.

Effective surface quality control during the manufacturing process requires a comprehensive consideration of the characteristics of raw materials, part design, process parameters, and melting and deposition conditions. Additionally, selecting an appropriate post-treatment process is vital for enhancing the quality of the final parts. Moreover, developing high-fidelity predictive models and reliable methods for assessing fatigue strength and life, which take surface roughness into account, is essential for ensuring the engineering applicability, reliability, and safety of additive components.

3.5. Structure-properties-performance relationship

In recent years, the effects of the WAAM fabrication process on microstructure, defects, residual stresses,

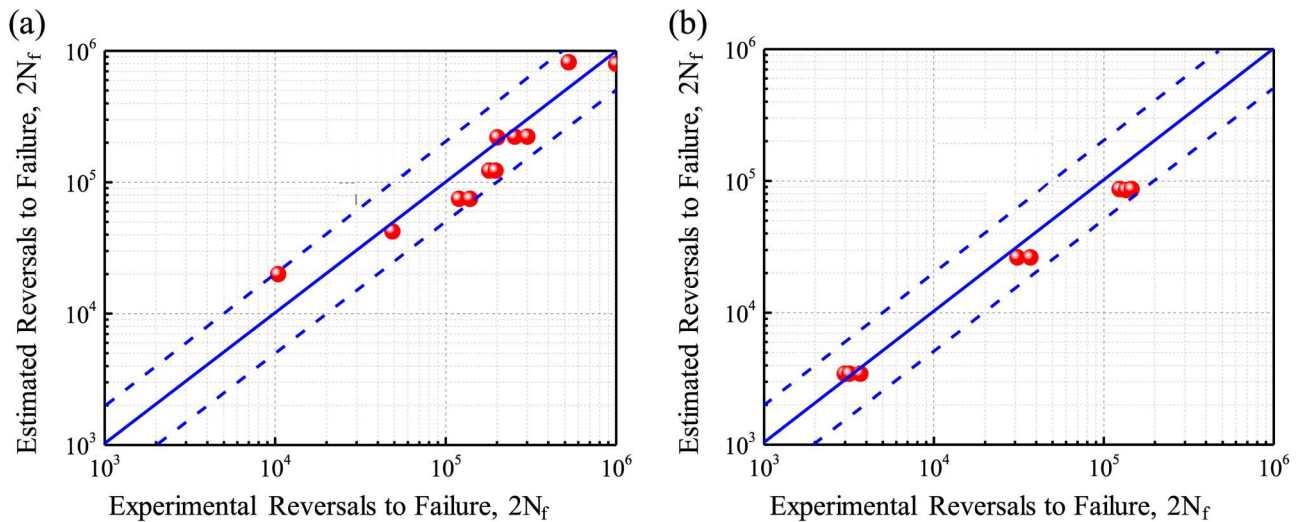


Figure 23. Comparison between predicted fatigue life and experimental value considering surface roughness (double error band): (a) Stress-controlled high-cycle fatigue; (b) Strain-controlled low cycle fatigue [176].

roughness and mechanical properties have been extensively investigated. The microstructure in WAAM-forming alloys tends to exhibit rough and textured columnar crystals, a microstructural feature which may lead to anisotropic behaviour in terms of the mechanical properties. In addition, the superheat generated during arc welding can lead to high residual stresses or distortions. Residual tensile stresses are known to adversely affect the mechanical properties and resistance to fatigue crack propagation of the material, because they facilitate crack initiation and propagation. Moreover, it's crucial to recognise that, due to its high surface roughness, WAAM is not a net-shape AM process, and typically requires post-processing treatments.

The main focus here, is to clarify the process-structure-properties characteristics of these materials. Fatigue damage is one of the most common and dominant forms of failure of engineered components in service. Ensuring the reliability of fatigue fracture performance requires a robust assessment and accurate prediction methodology. It is of paramount importance to ascertain the reliability of fatigue fracture performance through the implementation of a robust assessment, and accurate prediction methodology, if the application of WAAM is to be extended to real engineering components in service. Empirical evidence suggests that the mechanical properties of WAAM materials show comparable performance to those produced by conventional fabrication processes under static loading conditions [177], and development of improved fatigue resistance represents a significant research focus in this field [178].

Nevertheless, the WAAM fabrication process subjects the material to a complex thermal history, and the complex and variable thermodynamic, and geometric boundary conditions may result in metallurgical defects (pores, inclusions and cracks, etc.), between the deposited layers. Additionally, the misalignment of process parameters, including arc energy, cooling rate, wire feed rate, and other variables, can result in the formation of microstructural inhomogeneities within the material, leading to a range of defects, including organisational anisotropy, residual stresses, surface roughness, etc. [179]. It is evident that these properties exert control over the macroscopic properties of the material, thereby adversely affecting the reliability of the component for real-world applications. Among these properties, the complexity of defect size, morphology, and distribution, which are unavoidable and challenging to eliminate, play a critical role in determining the fatigue performance and service reliability of components. Attempts have been made to establish a correlation between

the fatigue strength and defect size, in AM materials. Kitagawa and Takahashi [180] proposed the concepts of stress intensity factor and critical short crack size, and based on this, El Haddad [181] derived a mathematical model that can be used to describe the relationship between fatigue strength and short crack size. Murakami [182] observed that the influence of defects on fatigue performance resembles that of short cracks. Expanding on this observation, Beretta et al. [183] replaced short crack sizes with small defect sizes in the El-Haddad model, aiming to use the refined model for predicting the performance of AM materials and components in a relatively small dimension. Nonetheless, the effects of the WAAM process on fatigue performance are intricate, with variations in defect size and location contributing to increased scatter in fatigue life, such that no general theory or model can fully describe the effects.

Establishing a qualitative link between defect characteristics and potential fatigue life is essential for ensuring safe material performance in service. Xie et al. [66] employed a novel approach, combining the peak-over-threshold method with the enhanced NASGRO model, to predict the fatigue life of materials subjected to defect-controlled fatigue. Wang et al. [184] established a fatigue cracking criterion with a specific physical meaning for a strength-toughness coordinate system containing equidistant inclusions size lines to reveal the relationship between UTS, fracture toughness, and critical inclusions sizes based on fracture mechanics when considering different inclusions types. This concept can be adapted to enhance our understanding of the structure-property relationships of WAAM. By doing so, it provides a robust theoretical framework for managing fatigue fractures caused by various types of inclusions in WAAM components.

In addition to establishing relationships between structure and properties, understanding the relationship between performance and properties is exactly the same important. Extensive work has been conducted in modelling and quantifying the fatigue strength. Numerous models and prediction formulæ have been developed. However, it's still necessary to address the numerous factors affecting fatigue, which include microstructure, defects, residual stress and the service environment. Furthermore, there is a discrepancy between the solutions offered by the research community, and those required by the industry side. After analysing a substantial quantity of available fatigue data, Pang et al. [185] established qualitative and quantitative relationships between fatigue strength and hardness, strength (tensile and yield strength) and toughness (static and impact toughness). Among these relationships, it was discovered for the first time that with increasing tensile strength, the

fatigue strength initially increases to a maximum value and then decreases, satisfying the quadratic parabolic equation relationship:

$$\sigma_w = \sigma_b(C - P \cdot \sigma_b) \quad (15)$$

The ideal linear fatigue strength factor, denoted by C , is defined as the ratio of the fatigue strength to the elastic limit. The fatigue defect sensitivity factor, denoted by P , is defined as the ratio of the fatigue strength to the elastic limit. This relationship is applicable to a wide range of materials, including traditional materials (e.g. steel, aluminium alloys, copper alloys, and titanium alloys), new materials (e.g. ultra-fine grain materials, mild steel, and copper-aluminium alloys), and engineering components (e.g. shafts, manual gears, and joy-sticks). Therefore, the tensile strength and fatigue strength of the quadratic equation are collectively referred to as the fatigue strength of the general relationship. This relationship also provides a satisfactory description of the relationship between fatigue strength and tensile strength. It allows for the prediction or design of materials by adjusting the material constants C or P (Figure 24). Also, it allows for the rapid prediction of the maximum fatigue strength and its critical tensile strength [186].

The correlation between defects and fatigue performance, as well as the relationship between fatigue performance and traditional mechanical properties, forms a crucial theoretical foundation for designing components using WAAM. Materials with higher yield stress can endure greater stress levels before experiencing plastic deformation, thereby lowering the risk of crack initiation and propagation. Consequently, materials with higher yield stresses generally exhibit superior performance in low-cycle fatigue [187].

4. Machine learning-enabled PSPP mapping

The success of WAAM is contingent on two key factors: component performance enhancement, and an extended service life. However, despite the growing interest in this field, the fundamental scientific principles underlying WAAM are not yet well established, with many aspects still dealt with empirically, and in a piecemeal manner. This is compounded by the lack of a unified approach that can systematically address the various challenges and complexities associated with WAAM technology, including the mesoscale interactions between the arc and the printed material, as well as the macroscale realisation of the component forming process, properties control, and in-service performance.

As it is now increasingly recognised that predictive ML can accelerate the development of WAAM

technology, it allows for the accumulation of datasets as well as the use of physical knowledge in conjunction with models. Furthermore, it enables the use of ML models to find PSPP links embedded in the data, thus completing the process-structure-properties-performance in the form of PSPP links. Consequently, a number of studies have begun incorporating ML techniques into WAAM with the objective of predicting the relationships within the dataset, in order to optimise the manufacturing process and enhance product performance for service. Examples of predictive machine learning algorithms include neural networks, decision trees, polynomial regression and support vector machines. It can be seen that the trend of integrating predictive ML research into WAAM is still on the rise, as depicted in Figure 25 [188], aiming to enhance understanding of the WAAM process and optimise decisions regarding component quality and control.

Influenced by various factors such as anisotropic structures, widespread defect distribution, deep residual stresses, and complex surface roughness, the efficiency and accuracy of predicting the mechanical properties of metals in AM, based on traditional empirical models and limited data, face serious challenges. In recent years, as an inevitable product of the development of big data and artificial intelligence, ML methods have provided opportunities for effectively handling the complex nonlinear relationships between high-dimensional physical quantities, and have been receiving ongoing sustained attention in the field of mechanical performance prediction for AM.

The four factors most commonly associated with the fatigue performance of additive components are microstructure, internal defects, residual stresses and surface roughness. These factors are closely related to the manufacturing process, and a significant body of research has been conducted to establish the correlation between process parameters and influencing factors. This research has employed ML techniques to gain deeper insights into the correlation mechanisms between the two. This section will provide a brief overview of the main applications of WAAM in ML, and the current research status of predicting the influencing factors of component performance based on ML.

4.1. Process-structure optimisation

The accurate modelling of crystal structures plays a crucial role in the optimisation of AM processes. However, there is a relative dearth of ML-based studies on WAAM grain modelling. Li et al. [189] proposed an Artificial Neural Network (ANN) method for predicting the competitive grain growth behaviour during DED.

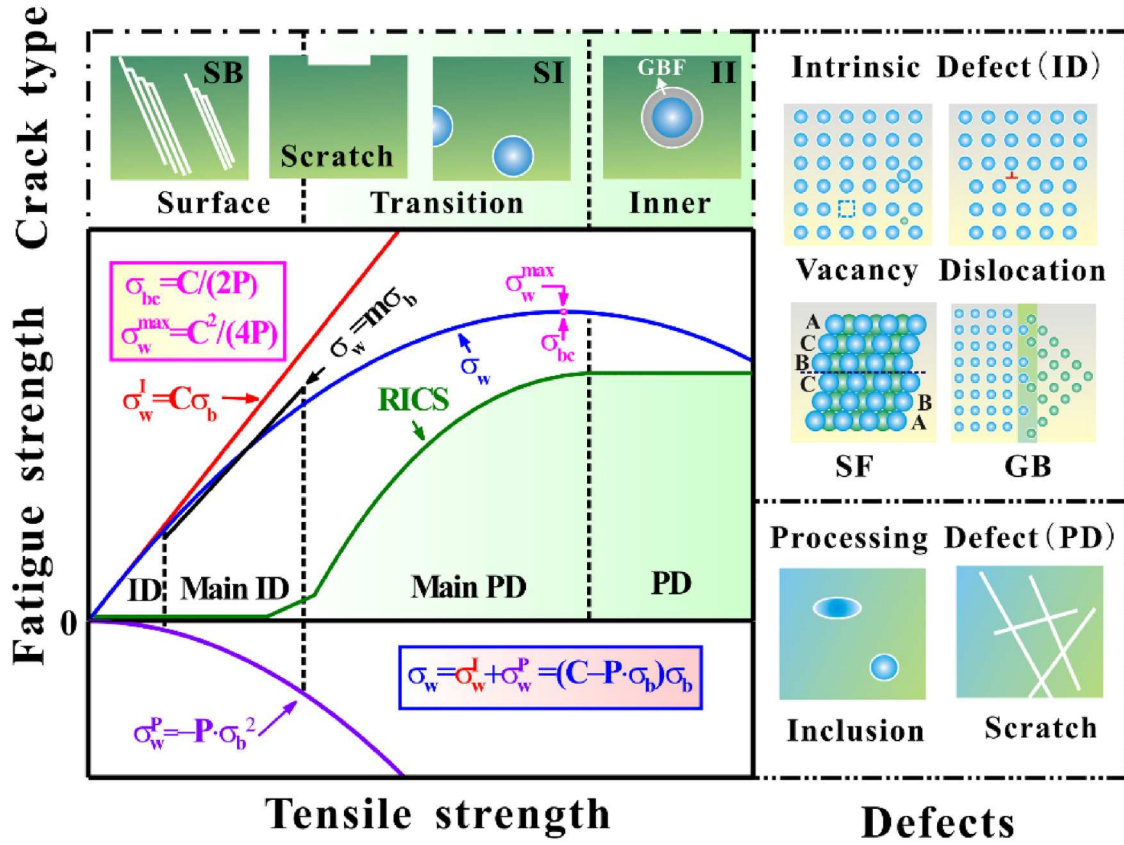


Figure 24. Schematic diagram of fatigue strength relationship and fatigue mechanism with tensile strength change [186].

ANN was used to investigate the relationship between grain boundary inclination, and thermal gradient, crystal orientation, and the Marangoni effect. Kats et al. [190] employed the Finite Volume Method (FVM) to derive the temperature field, which was also integrated with a metal cellular automaton to simulate the internal grain structure of the melt pool. Subsequently, the temperature gradient and cooling rate were linked to

the grain size and morphology through a neural network, which was then coupled with the FVM, in order to predict the microstructural features under the given process parameters in the DED process. This ultimately led to the development of a physically-informed ML algorithm, which can achieve fast and accurate prediction of the grain structure in the DED process. This is illustrated in Figure 26.

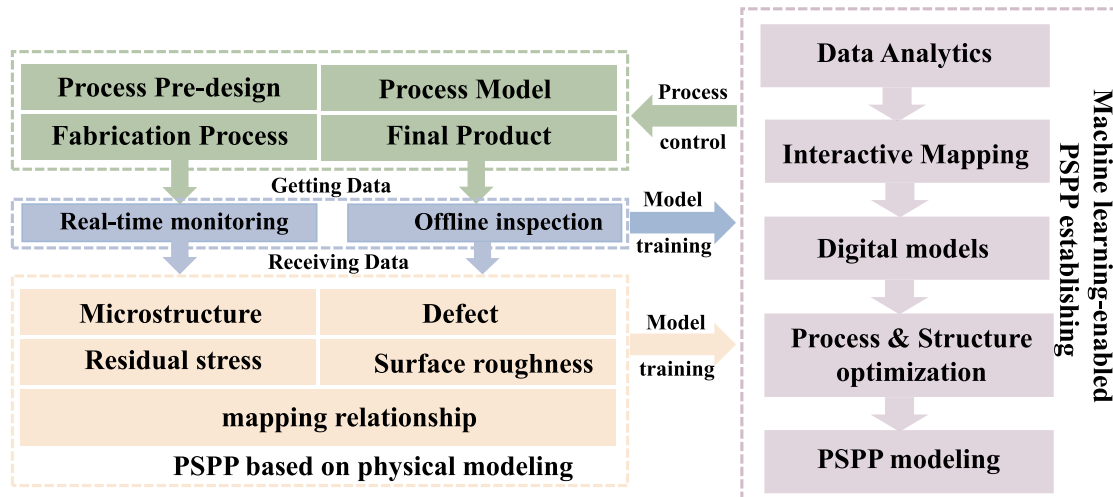


Figure 25. Model training and in-process updating of the proposed ML-WAAM framework.

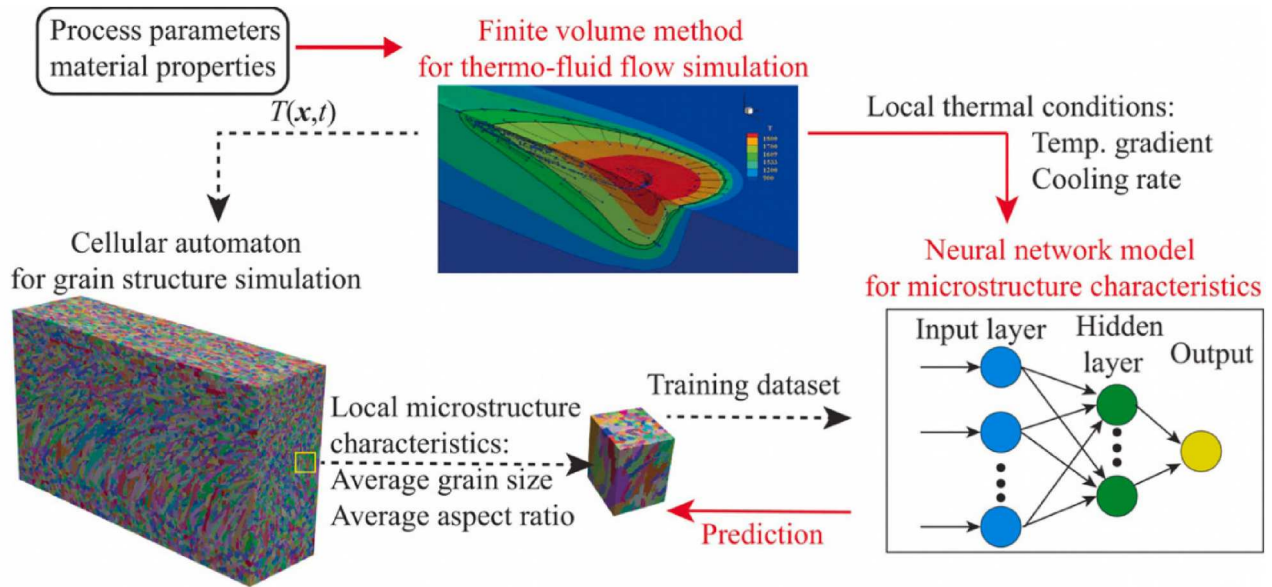


Figure 26. Schematic of the prediction of grain structure by ML [190].

Data-driven grain structure modelling is still in its early stages, with research focusing on establishing mapping relationships between simple microstructure descriptors and input features. The challenge lies in the explicit modelling of grain structure as a high-dimensional physical quantity. Other forms of data-driven modelling exist, such as lattice structure modelling, dendrite structure modelling, two-particle phase-field microstructure modelling, and regenerated scanning electron microscope photographs.

The structural and geometrical nature of WAAM treated components significantly influence both the final quality and the mechanical properties, as well as operational behaviour. Such models use the process parameters of WAAM as input variables, using ML to predict the interrelationships between these parameters and the features. This approach allows an analysis of their impact on the quality of deposition, thereby enhancing the precision of the process, and the integrity of weld geometry [191].

Numerous studies have correlated welding variables with weld geometry and depth, to predict the performance of ML models for straight monolayer beads [111–113, 192–194]. For instance, Ding et al. [195] employed an ANN model to correlate the between process parameters and bead geometry. They subsequently applied an adaptive medial axis transformation algorithm, to achieve precise geometric deposition, as depicted in Figure 27. Besides, Kumar et al. [196] characterised bead width, bead height, and cross-sectional area of beads using a second-order response surface model involving four processing parameters. They then

identified optimal processing conditions using a genetic algorithm.

Further, Li et al. [197] trained an ANN on linear single-layer magnetic beads, using the travel speed (TS) of the motion control system, and the wire feed speed (WFS) of the welding machine as input parameters. They used this model to derive a WFS that produces the same average magnetic bead height (BH), and average bead width (BW). In addition, Lambiase et al. [198] used a ML model to capture BH and BW, based on TS and WFS, predicting the geometry of the beads with good results. Gühr et al. [199] employed a multilayer perceptron (MLP) algorithm, to determine the relationship between excessive deposition and porosity by analysing data. The novelty of this study lies in demonstrating the capability of ML models to capture and compensate for geometric defects in beads at the turning points of deposition, providing a blueprint for geometric prediction research on different shape features in WAAM, which could be directly applied to hanging or circular features. By selecting appropriate processing parameters through bead geometry modelling, the porosity and post-processing requirements of WAAM can be carefully mitigated.

4.2. Residual stress control

The intensely localised heat source in WAAM creates steep temperature gradients, causing significant residual stresses that may lead to thermal cracking and deformation, thereby compromising part integrity. Understanding the WAAM process, especially temperature

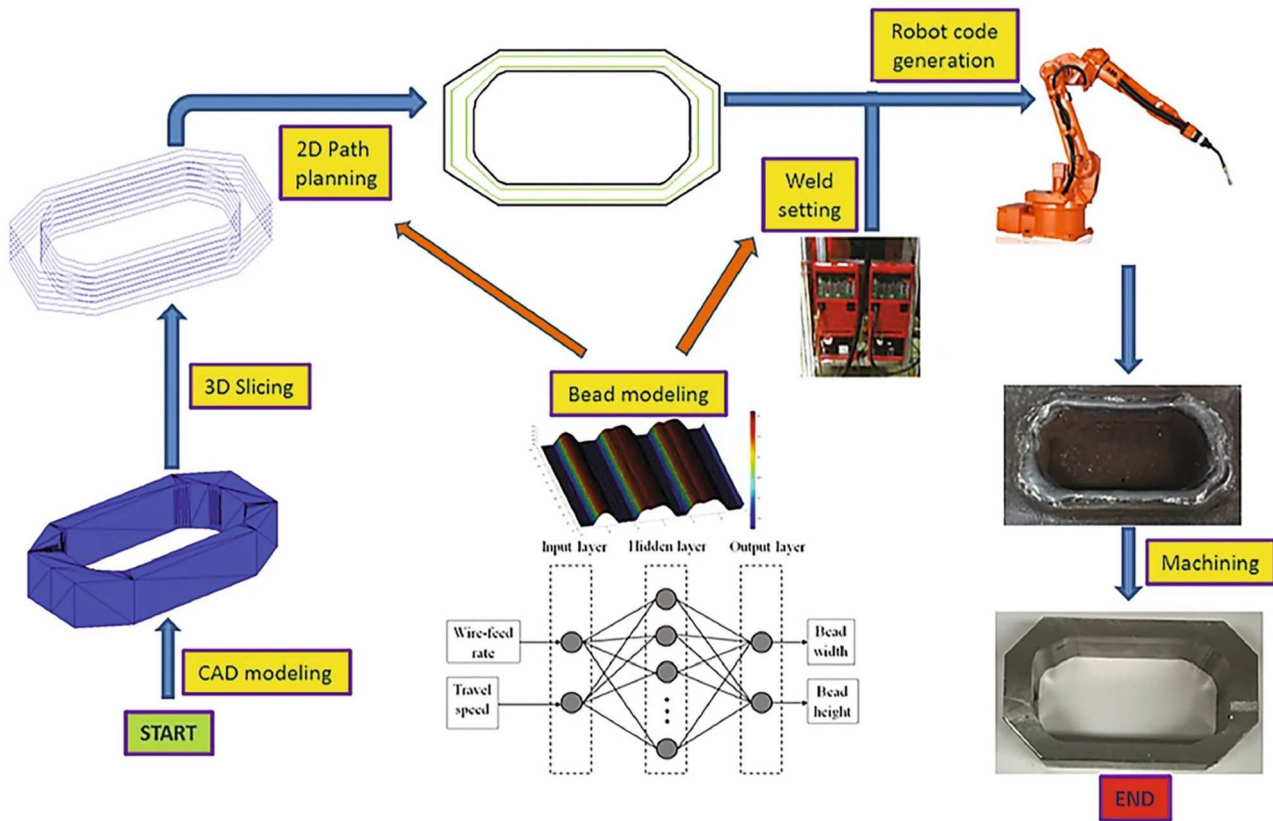


Figure 27. Automated process planning based on ML for robotic WAAM system [195].

distribution, is crucial for its broader industrial application. Le et al. [200] developed an efficient ML framework, integrated with numerical simulation to predict thermal history during single-bead track WAAM processes. Similarly, Xie et al. [201] integrated physical principles with data-driven methods, using a Physics-Informed Neural Network (PINN), to model the 3D temperature field of nickel-chromium alloy. This model, which employs approximations of partial differential equations for calculating thermal conductivity, and includes laser power, scanning speed, time, and coordinates as data-driven components, was found to require significantly less data to achieve high-precision predictions, compared with purely data-driven models. Moreover, Fagersand et al. [202] used finite element data to train and test a multilayer perceptron model, focused on predicting temperature evolution, and assessing the transferability of thermal history in the WAAM process.

During the WAAM process, discontinuities between adjacent weld beads can result in uneven temperature distribution, and significant residual stresses afterward [203]. Therefore, it is of vital importance to optimise the thermomechanical performance of continuous tool paths. Employing a data-driven approach, Zhou et al. [204] predicted the residual thermal stress fields in

situations with arbitrary component geometries and continuous toolpaths. This method offers an efficient and rational tool for optimising tool path planning in metal AM, particularly focusing on residual stresses. Notably, this approach bypasses the requirement for traditional finite element simulation to be used during online prediction, significantly boosting prediction efficiency, as illustrated in Figure 28.

Building on these findings, Zhou et al. [205] introduced an evolutionary method based on a genetic algorithm, to optimise the continuous tool paths with superior thermo-mechanical properties, aiming to achieve superior properties. This strategic approach yielded significant outcomes, with an enhancement exceeding 87% in thermos-mechanical performance, and a reduction of over 32 MPa in residual stress. It has been shown that the integration of ML with residual stresses is progressively establishing more dependable and efficient processes. Overall, the application of ML methods in controlling residual stresses is paving the way for more reliable WAAM processes. As ML methods continue to advance, they have offered the potential to revolutionise manufacturing, by enabling more precise control over complex variables that influence the quality and performance of manufactured parts.

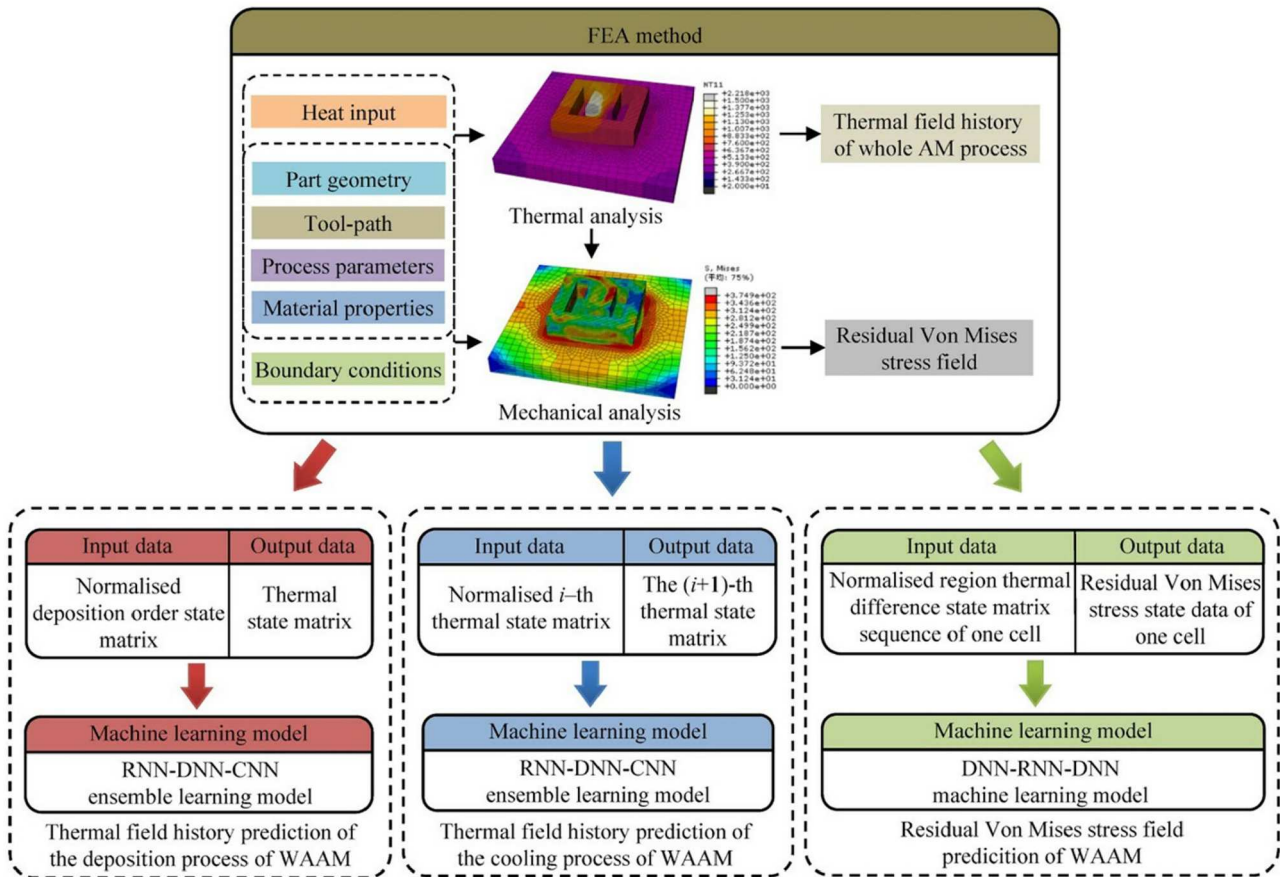


Figure 28. A methodology for the prediction of thermal field histories and residual stress fields [204].

4.3. Defect and roughness control

Before industrial implementation, WAAM requires surface finishing. This is due to the complex mass and heat transfer dynamics during deposition, which leads to irregularities in weld quality, and associated significant surface fluctuations and reduced quality. Even after mechanical finishing, residual defects at both the surface and sub-surface may persist, often imperceptible to visual inspection. Ignoring these defects can lead to major issues, thus affecting product performance, service life, and safety. Common issues like cracks, porosity, deformation, and insufficient fusion, impact mechanical properties and service behaviours. Therefore, product inspection for defect analysis is crucial during manufacturing. However, conventional examination methods and non-destructive techniques often fall short in enabling quality engineers to effectively address these defects.

Thus, the development of intelligent defect detection systems is essential for ensuring product quality. These systems must predict and optimise process parameters in WAAM. This could be done by utilising innovative modelling techniques using ML, which can link process

parameters to product quality and service performance. For instance, He et al. [206] introduced an intelligent defect classification method in WAAM products, by using a ML model. This method efficiently detects and identifies defects in magneto-optic images, with a limited number of defect samples from real inspections. Cheepu et al. [207] implemented an ML model to analyse defects in the initial and subsequent layers of WAAM data, enabling the prediction of defects in subsequent deposition layers. Their predictive model achieved a remarkable 99.78% accuracy while detecting and classifying defects in WAAM deposition layers. Additionally, Surovi et al. [208] proposed a method for constructing a geometrical defect detection model based on acoustic sensing. This model identifies defects in weld rod segments during the WAAM process, by monitoring bead segments and labelling datasets in terms of mean curvature thresholds, to distinguish between good and faulty bead segments. The primary novelty of this work lies in its focus on geometric defects, enabling precise localisation of defects and facilitating early intervention.

In the context of WAAM, which involves a layer-by-layer deposition process, the quality of each layer

significantly affects the final quality level. Li et al. [209] systematically evaluated the pivotal role of hybrid WAAM process, considering surface quality, material utilisation, and efficiency. This evaluation was based on the interplay between deposition and milling parameters. To enhance the performance, the researchers endeavoured to pinpoint the optimal combination of deposition and milling parameters, by leveraging a second-order regression model to predict the Surface Roughness (SR) of WAAM components. Xia et al. [210] compared the SR predictions from three ML algorithms: Extreme Learning Machine, Adaptive Neuro-Fuzzy Inference System, and Support Vector Regression. It is revealed that a non-linear correlation between SR, tool speed, and wire feed rate, posing a challenge for conventional modelling approaches. Yaseer et al. [211] utilised Random Forest (RF) and ANN to forecast WAAM's SR, which indicated that both ML algorithms effectively modelled layer roughness, with RF surpassing ANN in predictive accuracy and computational efficiency. Kazmi et al. [212] introduced three ML algorithms, including RF, ANN, and XGBoost, as illustrated in Figure 29, to predict the SR of WAAM-deposited aluminium alloy beads. These findings from XGBoost and ANN demonstrated notable capabilities in SR prediction.

These studies have laid the foundation for the advancement of universal ML models tailored for industrial settings, harnessing the capability of ML methods to enhance the component quality during the WAAM processes. At present, numerous ML investigations mainly focus on the defect detection, SR assessment, and optimisation of WAAM process parameters. However, research linking these advancements to fundamental mechanical properties and fatigue fracture performance remains relatively scarce.

4.4. PSPP cross scale modelling

It is identified that metallic materials properties are intimately connected to their processing, chemical composition, and microstructural characteristics. Understanding the impact of process conditions (e.g. process parameters and temperature history) on the mechanical properties, has become a central objective of advanced manufacturing and materials science. Accurately predicting these properties is a significant challenge [178].

In recent years, the integration of ML techniques in materials science and engineering has provided significant breakthroughs in understanding and optimising manufacturing processes. Particularly, ML has been instrumental in describing the complex interrelationships between the processes, microstructures, mechanical properties and performance. These progresses can be broadly classified into three categories: Process-Property modelling, Process-Microstructure-Property modelling, and Process-Structure-Property-Performance (PSPP) modelling. Such categorisations reflect an increasing complexity and integration of factors considered, which correspond to the depth and breadth of the correlations being studied.

(1) Process-Property modelling: This modelling primarily focuses on direct correlations between manufacturing parameters, and the resultant properties of the WAAM components. This category utilises regression analysis, neural networks, and other predictive models, to map process parameters such as the temperature, pressure, and duration, to mechanical properties such as the strength, ductility, and hardness. The main objective is to optimise processing conditions to achieve desired properties without requiring the for intermediate microstructural characterisation. Xie et al. [213]

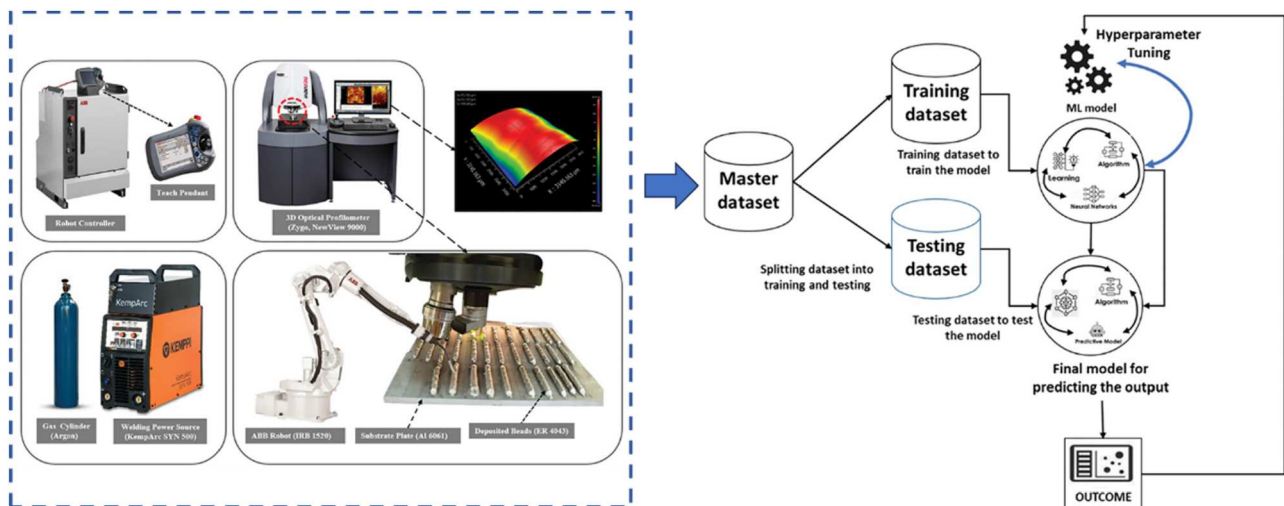


Figure 29. Flowchart of the experiment and data acquisition devices and the implementation of ML to the dataset [212].

introduced a data-driven supervised learning method, which employs infrared measurements from thermal images as input, to capture the intricate nonlinear relationship between local thermal history, and final mechanical properties. This approach is particularly valuable in industry, allowing for rapid adjustments to process parameters, based on the desired end properties.

(2) Process-Structure-Properties modelling: This modelling extends the analysis to include microstructural features as an intermediary between process parameters and properties. It examines how different manufacturing conditions affect the microstructure of the material, such as grain size, phase distribution, and defect density, and how these microstructural characteristics, in turn, influence the material's properties. ML models in this area are often more complex and may involve a combination of image analysis techniques to characterise microstructures, and predictive modelling to link these characteristics to properties. Brooke et al. [214] utilised ML models to predict manufacturing layer height and grain size based on process parameters. Fang et al. [215] employed a convolutional neural network (CNN) to extract features from simulated thermal histories, and predict mechanical properties in order to investigate the correlation between thermal history, microstructure and mechanical properties of Inconel 718 during the DED process. The entire process is depicted in Figure 30. Zhang et al. [216] developed a predictive

model for the microstructure and tensile properties of Ti-6Al-4 V alloys manufactured through the WAAM process.

(3) Process-Microstructure-Property-Performance modelling: The most comprehensive PSPP, routine considers the entire lifecycle of a material or component from manufacturing to performance in real-world applications. This approach not only accounts for the processing conditions and the resultant microstructure and properties, but also includes how these factors affect the final performance, such as fatigue life, corrosion resistance, and wear performance. PSPP modelling is integral to advanced engineering applications subjected to complex loading and environmental conditions. Li et al. [67] streamlined the PSPP relationship through material characterisation, integrating process factors into an ML model. Figure 31 illustrates the PSPP modelling approach employed in WAAM. This method can establish PSPP relationships through a systematic multi-scale characterisation and causal mapping of materials, significantly enhancing time efficiency over traditional iterative testing methods. By incorporating process factors into the PSPP model, it becomes possible to predict the fatigue life of components with greater accuracy.

Currently, there is a lack of effective methods to predict the intricate properties of metal materials solely through phenomenology. ML presents an opportunity for optimising this, by establishing connections

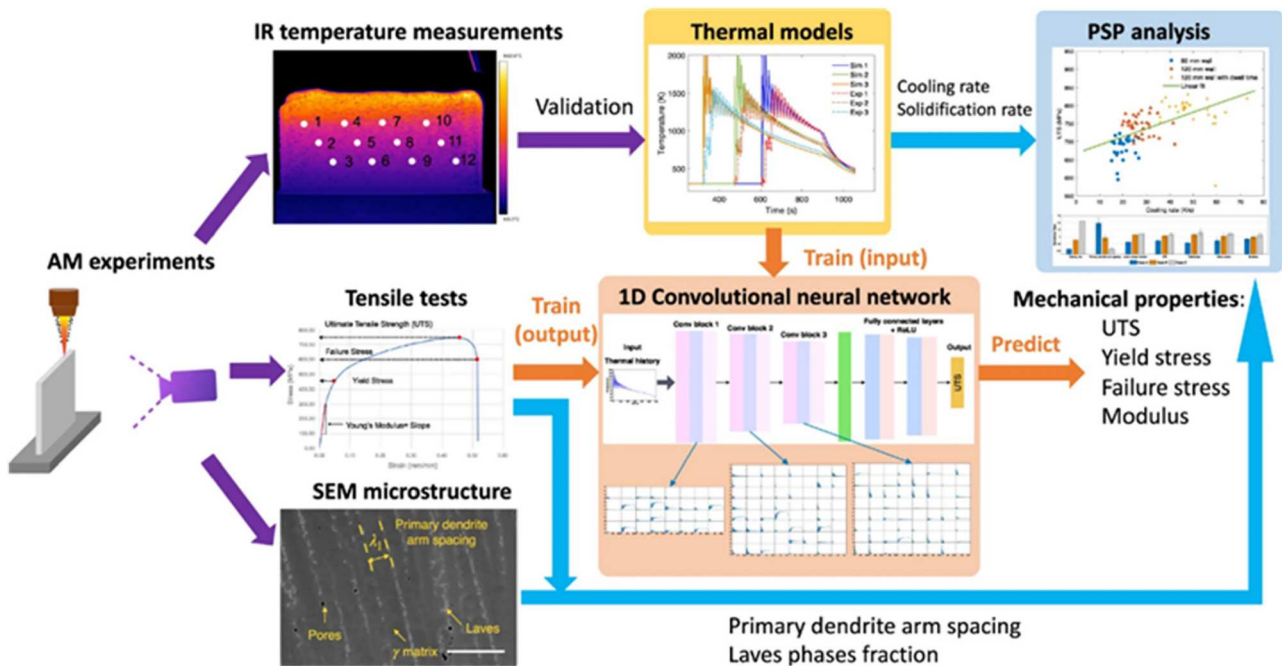


Figure 30. The simulated thermal process data, microstructure, and measured mechanical properties are analysed for process-structure-properties (PSP) relationship [215].

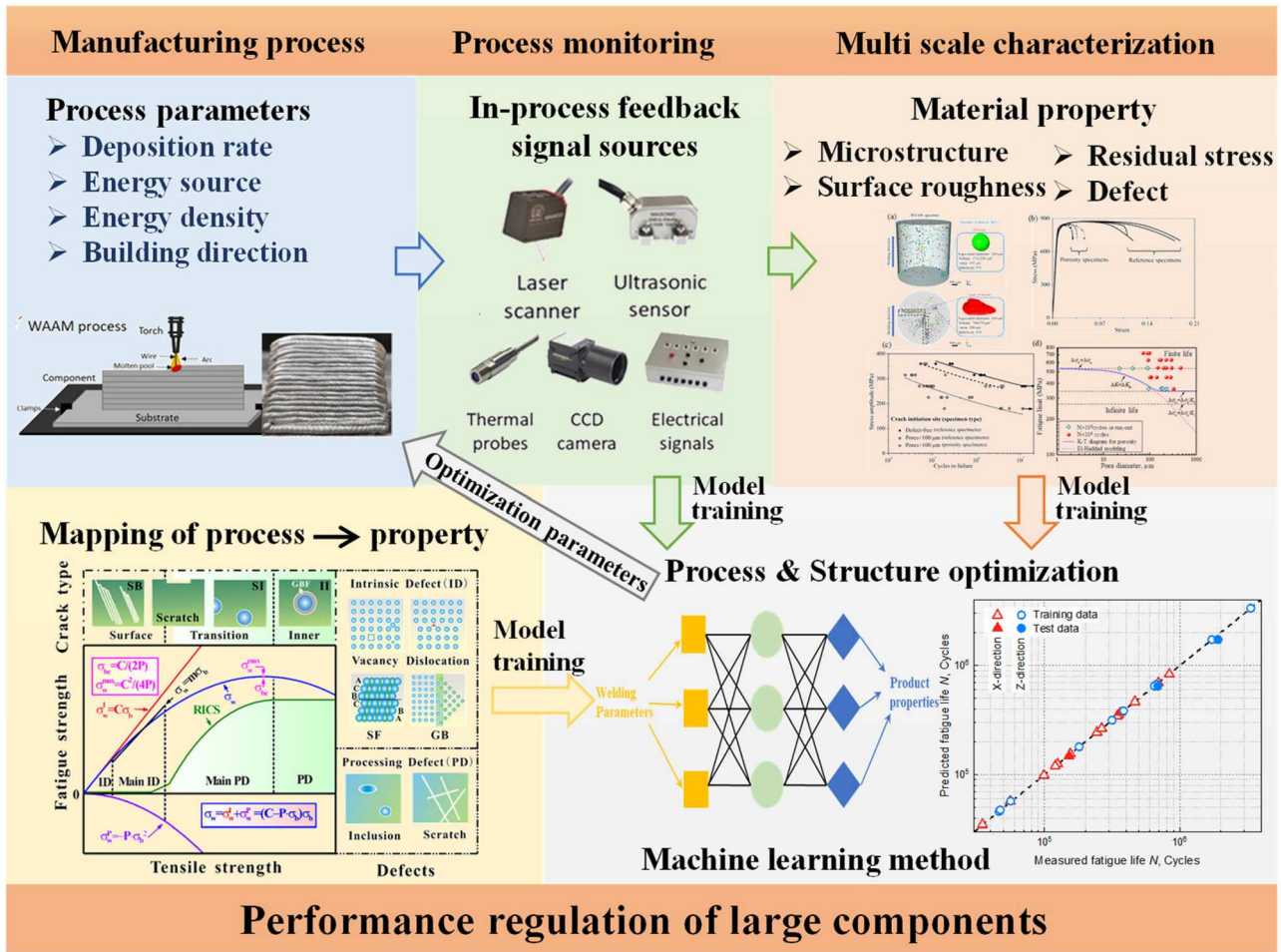


Figure 31. The PSPP modelling approach employed in WAAM.

between microstructures and various characteristics, thereby enhancing the performance of parts, based on sound scientific principles. Moreover, the integration of intelligent algorithms into WAAM workstations helps refine decision-making strategies for tool paths, leading to improved efficiency and sustainability. Consequently, the integration of advanced intelligent methods into material science and AM processes is useful for improving product quality, and streamlining manufacturing efficiency. However, this integration represents a fundamental step towards propelling additive manufacturing technology into the technological revolution.

5. Technological challenges and strategies

WAAM offers several advantages, such as higher deposition rates, better material utilisation and scalability, which makes it particularly suitable for producing larger components of moderate complexity. Besides, WAAM has found widespread application across various industries, including aerospace and automotive,

due to its efficiency, cost-effectiveness, and ability to produce high-quality metal components. Research on wire-feed AM of metal components is inherently interdisciplinary, involving the integration of materials science, thermo-mechanical engineering, and process planning. Despite significant advancements, there are several areas where further research and understanding are essential for the continued development and optimisation of WAAM technology. Based on extensive work in the field [10,21,31,54,217], the following issues concerning the integrity assessment of WAAM parts are of particular significance for future research.

5.1. Intricate PSPP relationship of WAAM parts

The PSPP relationship is fundamental to understanding and optimising the WAAM, which helps describe how process parameters affect the structure of WAAM materials, which in turn affects their properties and ultimately, their performance of WAAM components. Note that the PSPP relations in metallurgy are complex and not always quantitative. Establishing a reasonable PSPP

relationship in WAAM is a multifaceted challenge involving complex interactions between thermal, mechanical, and material science principles. The inherent variability in WAAM process parameters, material behaviour, and the difficulty of real-time monitoring and data collection all contribute to the challenge. Advanced modelling techniques, including mechanistic and ML models, are essential to tackle these complexities, but they also require extensive data and validation efforts.

Fortunately, the integration of metallurgy, mechanistic models, and ML method is essential for the design, process planning, production, characterisation, and performance evaluation of WAAM parts. From part design and process planning to process monitoring and control, ML can help reduce defects, achieve superior microstructures and properties, and facilitate product quality inspection, thus accelerating product qualification. As shown in Figure 32, both mechanistic models and ML can offer a quantitative framework for understanding the metallurgical characteristics of parts [203]. By using the joint applications of these advanced methodologies, WAAM can achieve improved part quality, enabling the production of high-performance components across various industries.

Multi-scale ML modelling for WAAM processes should be developed, which can well link processes not only to structure performance, but also to product performance. This may require the development of accurate and efficient algorithms that use in situ observations, combined with high-resolution direct simulations, to acquire rich training data. Enhanced concurrent modelling techniques are also useful for determining the

impact of local process-structure-property relationships for global product performance control.

5.2. Real-time monitoring and control of WAAM

WAAM represents a multifaceted domain encompassing multiple physical effects and scales, intertwining wire-arc interactions at the micro-scale, melt pool dynamics and columnar grain evolution at the mesoscale, and thermo-mechanical coupling at the macro-scale. This process operates across vast spatial and temporal dimensions, with WAAM structures spanning metres in volume and metal grains mere microns in size. While printing large WAAM structures or components can span hours, the heating and cooling of raw materials occurs within seconds. These extensive spatial and temporal scales pose significant challenges in monitoring and controlling the WAAM process.

Real-time monitoring and control are very essential for ensuring high-quality, consistent production, but they usually face numerous challenges. These mainly include dealing with harsh operating environments, complex thermal cycles, material and process variability, high data acquisition and processing demands, difficulties in defect detection, control system complexity, and sensor reliability issues. As depicted in Figure 33, ML prediction enable the implementation of anticipatory process control, ensuring that the AM process adheres to the necessary specifications to meet performance criteria [218].

Addressing the challenges of real-time monitoring and control in WAAM involves a combination of

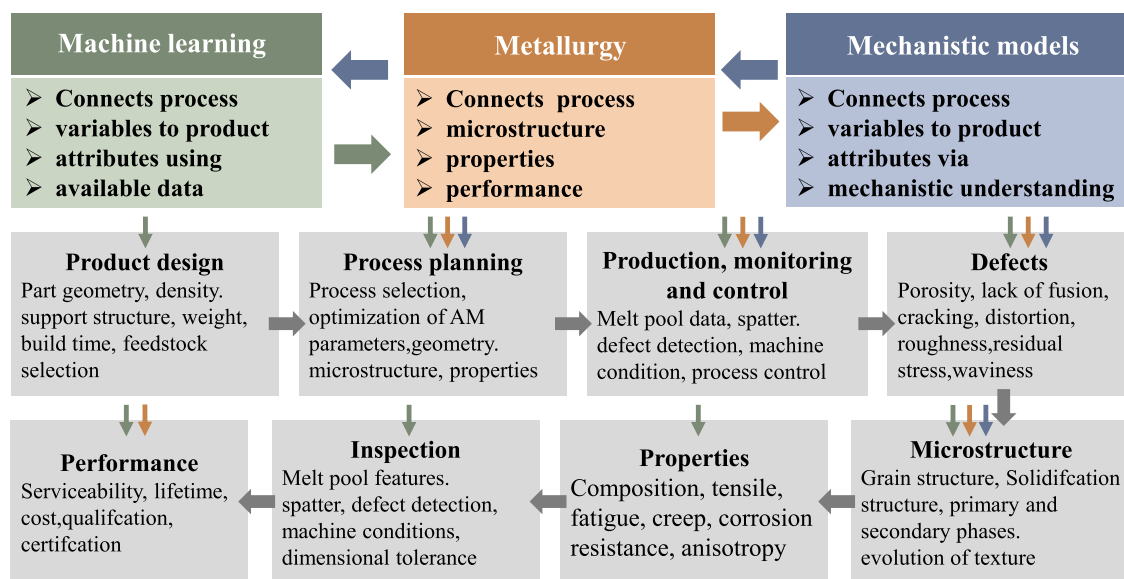


Figure 32. The interplay of machine learning and mechanistic models in understanding the physical metallurgy of AM processes and techniques [203].

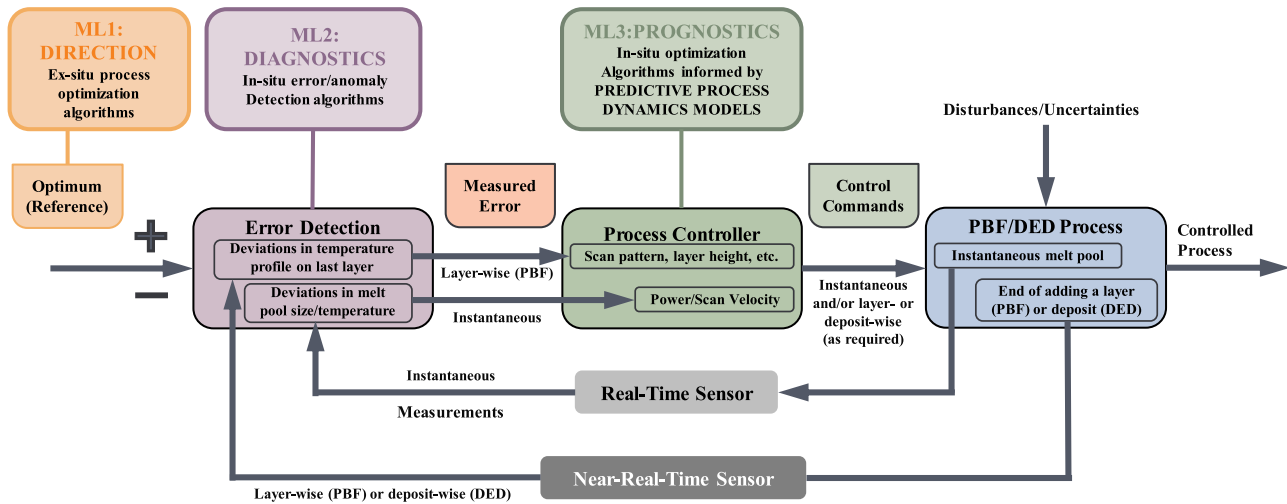


Figure 33. Example of ML application in real-time and near-real-time diagnostic-prognostic closed loop control for AM [218].

advanced technologies, innovative methods, and strategic planning. High-temperature sensors, protective measures, and sophisticated thermal management can help mitigate the harsh operating environment. Ensuring consistent feedstock quality, and optimising process parameters through advanced algorithms and ML are crucial for managing material and process variability. High-speed data acquisition, sensor fusion, and *in situ* monitoring technologies like high-resolution X-ray imaging and ultrasonic testing can enhance defect detection and quality control [219]. Developing adaptive control systems and predictive modelling, supported by cloud and edge computing, can manage the control system complexity and computational demands.

5.3. Data standardisation and physical mechanisms

It is anticipated that the utilisation of ML modelling to identify potential links between PSPP and WAAM will become increasingly prevalent in the near future. Further investigation of these core links is essential to improve our understanding and improve control over WAAM processes. Additionally, given the nonlinear, multi-scale, and multi-physical nature of PSPP relationships in WAAM, employing data-driven or physically-informed ML models appear to be the most suitable approach. The size and quality of the dataset play a crucial role in ensuring the robustness of these models, and accurately identifying the complex correlations between physical quantities.

However, gathering fatigue data to construct these datasets is both costly and time-consuming, presenting a significant challenge in developing large-scale datasets. This has become one of the primary obstacles in

applying ML to predict fatigue performance. To enhance the quality and quantity of training samples, data augmentation techniques can be utilised. These techniques allow for the integration of diverse data, encompassing different scales and physical quantities, sourced from experimental data, simulation results, or a priori knowledge [220]. Moreover, a series of transformations and modifications to the original training data can generate new samples, thereby expanding the size and diversity of the dataset. Alternatively, using external data or a priori knowledge can help generate new samples without relying solely on transformations of the original data.

Physical mechanism-driven ML represents an emerging paradigm that aims to utilise prior knowledge to inform ML modelling, thereby assisting in the interpretation of models [221]. In order to construct physical mechanism-driven ML models, it is necessary to grasp the implied physical damage mechanisms between input and target variables in advance, to select the most appropriate physical knowledge. An inaccurate understanding of the physical mechanisms will make it challenging to guarantee the correct interpretation, and physical consistency of the model, which will lead to an inaccurate description of the correlation relationship between the physical variables, reducing the prediction accuracy of the model. Hence, there is a critical need to establish a standardised method for extracting physical information from the WAAM thermal process, which is essential to ensure the accurate development of physical mechanism-driven models.

6. Conclusions

Wire Arc Additive Manufacturing (WAAM) is a prominent technique for fabricating solid free-form components,

renowned for its high deposition rates, and virtually unlimited build dimensions. These attributes significantly enhance the production speed of medium to large critical components. However, the service life prediction of WAAM components remain challenging, due to complex nonlinear relationships inherent in the thermo-mechanical process. Traditionally, physical modelling has focused on key elements of fatigue, such as microstructure, internal defects, residual stresses, and surface roughness, integrating these into comprehensive PSPP (process-structure-property-performance) models, to capture the full spectrum of interactions. On the other hand, machine learning (ML) offers a powerful alternative, providing a robust framework for precise predictions and outcome optimisation. Utilising historical data, real-time inputs, and advanced algorithms, ML models excel in delineating the physical factors that impact the service performance of WAAM products, thereby establishing detailed cross-scale PSPP relationships.

The present study commenced with a thorough review of current WAAM technologies, encompassing both standard and hybrid WAAM processes, alongside detection and control methods. Real-time monitoring is crucial for describing physical mechanisms, managing processes, and validating ML models. To facilitate multidimensional and multiscale correlation imaging, it is essential to place numerous sensors on the structure to monitor device operation in real time. Offline inspection of WAAM components provides insights into microstructure, defects, residual stresses, and surface roughness. The study further investigates how these critical factors: microstructure, internal defects, residual stresses, and surface roughness, influence the service performance. Physical modelling establishes the correlational relationships between these variables and performance outcomes. Ultimately, by integrating these insights with ML, a nonlinear PSPP relationship can be found to improve control over WAAM production quality, and predict service performance.

The development of PSPP relationships has markedly improved the evaluation of WAAM components. Yet, challenges persist in achieving cross-temporal and spatial scale modelling, *in situ* monitoring, and standardised data modelling within PSPP frameworks. Despite these challenges, using PSPP in WAAM holds significant promise for reducing time and labour costs, while simultaneously enhancing the material properties and performance. Looking forward, components manufactured using WAAM, are poised to play a crucial role in industries such as aerospace, automotive, and heavy machinery, etc.

Disclosure statement

No potential conflict of interest was reported by the author(s).

Funding

The authors sincerely thank the support from the Key Science & Technology Research Project of Taihang Laboratory (No. C2024-1-0405).

Data availability statement

The data that support the findings of this study are available from the corresponding authors upon reasonable request.

CRedit authorship contribution statement

Han Zhang: Conceptualisation, Data curation, Investigation, Methodology, Formal analysis, Visualisation, Writing – original draft. **Runsheng Li:** Data curation, Investigation, Validation, Methodology. **Junjiang Liu:** Methodology, Formal analysis, Writing – review & editing. **Kaiyun Wang:** Methodology, Funding acquisition, Validation, Writing – review & editing. **Weijian Qian:** Data curation, Formal analysis. **Lei Shi:** Data curation, Formal analysis. **Liming Lei:** Methodology, Funding acquisition, Supervision. **Weifeng He:** Validation, Writing – review & editing. **Shengchuan Wu:** Conceptualisation, Data curation, Methodology, Funding acquisition, Supervision, Writing – review & editing.

References

- [1] Tofail SAM, Koumoulos EP, Bandyopadhyay A, et al. Additive manufacturing: scientific and technological challenges, market uptake and opportunities. *Mater Today*. 2018;21:22–37. doi:10.1016/j.mattod.2017.07.001
- [2] DebRoy T, Mukherjee T, Milewski JO, et al. Scientific, technological and economic issues in metal printing and their solutions. *Nat Mater*. 2019;18:1026–1032. doi:10.1038/s41563-019-0408-2
- [3] Liu G, Zhang X, Chen X, et al. Additive manufacturing of structural materials. *Mater Sci Eng R Rep*. 2021;145:100596. doi:10.1016/j.mser.2020.100596
- [4] Wohlers Associates, ed.. *Wohlers report 2023: 3D printing and additive manufacturing global state of the industry*, Washington (DC): Wohlers Associates; 2023.
- [5] Leal R, Barreiros FM, Alves L, et al. Additive manufacturing tooling for the automotive industry. *Int J Adv Manuf Technol*. 2017;92:1671–1676. doi:10.1007/s00170-017-0239-8
- [6] Blakey-Milner B, Gradl P, Snedden G, et al. Metal additive manufacturing in aerospace: a review. *Mater Des*. 2021;209:110008. doi:10.1016/j.matdes.2021.110008
- [7] Sefene EM. State-of-the-art of selective laser melting process: a comprehensive review. *J Manuf Syst*. 2022;63:250–274. doi:10.1016/j.jmsy.2022.04.002

- [8] Kim H, Cha M, Kim BC, et al. Maintenance framework for repairing partially damaged parts using 3D printing. *Int J Precis Eng Manuf.* 2019;20:1451–1464. doi:10.1007/s12541-019-00132-x
- [9] Williams SW, Martina F, Addison AC, et al. Wire + arc additive manufacturing. *Mater Sci Technol.* 2016;32:641–647. doi:10.1179/1743284715Y.0000000073
- [10] Wu B, Pan Z, Ding D, et al. A review of the wire arc additive manufacturing of metals: properties, defects and quality improvement. *J. Manuf. Process.* 2018;35:127–139. doi:10.1016/j.jmapro.2018.08.001
- [11] Li JZ, Alkahari MR, Rosli NAB, et al. Malaysia, review of wire arc additive manufacturing for 3D metal printing., *Int. J. Autom. Technol.* 2019;13:346–353. doi:10.20965/ijat.2019.p0346
- [12] Rodríguez-González P, Ruiz-Navas EM, Gordo E. Wire arc additive manufacturing (WAAM) for aluminum-lithium alloys: a review., *Materials.* 2023;16:1375. doi:10.3390/ma16041375
- [13] Zhang H, Huang C, Wang G, et al. Comparison of energy consumption between hybrid deposition & micro-rolling and conventional approach for wrought parts. *J. Clean. Prod.* 2021;279:123307. doi:10.1016/j.jclepro.2020.123307
- [14] Mereddy S, Bermingham MJ, StJohn DH, et al. Grain refinement of wire arc additively manufactured titanium by the addition of silicon. *J. Alloys Compd.* 2017;695:2097–2103. doi:10.1016/j.jallcom.2016.11.049
- [15] Qi Z, Qi B, Cong B, et al. Microstructure and mechanical properties of wire + arc additively manufactured 2024 aluminum alloy components: as-deposited and post heat-treated. *J. Manuf. Process.* 2019;40:27–36. doi:10.1016/j.jmapro.2019.03.003
- [16] Singla YK, Miller JD, Raja K, et al. Toward single crystal nickel fabrication using WAAM – a first report. *J. Mater. Res. Technol.* 2023;27:4801–4804. doi:10.1016/j.jmrt.2023.11.016
- [17] Haden CV, Zeng G, Carter FM, et al. Wire and arc additive manufactured steel: tensile and wear properties. *Addit. Manuf.* 2017;16:115–123. doi:10.1016/j.addma.2017.05.010
- [18] Yi H, Jia L, Ding J, et al. Achieving material diversity in wire arc additive manufacturing: leaping from alloys to composites via wire innovation. *Int J Mach Tools Manuf.* 2024;194:104103. doi:10.1016/j.ijmachtools.2023.104103
- [19] Ge J, Lin J, Lei Y, et al. Location-related thermal history, microstructure, and mechanical properties of arc additively manufactured 2Cr13 steel using cold metal transfer welding. *Mater Sci Eng A.* 2018;715:144–153. doi:10.1016/j.msea.2017.12.076
- [20] Srivastava S, Garg RK, Sharma VS, et al. Measurement and mitigation of residual stress in wire-arc additive manufacturing: a review of macro-scale continuum modelling approach. *Arch. Comput. Methods Eng.* 2021;28:3491–3515. doi:10.1007/s11831-020-09511-4
- [21] Tomar, B, Shiva S, Nath T, A review on wire arc additive manufacturing: processing parameters, defects, quality improvement and recent advances. *Mater Today Commun.* 2022;31:103739. doi:10.1016/j.mtcomm.2022.103739
- [22] Stavropoulos P, Foteinopoulos P, Papacharalampopoulos A, et al. Addressing the challenges for the industrial application of additive manufacturing: towards a hybrid solution. *Int. J. Lightweight Mater. Manuf.* 2018;1:157–168. doi:10.1016/j.ijlmm.2018.07.002
- [23] Tapia G, Elwany A. A review on process monitoring and control in metal-based additive manufacturing. *J. Manuf. Sci. Eng.* 2014;136:060801. doi:10.1115/1.4028540
- [24] Jafari D, Vaneker THJ, Gibson I. Wire and arc additive manufacturing: opportunities and challenges to control the quality and accuracy of manufactured parts. *Mater. Des.* 2021;202:109471. doi:10.1016/j.matdes.2021.109471
- [25] Li Y, Su C, Zhu J. Comprehensive review of wire arc additive manufacturing: hardware system, physical process, monitoring, property characterization, application and future prospects. *Res Eng.* 2022;13:100330. doi:10.1016/j.rineng.2021.100330
- [26] Guo K, Yang Z, Yu C-H, et al. Artificial intelligence and machine learning in design of mechanical materials. *Mater. Horiz.* 2021;8:1153–1172. doi:10.1039/D0MH01451F
- [27] Guo S, Agarwal M, Cooper C, et al. Machine learning for metal additive manufacturing: towards a physics-informed data-driven paradigm. *J. Manuf. Syst.* 2022;62:145–163. doi:10.1016/j.jmsy.2021.11.003
- [28] Qin J, Hu F, Liu Y, et al. Research and application of machine learning for additive manufacturing. *Addit. Manuf.* 2022;52:102691. doi:10.1016/j.addma.2022.102691
- [29] Fang, AM, Xie M, He X, Zhang J, Hu J, Chen Y, Yang Y, Jin Q, Machine learning accelerates the materials discovery, *Mater. Today Commun.* 2022;33:104900. doi:10.1016/j.mtcomm.2022.104900
- [30] Svetlizky D, Das M, Zheng B, et al. Directed energy deposition (DED) additive manufacturing: physical characteristics, defects, challenges and applications. *Mater Today.* 2021;49:271–295. doi:10.1016/j.mattod.2021.03.020
- [31] Cunningham CR, Flynn JM, Shokrani A, et al. Invited review article: strategies and processes for high quality wire arc additive manufacturing. *Addit. Manuf.* 2018;22:672–686. doi:10.1016/j.addma.2018.06.020
- [32] Ding J, Colegrove P, Mehnen J, et al. Thermo-mechanical analysis of wire and arc additive layer manufacturing process on large multi-layer parts. *Comput. Mater. Sci.* 2011;50:3315–3322. doi:10.1016/j.commatsci.2011.06.023
- [33] Tan C, Li R, Su J, et al. Review on field assisted metal additive manufacturing. *Int J Mach Tools Manuf.* 2023;189:104032. doi:10.1016/j.ijmachtools.2023.104032
- [34] Huan P, Wei X, Wang X, et al. Comparative study on the microstructure, mechanical properties and fracture mechanism of wire arc additive manufactured Inconel 718 alloy under the assistance of alternating magnetic field. *Mater Sci Eng A.* 2022;854:143845. doi:10.1016/j.msea.2022.143845
- [35] Hu Y, Chen F, Gao X, et al. Enhancing the geometry accuracy and mechanical properties of wire arc additive manufacturing of an Al-5%Mg alloy through longitudinal magnetic field influence. *J. Manuf. Process.* 2024;118:407–418. doi:10.1016/j.jmapro.2024.03.054

- [36] Chen Y, Xu M, Zhang T, et al. Grain refinement and mechanical properties improvement of Inconel 625 alloy fabricated by ultrasonic-assisted wire and arc additive manufacturing. *J Alloys Compd* 2022;910:164957. doi:10.1016/j.jallcom.2022.164957
- [37] Fu R, Tang S, Lu J, et al. Hot-wire arc additive manufacturing of aluminum alloy with reduced porosity and high deposition rate. *Mater Des* 2021;199:109370. doi:10.1016/j.matdes.2020.109370
- [38] Hai-ou Z, Wang R, Liang L, et al. HDMR technology for the aircraft metal part. *Rapid Prototyp. J.* 2016;22:857–863. doi:10.1108/RPJ-05-2015-0047
- [39] Zhou X, Fu Z, Zhou X, et al. Numerical simulation of heat and mass transient behavior during WAAM overlapping deposition with external deflection magnetic field. *Int. J. Heat Mass Transf.* 2024;218:124780. doi:10.1016/j.ijheatmasstransfer.2023.124780
- [40] Al Noman A, Kumar BK, Dickens T. Field assisted additive manufacturing for polymers and metals: materials and methods. *Virtual Phys. Prototyp.* 2023;18:e2256707. doi:10.1080/17452759.2023.2256707
- [41] Wu B, Qiu Z, Dong B, et al. Effects of synchronized magnetic arc oscillation on microstructure, texture, grain boundary and mechanical properties of wire arc additively manufactured Ti6Al4V alloy. *Addit. Manuf.* 2022;54:102723. doi:10.1016/j.addma.2022.102723
- [42] Colegrove PA, Coules HE, Fairman J, et al. Microstructure and residual stress improvement in wire and arc additively manufactured parts through high-pressure rolling. *J. Mater. Process. Technol.* 2013;213:1782–1791. doi:10.1016/j.jmatprotec.2013.04.012
- [43] Zhang H, Wang X, Wang G, et al. Hybrid direct manufacturing method of metallic parts using deposition and micro continuous rolling. *Rapid Prototyp. J.* 2013;19:387–394. doi:10.1108/RPJ-01-2012-0006
- [44] Neto L, Williams S, Ding J, et al. Mechanical properties enhancement of additive manufactured Ti-6Al-4V by machine hammer peening. In: Itoh S, Shukla S, editors. *Advanced Surface Enhancement: Proceedings of the 1st International Conference on Advanced Surface Enhancement (INCASE 2019) – Research Towards Industrialisation*. Springer Link; 2020. p. 121–132. doi:10.1007/978-981-15-0054-1_13
- [45] Wang Y, Chen X, Shen Q, et al. Effect of magnetic field on the microstructure and mechanical properties of inconel 625 superalloy fabricated by wire arc additive manufacturing. *J. Manuf. Process.* 2021;64:10–19. doi:10.1016/j.jmapro.2021.01.008
- [46] Wang T, Mazánová V, Liu X. Ultrasonic effects on gas tungsten arc based wire additive manufacturing of aluminum matrix nanocomposite. *Mater Des* 2022;214:110393. doi:10.1016/j.matdes.2022.110393
- [47] Sang Y-X, Xiao M-Z, Zhang Z-J, et al. Effect of auxiliary heating process on low power pulsed laser wire feeding deposition. *Mater Des* 2022;218:110666. doi:10.1016/j.matdes.2022.110666
- [48] Fu Y, Zhang M, Chen X, et al. Mathematical analysis and process optimization of wire and arc additive manufactured Ti6Al4V ELI alloy with in-situ rolling. *J. Mater. Res. Technol.* 2024;30:210–222. doi:10.1016/j.jmrt.2024.02.176
- [49] Hu Y, Ao N, Wu S, et al. Influence of *in situ* micro-rolling on the improved strength and ductility of hybrid additively manufactured metals. *Eng. Fract. Mech.* 2021;253:107868. doi:10.1016/j.engfracmech.2021.107868
- [50] Wu Z, Wu S, Qian W, et al. Structural integrity issues of additively manufactured railway components: progress and challenges. *Eng Fail Anal* 2023;149:107265. doi:10.1016/j.engfailanal.2023.107265
- [51] Arbogast A, Nycz A, Noakes MW, et al. Strategies for a scalable multi-robot large scale wire arc additive manufacturing system. *Addit. Manuf. Lett.* 2024;8:100183. doi:10.1016/j.addlet.2023.100183
- [52] Li Y, Meng L, Li M, et al. Allocation and scheduling of deposition paths in a layer for multi-robot coordinated wire and arc additive manufacturing of large-scale parts. *Virtual Phys. Prototyp.* 2024;19:e2300680. doi:10.1080/17452759.2023.2300680
- [53] Lehmann T, Rose D, Ranjbar E, et al. Large-scale metal additive manufacturing: a holistic review of the state of the art and challenges. *Int. Mater. Rev.* 2022;67:410–459. doi:10.1080/09506608.2021.1971427
- [54] Chen X, Kong F, Fu Y, et al. A review on wire-arc additive manufacturing: typical defects, detection approaches, and multisensor data fusion-based model. *Int. J. Adv. Manuf. Technol.* 2021;117:707–727. doi:10.1007/s00170-021-07807-8
- [55] Xiong Y, Dharmawan AG, Tang Y, et al. A knowledge-based process planning framework for wire arc additive manufacturing. *Adv. Eng. Inform.* 2020;45:101135. doi:10.1016/j.aei.2020.101135
- [56] Li H, Shi X, Wu B, et al. Wire arc additive manufacturing: a review on digital twinning and visualization process. *J. Manuf. Process.* 2024;116:293–305. doi:10.1016/j.jmapro.2024.03.001
- [57] Sampson R, Lancaster R, Sutcliffe M, et al. An improved methodology of melt pool monitoring of direct energy deposition processes. *Opt Laser Technol* 2020;127:106194. doi:10.1016/j.optlastec.2020.106194
- [58] Everton SK, Hirsch M, Stravroulakis P, et al. Review of in-situ process monitoring and in-situ metrology for metal additive manufacturing. *Mater Des* 2016;95:431–445. doi:10.1016/j.matdes.2016.01.099
- [59] Xia C, Pan Z, Polden J, et al. A review on wire arc additive manufacturing: monitoring, control and a framework of automated system. *J. Manuf. Syst.* 2020;57:31–45. doi:10.1016/j.jmsy.2020.08.008
- [60] Maire E, Withers PJ. Quantitative X-ray tomography. *Int. Mater. Rev.* 2014;59:1–43. doi:10.1179/1743280413Y.0000000023
- [61] Aucott L, Dong H, Mirihanage W, et al. Revealing internal flow behaviour in arc welding and additive manufacturing of metals. *Nat Commun* 2018;9:5414. doi:10.1038/s41467-018-07900-9
- [62] Xing HZ, Zhang QB, Ruan D, et al. Full-field measurement and fracture characterisations of rocks under dynamic loads using high-speed three-dimensional digital image correlation. *Int. J. Impact Eng.* 2018;113:61–72. doi:10.1016/j.ijimpeng.2017.11.011
- [63] Nycz A, Lee Y, Noakes M, et al. Effective residual stress prediction validated with neutron diffraction method

- for metal large-scale additive manufacturing. *Mater Des* **2021**;205:109751. doi:10.1016/j.matdes.2021.109751
- [64] Plotkowski A, Saleeby K, Fancher CM, et al. Operando neutron diffraction reveals mechanisms for controlled strain evolution in 3D printing. *Nat Commun* **2023**;14:4950. doi:10.1038/s41467-023-40456-x
- [65] Burnett TL, Withers PJ. Completing the picture through correlative characterization. *Nat Mater* **2019**;18:1041–1049. doi:10.1038/s41563-019-0402-8
- [66] Xie C, Wu S, Yu Y, et al. Defect-correlated fatigue resistance of additively manufactured Al-Mg4.5Mn alloy with *in situ* micro-rolling. *J. Mater. Process. Technol.* **2021**;291:117039. doi:10.1016/j.jmatprotec.2020.117039
- [67] Li S, Yuan S, Zhu J, et al. Multidisciplinary topology optimization incorporating process-structure-property-performance relationship of additive manufacturing. *Struct. Multidiscip. Optim.* **2021**;63:2141–2157. doi:10.1007/s00158-021-02856-9
- [68] Smith J, Xiong W, Yan W, et al. Linking process, structure, property, and performance for metal-based additive manufacturing: computational approaches with experimental support. *Comput Mech* **2016**;57:583–610. doi:10.1007/s00466-015-1240-4
- [69] Gu D, Shi X, Poprawe R, et al. Material-structure-performance integrated laser-metal additive manufacturing. *Science*. **2021**;372:eabg1487. doi:10.1126/science.abg1487
- [70] Hashemi SM, Parvizi S, Baghbaniavid H, et al. Computational modelling of process-structure-property-performance relationships in metal additive manufacturing: a review. *Int. Mater. Rev.* **2022**;67:1–46. doi:10.1080/09506608.2020.1868889
- [71] Flores Ituarte I, Panicker S, Nagarajan HPN, et al. Optimisation-driven design to explore and exploit the process-structure-property-performance linkages in digital manufacturing. *J. Intell. Manuf.* **2022**;34:219–241. doi:10.1007/s10845-022-02010-2
- [72] Pant H, Arora A, Gopakumar GS, et al. Applications of wire arc additive manufacturing (WAAM) for aerospace component manufacturing. *Int. J. Adv. Manuf. Technol.* **2023**;127:4995–5011. doi:10.1007/s00170-023-11623-7
- [73] Barath Kumar MD, Manikandan M. Assessment of process, parameters, residual stress mitigation, post treatments and finite element analysis simulations of wire arc additive manufacturing technique. *Met. Mater. Int.* **2022**;28:54–111. doi:10.1007/s12540-021-01015-5
- [74] Niu X, He C, Zhu S-P, et al. Defect sensitivity and fatigue design: deterministic and probabilistic aspects in additively manufactured metallic materials. *Prog Mater Sci* **2024**;144:101290. doi:10.1016/j.pmatsci.2024.101290
- [75] Lan B, Wang Y, Liu Y, et al. The influence of microstructural anisotropy on the hot deformation of wire arc additive manufactured (WAAM) Inconel 718. *Mater Sci Eng A*. **2021**;823:141733. doi:10.1016/j.msea.2021.141733
- [76] Ouyang JH, Wang H, Kovacevic R. Rapid prototyping of 5356-aluminum alloy based on variable polarity gas tungsten arc welding: process control and microstructure. *Mater. Manuf. Process.* **2002**;17:103–124. doi:10.1081/AMP-120002801
- [77] Columnar to equiaxed grain transition in as solidified alloys, (n.d.). doi:10.1179/174328006X102493
- [78] Easton MA, StJohn DH. A model of grain refinement incorporating alloy constitution and potency of heterogeneous nucleant particles. *Acta Mater.* **2001**;49:1867–1878. doi:10.1016/S1359-6454(00)00368-2
- [79] Narasimharaju SR, Zeng W, See TL, et al. A comprehensive review on laser powder bed fusion of steels: processing, microstructure, defects and control methods, mechanical properties, current challenges and future trends. *J. Manuf. Process.* **2022**;75:375–414. doi:10.1016/j.jmapro.2021.12.033
- [80] Liu Z, Zhao D, Wang P, et al. Additive manufacturing of metals: microstructure evolution and multistage control. *J. Mater. Sci. Technol.* **2022**;100:224–236. doi:10.1016/j.jmst.2021.06.011
- [81] Bermingham M, StJohn D, Easton M, et al. Revealing the mechanisms of grain nucleation and formation during additive manufacturing. *JOM*. **2020**;72:1065–1073. doi:10.1007/s11837-020-04019-5
- [82] Hunt JD. Steady state columnar and equiaxed growth of dendrites and eutectic. *Mater. Sci. Eng.* **1984**;65:75–83. doi:10.1016/0025-5416(84)90201-5
- [83] Wu SC, Liu GR, Cui XY, et al. An edge-based smoothed point interpolation method (ES-PIM) for heat transfer analysis of rapid manufacturing system. *Int. J. Heat Mass Transf.* **2010**;53:1938–1950. doi:10.1016/j.ijheatmasstransfer.2009.12.062
- [84] Montevecchi F, Venturini G, Grossi N, et al. Finite element mesh coarsening for effective distortion prediction in wire arc additive manufacturing. *Addit. Manuf.* **2017**;18:145–155. doi:10.1016/j.addma.2017.10.010
- [85] Hackenhaar W, Mazzaferro JAE, Montevecchi F, et al. An experimental-numerical study of active cooling in wire arc additive manufacturing. *J. Manuf. Process.* **2020**;52:58–65. doi:10.1016/j.jmapro.2020.01.051
- [86] Ou W, Mukherjee T, Knapp GL, et al. Fusion zone geometries, cooling rates and solidification parameters during wire arc additive manufacturing. *Int. J. Heat Mass Transf.* **2018**;127:1084–1094. doi:10.1016/j.ijheatmasstransfer.2018.08.111
- [87] Cadiou S, Courtois M, Carin M, et al. Heat transfer, fluid flow and electromagnetic model of droplets generation and melt pool behaviour for wire arc additive manufacturing. *Int. J. Heat Mass Transf.* **2020**;148:119102. doi:10.1016/j.ijheatmasstransfer.2019.119102
- [88] Gao Z, Li Y, Shi H, et al. Microstructure characteristics under varying solidification parameters in different zones during CMT arc additive manufacturing process of 2319 aluminum alloy. *Vacuum*. **2023**;214:112177. doi:10.1016/j.vacuum.2023.112177
- [89] Hu J, Tsai HL. Heat and mass transfer in gas metal arc welding. Part II: the metal. *Int. J. Heat Mass Transf.* **2007**;50:808–820. doi:10.1016/j.ijheatmasstransfer.2006.08.026
- [90] Sampaio RFV, Pragana JPM, Bragança IMF, et al. Modelling of wire-arc additive manufacturing – a review. *Adv. Ind. Manuf. Eng.* **2023**;6:100121. doi:10.1016/j.aime.2023.100121
- [91] Yang H, Wu C, Li H, et al. Review on cellular automata simulations of microstructure evolution during metal forming process: grain coarsening, recrystallization and phase transformation. *Sci. China Technol. Sci.* **2011**;54:2107–2118. doi:10.1007/s11431-011-4464-3

- [92] Wang D, Wang Y, Liu W, et al. Multiscale investigation of microstructure optimization in the arc additive manufacturing and arc welding by self-induced ultrasound. *Int. J. Heat Mass Transf.* **2021**;180:121790. doi:10.1016/j.ijheatmasstransfer.2021.121790
- [93] Rodrigues TA, Duarte V, Miranda RM, et al. Current status and perspectives on wire and arc additive manufacturing (WAAM). *Materials (Basel)*. **2019**;12:1121. doi:10.3390/ma12071121
- [94] Liu J, Xu Y, Ge Y, et al. Wire and arc additive manufacturing of metal components: a review of recent research developments. *Int. J. Adv. Manuf. Technol.* **2020**;111:149–198. doi:10.1007/s00170-020-05966-8
- [95] Jin P, Liu Y, Sun Q. Evolution of crystallographic orientation, columnar to equiaxed transformation and mechanical properties realized by adding TiC in wire and arc additive manufacturing 2219 aluminum alloy. *Addit. Manuf.* **2021**;39:101878. doi:10.1016/j.addma.2021.101878
- [96] Wu S, Zhang Y, Xue M, et al. Grain refinement of flux-cored wire arc additively manufactured duplex stainless steel through in-situ alloying of Ti. *Mater Charact* **2024**;209:113749. doi:10.1016/j.matchar.2024.113749
- [97] Zhuo Y, Yang C, Fan C, et al. Grain morphology evolution mechanism of titanium alloy by the combination of pulsed arc and solution element during wire arc additive manufacturing. *J. Alloys Compd.* **2021**;888:161641. doi:10.1016/j.jallcom.2021.161641
- [98] Wang L, Xue J, Wang Q. Correlation between arc mode, microstructure, and mechanical properties during wire arc additive manufacturing of 316L stainless steel. *Mater Sci Eng A*. **2019**;751:183–190. doi:10.1016/j.msea.2019.02.078
- [99] Abe T, Kaneko J, Sasahara H. Thermal sensing and heat input control for thin-walled structure building based on numerical simulation for wire and arc additive manufacturing. *Addit. Manuf.* **2020**;35:101357. doi:10.1016/j.addma.2020.101357
- [100] Tröger J-A, Hartmann S, Treutler K, Potschka A, Wesling V. Simulation-based process parameter optimization for wire arc additive manufacturing. *Prog Addit Manuf.* **2024**;1–14. doi:10.1007/s40964-024-00597-x
- [101] Cai Y, Peng Z, Chen J, et al. Grain refinement and anisotropy improvement of arc-directed energy deposited Ti-6Al-4V with oscillating laser. *Mater Sci Eng A*. **2024**;893:146144. doi:10.1016/j.msea.2024.146144
- [102] Zhang W, Xu C, Li W, et al. The strengthening effect of high-energy ultrasound treatment on the additively manufactured ZL114A aluminum alloy. *Mater. Today Commun.* **2023**;37:107254. doi:10.1016/j.mtcomm.2023.107254
- [103] Gong M, Zhang S, Lu Y, et al. Achieving impressive strength and mitigated anisotropy in high-power laser-arc hybrid additive manufacturing of stainless steel through tailored microstructures composition. *Mater Sci Eng A*. **2024**;894:146204. doi:10.1016/j.msea.2024.146204
- [104] Guo Y, Han Q, Lu W, et al. Microstructure tuning enables synergistic improvements in strength and ductility of wire-arc additive manufactured commercial Al-Zn-Mg-Cu alloys. *Virtual Phys. Prototyp.* **2022**;17:649–661. doi:10.1080/17452759.2022.2048236
- [105] Liao Z, Yang B, Xiao S, et al. Fatigue crack growth behaviour of an Al-Mg4.5Mn alloy fabricated by hybrid *in situ* rolled wire + arc additive manufacturing. *Int J Fatigue*. **2021**;151:106382. doi:10.1016/j.ijfatigue.2021.106382
- [106] Sasikumar C, Oyyaravelu R. Mechanical properties and microstructure of SS 316 L created by WAAM based on GMAW. *Mater. Today Commun.* **2024**;38:107807. doi:10.1016/j.mtcomm.2023.107807
- [107] Su C, Chen X, Gao C, et al. Effect of heat input on microstructure and mechanical properties of Al-Mg alloys fabricated by WAAM. *Appl. Surf. Sci.* **2019**;486:431–440. doi:10.1016/j.apsusc.2019.04.255
- [108] Rodideal N, Machado CM, Infante V, et al. Mechanical characterization and fatigue assessment of wire and arc additively manufactured HSLA steel parts. *Int J Fatigue*. **2022**;164:107146. doi:10.1016/j.ijfatigue.2022.107146
- [109] Yang X, Liu J, Wang Z, et al. Microstructure and mechanical properties of wire and arc additive manufactured AZ31 magnesium alloy using cold metal transfer process. *Mater Sci Eng A*. **2020**;774:138942. doi:10.1016/j.msea.2020.138942
- [110] Guo Y, Han Q, Hu J, et al. Comparative study on wire-arc additive manufacturing and conventional casting of Al-Si alloys: porosity. *Microstruct Mech Prop Acta Metall. Sin. Engl. Lett.* **2022**;35:475–485. doi:10.1007/s40195-021-01314-1
- [111] Cai X, Yang M, Wang S, et al. Experimental investigations on corrosion behavior and antibacterial property of nickel-aluminum bronze fabricated through wire-arc additive manufacturing (WAAM). *Corros Sci* **2023**;214:111040. doi:10.1016/j.corsci.2023.111040
- [112] Huang C, Kyvelou P, Zhang R, et al. Mechanical testing and microstructural analysis of wire arc additively manufactured steels. *Mater Des* **2022**;216:110544. doi:10.1016/j.matdes.2022.110544
- [113] Dong B, Cai X, Lin S, et al. Microstructures and mechanical properties of wire arc additive manufactured 5183-Al: Influences of deposition dimensions. *CIRP J. Manuf. Sci. Technol.* **2021**;35:744–752. doi:10.1016/j.cirpj.2021.08.014
- [114] Wei J, He C, Zhao Y, et al. Evolution of microstructure and properties in 2219 aluminum alloy produced by wire arc additive manufacturing assisted by interlayer friction stir processing. *Mater Sci Eng A*. **2023**;868:144794. doi:10.1016/j.msea.2023.144794
- [115] Webster GA, Behvar A, Shakil SI, et al. Wire arc additive manufactured AWS ER100S-G steel: Very high cycle fatigue characterization. *Eng. Fail. Anal.* **2023**;154:107721. doi:10.1016/j.engfailanal.2023.107721
- [116] Zhang Y, Liu Z, Wang Y, Zhai Y, Cui C, Zhang Q, Du Z, Yuan Y, Wang X, Study on the role of chromium addition on sliding wear and corrosion resistance of high-manganese steel coating fabricated by wire arc additive manufacturing. *Wear*. **2024**;540–541:205242. doi:10.1016/j.wear.2024.205242
- [117] Penot C, Wharton J, Addison A, et al. Heat treatment effects on the corrosion performance of wire arc additively manufactured ER316LSi stainless steel. *Npj Mater. Degrad.* **2023**;7:1–13. doi:10.1038/s41529-023-00359-0

- [118] Li C, Gu H, Wang W, et al. Investigation on high-temperature mechanical properties of Al-7Si-0.6Mg alloy by wire + arc additive manufacturing. *Mater. Sci. Technol.* **2020**;36:1516–1522. doi:[10.1080/02670836.2020.1799136](https://doi.org/10.1080/02670836.2020.1799136)
- [119] Gu J, Yang S, Gao M, et al. Micropore evolution in additively manufactured aluminum alloys under heat treatment and inter-layer rolling. *Mater Des* **2020**;186:108288. doi:[10.1016/j.matdes.2019.108288](https://doi.org/10.1016/j.matdes.2019.108288)
- [120] Li S, Zhang L-J, Ning J, et al. Microstructures and mechanical properties of Al-Zn-Mg aluminium alloy samples produced by wire + arc additive manufacturing. *J. Mater. Res. Technol.* **2020**;9:13770–13780. doi:[10.1016/j.jmrt.2020.09.114](https://doi.org/10.1016/j.jmrt.2020.09.114)
- [121] Anyalebechi PN. Hydrogen-induced gas porosity formation in Al-4.5wt% Cu-1.4wt% Mg alloy. *J. Mater. Sci.* **2013**;48:5342–5353. doi:[10.1007/s10853-013-7329-2](https://doi.org/10.1007/s10853-013-7329-2)
- [122] Chen S, Xu M, Yuan T, et al. Thermal-microstructural analysis of the mechanism of liquation cracks in wire-arc additive manufacturing of Al-Zn-Mg-Cu alloy. *J. Mater. Res. Technol.* **2022**;16:1260–1271. doi:[10.1016/j.jmrt.2021.12.016](https://doi.org/10.1016/j.jmrt.2021.12.016)
- [123] Kang K, Liu Y, Ren H, et al. A novel magnetic field assisted powder arc additive manufacturing for Ti60 titanium alloy: method, microstructure and mechanical properties. *Addit. Manuf.* **2024**;83:104065. doi:[10.1016/j.addma.2024.104065](https://doi.org/10.1016/j.addma.2024.104065)
- [124] Hou X, Zhao L, Ren S, et al. A comparative study on Al-Mg-Sc-Zr alloy fabricated by wire arc additive manufacturing with controlling interlayer temperature and continuous printing: porosity, microstructure, and mechanical properties. *J. Mater. Sci. Technol.* **2024**;193:199–216. doi:[10.1016/j.jmst.2023.12.062](https://doi.org/10.1016/j.jmst.2023.12.062)
- [125] Yi H, Yang L, Jia L, et al. Porosity in wire-arc directed energy deposition of aluminum alloys: formation mechanisms, influencing factors and inhibition strategies. *Addit. Manuf.* **2024**;84:104108. doi:[10.1016/j.addma.2024.104108](https://doi.org/10.1016/j.addma.2024.104108)
- [126] Jeon I, Liu P, Sohn H, Real-time melt pool depth estimation and control during metal-directed energy deposition for porosity reduction. *Int J Adv Manuf Technol.* **2023**;1–16. doi:[10.1007/s00170-023-11689-3](https://doi.org/10.1007/s00170-023-11689-3)
- [127] Hu YN, Wu SC, Wu ZK, et al. A new approach to correlate the defect population with the fatigue life of selective laser melted Ti-6Al-4V alloy. *Int J Fatigue.* **2020**;136:105584. doi:[10.1016/j.ijfatigue.2020.105584](https://doi.org/10.1016/j.ijfatigue.2020.105584)
- [128] Wang F, Williams S, Colegrove P, et al. Microstructure and mechanical properties of wire and arc additive manufactured Ti-6Al-4V. *Metall Mater Trans A.* **2013**;44:968–977. doi:[10.1007/s11661-012-1444-6](https://doi.org/10.1007/s11661-012-1444-6)
- [129] Baufeld B, der Biest OV, Gault R. Additive manufacturing of Ti-6Al-4V components by shaped metal deposition: microstructure and mechanical properties. *Mater Des* **2010**;31:S106–S111. doi:[10.1016/j.matdes.2009.11.032](https://doi.org/10.1016/j.matdes.2009.11.032)
- [130] Yi H, Wang Q, Zhang W, et al. Wire-arc directed energy deposited Mg-Al alloy assisted by ultrasonic vibration: improving properties via controlling grain structures. *J. Manuf. Process. Technol.* **2023**;321:118134. doi:[10.1016/j.jmatprotec.2023.118134](https://doi.org/10.1016/j.jmatprotec.2023.118134)
- [131] Cong B, Ding J, Williams S. Effect of arc mode in cold metal transfer process on porosity of additively manufactured Al-6.3%Cu alloy. *Int. J. Adv. Manuf. Technol.* **2015**;76:1593–1606. doi:[10.1007/s00170-014-6346-x](https://doi.org/10.1007/s00170-014-6346-x)
- [132] Biswal R, Zhang X, Syed AK, et al. Criticality of porosity defects on the fatigue performance of wire + arc additive manufactured titanium alloy. *Int J Fatigue.* **2019**;122:208–217. doi:[10.1016/j.ijfatigue.2019.01.017](https://doi.org/10.1016/j.ijfatigue.2019.01.017)
- [133] Soysal T, Kou S. A simple test for assessing solidification cracking susceptibility and checking validity of susceptibility prediction. *Acta Mater.* **2018**;143:181–197. doi:[10.1016/j.actamat.2017.09.065](https://doi.org/10.1016/j.actamat.2017.09.065)
- [134] Seow CE, Zhang J, Coules HE, et al. Effect of crack-like defects on the fracture behaviour of wire + arc additively manufactured nickel-base alloy 718. *Addit. Manuf.* **2020**;36:101578. doi:[10.1016/j.addma.2020.101578](https://doi.org/10.1016/j.addma.2020.101578)
- [135] Serrano-Munoz I, Buffiere J-Y, Verdu C. Casting defects in structural components: are they all dangerous? A 3D study. *Int J Fatigue.* **2018**;117:471–484. doi:[10.1016/j.ijfatigue.2018.08.019](https://doi.org/10.1016/j.ijfatigue.2018.08.019)
- [136] Javidrad H, Koc B, Bayraktar H, et al. Fatigue performance of metal additive manufacturing: a comprehensive overview. *Virtual Phys. Prototyp.* **2024**;19:e2302556. doi:[10.1080/17452759.2024.2302556](https://doi.org/10.1080/17452759.2024.2302556)
- [137] Wu SC, Song Z, Kang GZ, et al. The Kitagawa-Takahashi fatigue diagram to hybrid welded AA7050 joints via synchrotron X-ray tomography. *Int J Fatigue.* **2019**;125:210–221. doi:[10.1016/j.ijfatigue.2019.04.002](https://doi.org/10.1016/j.ijfatigue.2019.04.002)
- [138] Zerbst U, Vormwald M, Pippan R, et al. About the fatigue crack propagation threshold of metals as a design criterion – a review. *Eng Fract Mech* **2016**;153:190–243. doi:[10.1016/j.engfracmech.2015.12.002](https://doi.org/10.1016/j.engfracmech.2015.12.002)
- [139] El Haddad MH, Topper TH, Smith KN. Prediction of non propagating cracks. *Eng Fract Mech* **1979**;11:573–584. doi:[10.1016/0013-7944\(79\)90081-X](https://doi.org/10.1016/0013-7944(79)90081-X)
- [140] Wu SC, Xiao TQ, Withers PJ. The imaging of failure in structural materials by synchrotron radiation X-ray microtomography. *Eng. Fract. Mech.* **2017**;182:127–156. doi:[10.1016/j.engfracmech.2017.07.027](https://doi.org/10.1016/j.engfracmech.2017.07.027)
- [141] Withers PJ, Bhadeshia HKDH. Residual stress. Part 2 – nature and origins., *Mater. Sci. Technol.* **2001**;17:366–375. doi:[10.1179/026708301101510087](https://doi.org/10.1179/026708301101510087)
- [142] Hönnige JR, Colegrove PA, Ahmad B, et al. Residual stress and texture control in Ti-6Al-4V wire + arc additively manufactured intersections by stress relief and rolling. *Mater Des* **2018**;150:193–205. doi:[10.1016/j.matdes.2018.03.065](https://doi.org/10.1016/j.matdes.2018.03.065)
- [143] Wu Q, Mukherjee T, Liu C, et al. Residual stresses and distortion in the patterned printing of titanium and nickel alloys. *Addit. Manuf.* **2019**;29:100808. doi:[10.1016/j.addma.2019.100808](https://doi.org/10.1016/j.addma.2019.100808)
- [144] Huang W, Wang Q, Ma N, et al. Distribution characteristics of residual stresses in typical wall and pipe components built by wire arc additive manufacturing. *J. Manuf. Process.* **2022**;82:434–447. doi:[10.1016/j.jmapro.2022.08.010](https://doi.org/10.1016/j.jmapro.2022.08.010)
- [145] Derekar KS, Ahmad B, Zhang X, et al. Effects of process variants on residual stresses in wire arc additive manufacturing of aluminum alloy 5183. *J. Manuf. Sci. Eng.* **2022**;144:071005. doi:[10.1115/1.4052930](https://doi.org/10.1115/1.4052930)
- [146] Assessment of Process, Parameters, Residual Stress Mitigation, Post Treatments and Finite Element

- Analysis Simulations of Wire Arc Additive Manufacturing Technique | Metals and Materials International, (n.d.). [accessed 2024 April 9]. doi: [10.1007/s12540-021-01015-5](https://doi.org/10.1007/s12540-021-01015-5)
- [147] Zhang C, Shen C, Hua X, et al. Influence of wire-arc additive manufacturing path planning strategy on the residual stress status in one single buildup layer. *Int. J. Adv. Manuf. Technol.* 2020;111:797–806. doi:[10.1007/s00170-020-06178-w](https://doi.org/10.1007/s00170-020-06178-w)
- [148] Shen H, Lin J, Zhou Z, et al. Effect of induction heat treatment on residual stress distribution of components fabricated by wire arc additive manufacturing. *J. Manuf. Process.* 2022;75:331–345. doi:[10.1016/j.jmapro.2022.01.018](https://doi.org/10.1016/j.jmapro.2022.01.018)
- [149] Gorniyakov V, Ding J, Sun Y, et al. Understanding and designing post-build rolling for mitigation of residual stress and distortion in wire arc additively manufactured components. *Mater Des* 2022;213:110335. doi:[10.1016/j.matdes.2021.110335](https://doi.org/10.1016/j.matdes.2021.110335)
- [150] Saleh B, Fathi R, Tian Y, et al. Fundamentals and advances of wire arc additive manufacturing: materials, process parameters, potential applications, and future trends. *Arch. Civ. Mech. Eng.* 2023;23:96. doi:[10.1007/s43452-023-00633-7](https://doi.org/10.1007/s43452-023-00633-7)
- [151] Mughal MP, Fawad H, Mufti RA, et al. Deformation modelling in layered manufacturing of metallic parts using gas metal arc welding: effect of process parameters. *Model. Simul. Mater. Sci. Eng.* 2005;13:1187. doi:[10.1088/0965-0393/13/7/013](https://doi.org/10.1088/0965-0393/13/7/013)
- [152] Ujjwal K, Anand M, Bishwakarma H, et al. Effect of clamping position on the residual stress in wire arc additive manufacturing. *Int. J. Mater. Res.* 2023;114:872–878. doi:[10.1515/ijmr-2022-0249](https://doi.org/10.1515/ijmr-2022-0249)
- [153] Sun J, Hensel J, Köhler M, et al. Residual stress in wire and arc additively manufactured aluminum components. *J. Manuf. Process.* 2021;65:97–111. doi:[10.1016/j.jmapro.2021.02.021](https://doi.org/10.1016/j.jmapro.2021.02.021)
- [154] Abusalma H, Eisazadeh H, Hejripour F, et al. Parametric study of residual stress formation in wire and arc additive manufacturing. *J. Manuf. Process.* 2022;75:863–876. doi:[10.1016/j.jmapro.2022.01.043](https://doi.org/10.1016/j.jmapro.2022.01.043)
- [155] Feng G, Wang H, Wang Y, et al. Numerical simulation of residual stress and deformation in wire arc additive manufacturing. *Crystals (Basel)*. 2022;12:803. doi:[10.3390/cryst12060803](https://doi.org/10.3390/cryst12060803)
- [156] Fan D, Gao M, Li C, et al. Residual stress and microstructure properties by trailing cooling of argon gas of wire and arc additive manufacturing. *J. Manuf. Process.* 2022;77:32–39. doi:[10.1016/j.jmapro.2022.03.007](https://doi.org/10.1016/j.jmapro.2022.03.007)
- [157] Yang Y, Lin H, Li Q. A computationally efficient thermo-mechanical model with temporal acceleration for prediction of residual stresses and deformations in WAAM. *Virtual Phys. Prototyp.* 2024;19:e2349683. doi:[10.1080/17452759.2024.2349683](https://doi.org/10.1080/17452759.2024.2349683)
- [158] Huang H, Ma N, Chen J, et al. Toward large-scale simulation of residual stress and distortion in wire and arc additive manufacturing. *Addit. Manuf.* 2020;34:101248. doi:[10.1016/j.addma.2020.101248](https://doi.org/10.1016/j.addma.2020.101248)
- [159] Li C, Liu JF, Guo YB. Prediction of residual stress and part distortion in selective laser melting. *Procedia CIRP.* 2016;45:171–174. doi:[10.1016/j.procir.2016.02.058](https://doi.org/10.1016/j.procir.2016.02.058)
- [160] Michaleris P. Modeling metal deposition in heat transfer analyses of additive manufacturing processes. *Finite Elem. Anal. Des.* 2014;86:51–60. doi:[10.1016/j.finel.2014.04.003](https://doi.org/10.1016/j.finel.2014.04.003)
- [161] Denlinger ER, Michaleris P. Effect of stress relaxation on distortion in additive manufacturing process modeling. *Addit. Manuf.* 2016;12:51–59. doi:[10.1016/j.addma.2016.06.011](https://doi.org/10.1016/j.addma.2016.06.011)
- [162] Kolossov S, Boillat E, Glardon R, et al. 3D FE simulation for temperature evolution in the selective laser sintering process. *Int J Mach Tools Manuf.* 2004;44:117–123. doi:[10.1016/j.ijmachtools.2003.10.019](https://doi.org/10.1016/j.ijmachtools.2003.10.019)
- [163] Yang G, Ma J, Carlson BE, et al. Decreasing the surface roughness of aluminum alloy welds fabricated by a dual beam laser. *Mater Des* 2017;127:287–296. doi:[10.1016/j.matdes.2017.04.085](https://doi.org/10.1016/j.matdes.2017.04.085)
- [164] Xiong J, Li Y, Li R, et al. Influences of process parameters on surface roughness of multi-layer single-pass thin-walled parts in GMAW-based additive manufacturing. *J. Mater. Process. Technol.* 2018;252:128–136. doi:[10.1016/j.jmatprotec.2017.09.020](https://doi.org/10.1016/j.jmatprotec.2017.09.020)
- [165] Le VT, Mai DS, Hoang QH. Effects of cooling conditions on the shape, microstructures, and material properties of SS308L thin walls built by wire arc additive manufacturing. *Mater. Lett.* 2020;280:128580. doi:[10.1016/j.matlet.2020.128580](https://doi.org/10.1016/j.matlet.2020.128580)
- [166] Qiu Z, Dong B, Wu B, et al. Tailoring the surface finish, dendritic microstructure and mechanical properties of wire arc additively manufactured Hastelloy C276 alloy by magnetic arc oscillation. *Addit. Manuf.* 2021;48:102397. doi:[10.1016/j.addma.2021.102397](https://doi.org/10.1016/j.addma.2021.102397)
- [167] Li W, Amanov A, Nagaraja KM, et al. Processing aluminum alloy with hybrid wire arc additive manufacturing and ultrasonic nanocrystalline surface modification to improve porosity, surface finish, and hardness. *J. Manuf. Process.* 2023;103:181–192. doi:[10.1016/j.jmapro.2023.08.047](https://doi.org/10.1016/j.jmapro.2023.08.047)
- [168] Maleki E, Bagherifard S, Bandini M, et al. Surface post-treatments for metal additive manufacturing: progress, challenges, and opportunities. *Addit. Manuf.* 2021;37:101619. doi:[10.1016/j.addma.2020.101619](https://doi.org/10.1016/j.addma.2020.101619)
- [169] Ermakova A, Razavi N, Cabeza S, et al. The effect of surface treatment and orientation on fatigue crack growth rate and residual stress distribution of wire arc additively manufactured low carbon steel components. *J. Mater. Res. Technol.* 2023;24:2988–3004. doi:[10.1016/j.jmrt.2023.03.227](https://doi.org/10.1016/j.jmrt.2023.03.227)
- [170] Thakur VS, Manikandan M, Singh S, et al. Laser polishing of wire arc additive manufactured SS316L. In: Shunmugam MS, Kanthababu M, editors. *Advances in Additive Manufacturing and Joining*. Singapore: Springer; 2020. p. 127–135. doi:[10.1007/978-981-32-9433-2_10](https://doi.org/10.1007/978-981-32-9433-2_10)
- [171] Selvabharathi R. Microstructure and corrosion resistance of 23Cr9Ni4Mo2Mn filler duplex stainless steel 2205 fabricated by wire arc additive manufacturing with subsequent severe shot peening and Ni58Cr20Fe5Mo10 plasma spray coating. *Mater. Today Commun.* 2023;37:107560. doi:[10.1016/j.mtcomm.2023.107560](https://doi.org/10.1016/j.mtcomm.2023.107560)
- [172] Kim S-G, Lee C-M, Kim D-H. Plasma-assisted machining characteristics of wire arc additive manufactured stainless steel with different deposition directions. *J. Mater. Res. Technol.* 2021;15:3016–3027. doi:[10.1016/j.jmrt.2021.09.130](https://doi.org/10.1016/j.jmrt.2021.09.130)

- [173] Rauch M, Hascoet J-Y. A comparison of post-processing techniques for additive manufacturing components. *Procedia CIRP*. 2022;108:442–447. doi:10.1016/j.procir.2022.03.069
- [174] Rubino F, Scherillo F, Franchitti S, et al. Microstructure and surface analysis of friction stir processed Ti-6Al-4V plates manufactured by electron beam melting. *J. Manuf. Process*. 2019;37:392–401. doi:10.1016/j.jmapro.2018.12.015
- [175] Liu M, Zou T, Wang Q, et al. Microstructure evolution, failure mechanism and life prediction of additively manufactured Inconel 625 superalloy with comparable low cycle fatigue performance. *Int J Fatigue*. 2024;181:108142. doi:10.1016/j.ijfatigue.2023.108142
- [176] Lee S, Pegues JW, Shamsaei N. Fatigue behavior and modeling for additive manufactured 304L stainless steel: the effect of surface roughness. *Int J Fatigue*. 2020;141:105856. doi:10.1016/j.ijfatigue.2020.105856
- [177] Bian L, Thompson SM, Shamsaei N. Mechanical properties and microstructural features of direct laser-deposited Ti-6Al-4V. *JOM*. 2015;67:629–638. doi:10.1007/s11837-015-1308-9
- [178] Yadollahi A, Shamsaei N. Additive manufacturing of fatigue resistant materials: challenges and opportunities. *Int J Fatigue*. 2017;98:14–31. doi:10.1016/j.ijfatigue.2017.01.001
- [179] Qi Z, Cong B, Qi B, et al. Microstructure and mechanical properties of double-wire + arc additively manufactured Al-Cu-Mg alloys. *J. Mater. Process. Technol*. 2018;255:347–353. doi:10.1016/j.jmatprotec.2017.12.019
- [180] Kitagawa H. Applicability of fracture mechanics to very small cracks or the cracks in the early stage. *Int Conf Mech Behav Mater 2nd*. 1976: 627–631.
- [181] El Haddad MH, Smith KN, Topper TH. Fatigue crack propagation of short cracks. *J. Eng. Mater. Technol*. 1979;101:42–46. doi:10.1115/1.3443647
- [182] Metal Fatigue: Effects of Small Defects and Nonmetallic Inclusions - 2nd Edition | Elsevier Shop, (n.d.). [Accessed 2024 April 25]. <https://shop.elsevier.com/books/metal-fatigue-effects-of-small-defects-and-nonmetallic-inclusions/murakami/978-0-12-813876-2>
- [183] Beretta S, Carboni M, Madia M. Modelling of fatigue thresholds for small cracks in a mild steel by “Strip-Yield” model. *Eng Fract Mech*. 2009;76:1548–1561. doi:10.1016/j.engfracmech.2009.04.015
- [184] Wang P, Zhang P, Wang B, et al. Fatigue cracking criterion of high-strength steels induced by inclusions under high-cycle fatigue. *J. Mater. Sci. Technol*. 2023;154:114–128. doi:10.1016/j.jmst.2023.02.006
- [185] Pang JC, Li SX, Wang ZG, et al. Relations between fatigue strength and other mechanical properties of metallic materials. *Fatigue Fract. Eng. Mater. Struct*. 2014;37:958–976. doi:10.1111/ffe.12158
- [186] Pang JC, Li SX, Wang ZG, et al. General relation between tensile strength and fatigue strength of metallic materials. *Mater Sci Eng A*. 2013;564:331–341. doi:10.1016/j.msea.2012.11.103
- [187] Webster GA, Ribble R, Chou K, et al. Fatigue characterization of wire arc additive manufactured AWS ER100S-G steel: fully reversed condition. *Eng. Fail. Anal*. 2023;153:107562. doi:10.1016/j.engfailanal.2023.107562
- [188] Mu H, He F, Yuan L, Commins P, Wang H, Pan H, Toward a smart wire arc additive manufacturing system: a review on current developments and a framework of digital twin. *J. Manuf. Syst*. 2023;67:174–189. doi:10.1016/j.jmsy.2023.01.012
- [189] Li J, Sage M, Guan X, et al. Machine learning-enabled competitive grain growth behavior study in directed energy deposition fabricated Ti6Al4V. *JOM*. 2020;72:458–464. doi:10.1007/s11837-019-03917-7
- [190] Kats D, Wang Z, Gan Z, et al. A physics-informed machine learning method for predicting grain structure characteristics in directed energy deposition. *Comput. Mater. Sci*. 2022;202:110958. doi:10.1016/j.commatsci.2021.110958
- [191] Chandra M, Vimal KEK, Rajak S, A comparative study of machine learning algorithms in the prediction of bead geometry in wire-arc additive manufacturing. *Int. J. Interact. Des. Manuf. IJIDeM*. 2023:1–14. doi:10.1007/s12008-023-01326-4
- [192] Nagesh DS, Datta GL. Prediction of weld bead geometry and penetration in shielded metal-arc welding using artificial neural networks. *J. Mater. Process. Technol*. 2002;123:303–312. doi:10.1016/S0924-0136(02)00101-2
- [193] Gokhale NP, Kala P, Sharma V. Thin-walled metal deposition with GTAW welding-based additive manufacturing process. *J. Braz. Soc. Mech. Sci. Eng*. 2019;41:569. doi:10.1007/s40430-019-2078-z
- [194] Venkata Rao K, Parimi S, Suvarna Raju L, et al. Modelling and optimization of weld bead geometry in robotic gas metal arc-based additive manufacturing using machine learning, finite-element modelling and graph theory and matrix approach. *Soft Comput*. 2022;26:3385–3399. doi:10.1007/s00500-022-06749-x
- [195] Ding D, Pan Z, Cuiuri D, et al. Bead modelling and implementation of adaptive MAT path in wire and arc additive manufacturing. *Robot Comput-Integr Manuf*. 2016;39:32–42. doi:10.1016/j.rcim.2015.12.004
- [196] Kumar A, Maji K. Selection of process parameters for near-net shape deposition in wire arc additive manufacturing by genetic algorithm. *J. Mater. Eng. Perform*. 2020;29:3334–3352. doi:10.1007/s11665-020-04847-1
- [197] Li F, Chen S, Wu Z, et al. Adaptive process control of wire and arc additive manufacturing for fabricating complex-shaped components. *Int. J. Adv. Manuf. Technol*. 2018;96:871–879. doi:10.1007/s00170-018-1590-0
- [198] Lambiase F, Scipioni SI, Paoletti A. Accurate prediction of the bead geometry in wire arc additive manufacturing process. *Int. J. Adv. Manuf. Technol*. 2022;119:7629–7639. doi:10.1007/s00170-021-08588-w
- [199] Gühr M, Rashid A, Melkote SN. Bead geometry prediction and optimization for corner structures in directed energy deposition using machine learning. *Addit. Manuf*. 2024;84:104080. doi:10.1016/j.addma.2024.104080
- [200] Le VT, Bui MC, Pham TQD, et al. Efficient prediction of thermal history in wire and arc additive manufacturing combining machine learning and numerical simulation. *Int. J. Adv. Manuf. Technol*. 2023;126:4651–4663. doi:10.1007/s00170-023-11473-3
- [201] Xie J, Chai Z, Xu L, et al. 3D temperature field prediction in direct energy deposition of metals using physics informed neural network. *Int. J. Adv. Manuf. Technol*. 2022;119:3449–3468. doi:10.1007/s00170-021-08542-w

- [202] Fagersand HM, Morin D, Mathisen KM, et al. Transferability of temperature evolution of dissimilar wire-arc additively manufactured components by machine learning. *Materials* (Basel). 2024;17:742. doi:10.3390/ma17030742
- [203] DebRoy T, Mukherjee T, Wei HL, et al. Metallurgy, mechanistic models and machine learning in metal printing. *Nat. Rev. Mater.* 2021;6:48–68. doi:10.1038/s41578-020-00236-1
- [204] Zhou Z, Shen H, Liu B, et al. Residual thermal stress prediction for continuous tool-paths in wire-arc additive manufacturing: a three-level data-driven method. *Virtual Phys. Prototyp.* 2022;17:105–124. doi:10.1080/17452759.2021.1997259
- [205] Zhou Z, Shen H, Lin J, et al. Continuous tool-path planning for optimizing thermo-mechanical properties in wire-arc additive manufacturing: an evolutionary method. *J. Manuf. Process.* 2022;83:354–373. doi:10.1016/j.jmapro.2022.09.009
- [206] He X, Wang T, Wu K, et al. Automatic defects detection and classification of low carbon steel WAAM products using improved remanence/magneto-optical imaging and cost-sensitive convolutional neural network. *Measurement* (Mahwah N J). 2021;173:108633. doi:10.1016/j.measurement.2020.108633
- [207] Cheepu M. Machine learning approach for the prediction of defect characteristics in wire arc additive manufacturing. *Trans Indian Inst Met* 2023;76:447–455. doi:10.1007/s12666-022-02715-1
- [208] Surovi NA, Soh GS. Acoustic feature based geometric defect identification in wire arc additive manufacturing. *Virtual Phys. Prototyp.* 2023;18:e2210553. doi:10.1080/17452759.2023.2210553
- [209] Li F, Chen S, Shi J, et al. Evaluation and optimization of a hybrid manufacturing process combining wire arc additive manufacturing with milling for the fabrication of stiffened panels. *Appl Sci* 2017;7:1233. doi:10.3390/app7121233
- [210] Xia C, Pan Z, Polden J, et al. Modelling and prediction of surface roughness in wire arc additive manufacturing using machine learning. *J. Intell. Manuf.* 2022;33:1467–1482. doi:10.1007/s10845-020-01725-4
- [211] Yaseer A, Chen H. Machine learning based layer roughness modeling in robotic additive manufacturing. *J. Manuf. Process.* 2021;70:543–552. doi:10.1016/j.jmapro.2021.08.056
- [212] Kazmi KH, Chandra M, Rajak S, et al. Implementing machine learning in robotic wire arc additive manufacturing for minimizing surface roughness. *Int. J. Comput. Integr. Manuf.* 2024;0:1–16. doi:10.1080/0951192X.2024.2330091
- [213] Xie X, Bennett J, Saha S, et al. Mechanistic data-driven prediction of as-built mechanical properties in metal additive manufacturing. *Npj Comput. Mater.* 2021;7:1–12. doi:10.1038/s41524-021-00555-z
- [214] Brooke R, Qiu D, Le T, et al. Optimising the manufacturing of a β -Ti alloy produced via direct energy deposition using small dataset machine learning. *Sci Rep* 2024;14:6975. doi:10.1038/s41598-024-57498-w
- [215] Fang L, Cheng L, Glerum JA, et al. Data-driven analysis of process, structure, and properties of additively manufactured Inconel 718 thin walls. *Npj Comput. Mater.* 2022;8:1–15. doi:10.1038/s41524-022-00808-5
- [216] Zhang Y, Karnati S, Nag S, et al. Accelerating additive design with probabilistic machine learning. *ASCE-ASME J Risk Uncert Engrg Sys Part B Mech Eng.* 2021;8:011109. doi:10.1115/1.4051699
- [217] Lin Z, Song K, Yu X. A review on wire and arc additive manufacturing of titanium alloy. *J. Manuf. Process.* 2021;70:24–45. doi:10.1016/j.jmapro.2021.08.018
- [218] Gunasegaram DR, Barnard AS, Matthews MJ, et al. Machine learning-assisted in-situ adaptive strategies for the control of defects and anomalies in metal additive manufacturing. *Addit. Manuf.* 2024;81:104013. doi:10.1016/j.addma.2024.104013
- [219] AbouelNour Y, Gupta N. In-situ monitoring of sub-surface and internal defects in additive manufacturing: a review. *Mater Des* 2022;222:111063. doi:10.1016/j.matdes.2022.111063
- [220] Niu S, Peng Y, Li B, et al. A novel deep learning motivated data augmentation system based on defect segmentation requirements. *J. Intell. Manuf.* 2024;35:687–701. doi:10.1007/s10845-022-02068-y
- [221] Mozaffar M, Liao S, Xie X, et al. Mechanistic artificial intelligence (mechanistic-AI) for modeling, design, and control of advanced manufacturing processes: current state and perspectives. *J. Mater. Process. Technol.* 2022;302:117485. doi:10.1016/j.jmatprotec.2021.117485